2010

The Role of the Ca2+-dependent protein kinase, CaMK-II, in Heart and Kidney Development in the Zebrafish, Danio rerio

Sarah Rothschild
Virginia Commonwealth University

VCU Graduate School

Approval form for thesis/dissertation and final oral examination

Student name: Rothschild (Last) Sarah (First) C (Middle initial) **V number:** V00228560

Document type: (check one) ☐ Master's thesis ☐ ■ Doctoral dissertation

Department: Life Sciences

Thesis/dissertation title: The Role of the Ca(2+)-dependent Protein Kinase, CaMK-II, in Heart and Kidney Development in the Zebrafish, Danio rerio.

Approval numbers

- ☐ IRB
- ☐ IACUC AM10356
- ☐ Exempt
- ☐ Not applicable

Thesis/dissertation and final oral defense

Date: April 16, 2010

Graduate Advisory Committee (type name and sign)

	Failed	Passed
Robert M. Tombes		✓
James Lister		✓
Paul Fawcett		✓
Babette Fuss		✓
Shirley Taylor		✓

Graduate program director/department chair: Robert M Tombes **Date:** 4/16/10

School/college dean: Thomas F Hewett **Date:** 4/16/10

The Role of the Ca^{2+}-dependent protein kinase, CaMK-II, in Heart and Kidney Development in the Zebrafish, *Danio rerio*

A dissertation submitted in partial fulfillment of the requirements for the degree of Doctor of Philosophy at Virginia Commonwealth University.

by

Sarah Chase Rothschild
B.A., University of Mary Washington 2000

Robert M. Tombes, Ph.D.
Professor of Biology

Virginia Commonwealth University
Richmond, VA
April 2010

Acknowledgments

I would like to express my gratitude to a number of individuals who have made significant contributions to this dissertation project. First, I would like to thank Dr. Robert Tombes for his guidance, both scientifically and professionally, positive influence and continued support. Words will never be able to express how grateful I am to be a part of his lab. I would also like to thank Dr. James Lister for teaching me zebrafish experimental techniques and for his continued collaboration. I am truly grateful for both his participation on my committee as well as his continued advice on my research. I would also like to thank my committee members Drs Shirley Taylor, Babette Fuss, and Paul Fawcett. You have helped me to think critically about my research and to see the big picture.

I would like to thank former members of the Tombes Lab for their assistance. Dr. Charles Easley IV introduced me to the lab and taught me so much about CaMK-II and protein biology. I will always be grateful that Chas was a Biology teaching assistant. I would also like to thank Matt Seward for his continued support and scientific discussions.

I would also like to thank Ludmila Francescatto for her continued advice, and friendship. I am so thankful for all our scientific discussions and all her support. I am also grateful for Jamie McLeod, Alexandra Myers, Amritha Yellamilli, Jeannette Aiken and Bennett Childs who all helped me immensely during this process. The support from all the Tombes lab members was invaluable.

I would also like to thank our collaborators. Dr. Iain Drummond for providing the Tg(Na^+K^+-ATPase:GFP) line of fish, Dr. Debbie Garrity for providing us with heterozygous tbx5 mutant fish (*heartstring*) and her expertise on our 2009 article, Dr. Alan Davidson for providing *ret1, wt1a, gata3,* and *cdh17* cDNAs, Dr. Lilliana Solnica-Krezel for the Tg(CAAX:GFP) fish and Dr. Lister for providing *pax2a* cDNA and Tg(cmlc2:DsRed) fish. I also would like to thank Julie Farnsworth for her assistance in using the flow cytometer at the shared resource facility.

Finally I would like to thank my family; my parents, Chip and Lynne Chase, my sister, Amy Chase, my mother and father-in-law, Ed and Susy Rothschild, my sister-in-law, Elizabeth Rothschild, and most of all my husband, Andrew Rothschild, for their unconditional support and love.

Table of Contents

List of Tables

List of Figures

List of Abbreviations

ADPKD	Autosomal Dominant Polycystic Kidney disease
AER	Apical ectodermal ridge
AIP	Autoinhibitory peptide for CaMK-II
aPKC	Atypical protein kinase C
Amhc	Atrial myosin heavy chain
BAPTA	(1,2-bis(o-aminophenoxy)ethane-N,N,N',N'-tetraacetic acid)
BLAST	Basic Local Alignment Search Tool
Bmp4	Bone morphogenetic protein 4
Bmp6	Bone morphogenetic protein 6
bp	Base pair
Ca^{2+}	Calcium, ionized
CAAX	Membrane targeting sequence
$CaCO_3$	Calcium carbonate
CaMK-II	Ca^{2+}/calmodulin-dependent protein kinase II
CaM	Calmodulin
Cdh17	Cadherin-17
CG	Cortical granule
CICR	Calcium-induced calcium release

Cmlc2	Cardiac myosin light chain 2
CNS	Central Nervous System
CREB	cAMP response element-binding
cWnt	Canonical Wnt
dpf	Days post fertilization
DFISH	Double fluorescent *in situ* hybridization
DIC	Differential Interferene Contrast
DsRed	Discosoma sp. (coral) red fluorescent protein
EGFR	Epidermal growth factor receptor
EGTA	Ethylene glycol tetraacetic acid
ENU	N-ethyl-N-nitrosourea
ER	Endoplasmic Reticulum
FAK	Focal adhesion kinase
Fgf10	Fibroblast growth factor 10
FISH	Fluorescent *in situ* hybridization
Fli-I	Flightless-I
Gas8	Growth-arrest specific 8
Gata3	GATA transcription factor 3
Gata4	GATA transcription factor 4
GFP	Green fluorescent protein
GPCR	G-protein coupled receptor
HDAC	Histone deacetylase
HOS	Holt-Oram Syndrome

hpf	Hours post fertilization
hst	Heartstring mutant tbx5
Ift88	Intraflagellar transport protein 88
IP3R	Inositol Triphosphate Receptor
kDa	Kilodaltons
LEF	Lymphocyte enhancer factor
KN-92	Inactive analog of KN-93
KN-93	Calmodulin binding antagonist, inhibits CaMK-II
MS-222	3-amino-benzoic acid ethyl ester, Tricaine
MBT	Midblastula transition
mDia(1)	Mammalian Diaphanous homolog(1)
MIM	Missing in metastasis
MO	Antisense morpholino oligonucleotide
mPCTs	Mouse proximal tubule cells
Na^+/K^+ ATPase	Sodium potassium ATPase
ncWnt	Noncanonical Wnt
NLS	Nuclear localization signal
nt	Nucleotide
Nkx2.5	Homeodomain transcription factor
Pax2a	Paired box transcription factor
PCR	Polymerase chain reaction
PKC	Protein kinase C
PKD1	Polycystic kidney disease 1

PKD2	Polycystic kidney disease 2
PTU	1-phenyl-2-thiourea
Rac	Rho family of GTPases
Ret1	The ret1 tyrosine-kinase receptor
Sal4	Allosuppressor 4
SERCA	Sarco-endoplasmic reticulum Ca^{2+} -ATPase
SHP2	Protein-tyrosine phosphatase
SR	Sarcoplasmic reticulum
SynGAP	Synaptic RasGAP
Tbx4	T-box transcription factor 4
Tbx5	T-box transcription factor 5
Tbx20	T-box transcription factor 20
TCF	T-cell factor transcription factor
Tg	Transgenic
Tiam1	T-cell lymphoma invasion and metastasis 1
TOPO TA	TOPO cloning system (Invitrogen)
Tm	Melting Temperature
TRP	Transient receptor potential family
Vmhc	Ventricular myosin heavy chain
WISH	Whole mount *in situ* hybridization
Wnt	Wingless integrated
Wt1a	Wilm's tumor suppressor gene 1a

Abstract

THE ROLE OF THE Ca^{2+}-DEPENDENT PROTEIN KINASE, CAMK-II, IN HEART AND KIDNEY DEVELOPMENT IN THE ZEBRAFISH, *DANIO RERIO*

By Sarah Chase Rothschild, B.A.

A dissertation submitted in partial fulfillment of the requirements for the degree of Doctor of Philosophy at Virginia Commonwealth University

Virginia Commonwealth University, 2010

Robert M. Tombes, Ph.D.
Professor of Biology

$Ca^{2+/}$calmodulin-dependent protein kinase type II (CaMK-II) is a multifunctional serine/threonine kinase that is ubiquitously expressed throughout the lifespan of metazoans. Mammals encode four genes (α, β, γ, δ) that generate over forty splice-variants. CaMK-II is important in a myriad of functions, including ion channel regulation, cell-cycle progression, and long term potentiation. In adults, alterations in activation of CaMK-II induce cardiac arrhythmias and heart failure. Developmental roles for CaMK-II are not as well understood since mouse knockouts are embryonic lethal. Therefore the identification of other vertebrate CaMK-II genes will add to our understanding of development. Zebrafish encode seven catalytically active CaMK-II genes (α1, β1, β2, γ1, γ2, δ1, δ2) due to a genome wide duplication event that occurred approximately 250 million years ago. Although, only 20-30% of all duplicated genes were retained, 75% of CaMK-II duplicated genes are transcriptionally active, pointing to a critical role for this signaling protein. mRNA expression patterns demonstrate that CaMK-II is expressed in diverse tissues including retina, pectoral fins, somites, heart, and kidney. Suppression of each

gene generates unique phenotypes that mirror the mRNA expression patterns. Of the seven genes, *camk2b2* and *camk2g1* have the highest maternal contribution in zebrafish, are expressed in mesodermally derived organs, and develop defects similar to human syndromes. In fact, suppression of *camk2b2* mimics the phenotype observed in zebrafish mutants of *tbx5*, the gene mutated in patients with Holt-Oram Syndrome. *Camk2g1* morphants also exhibit similar defects as suppression of *pkd2*, the gene mutated in patients with Autosomal Dominant Polycystic Kidney disease. These roles implicate CaMK-II as an integral protein in the development and maintenance of mesodermally derived tissues.

Chapter 1: Background

Ca^{2+} and Development

Ca^{2+} is an integral second messenger at fertilization, during development, and throughout adulthood. Ca^{2+} is required for cell proliferation, cell differentiation, pattern formation, axis determination, organ development, and thus, formation of the overall body plan in vertebrates (Whitaker, 2006). The activity of Ca^{2+} dependent proteins is determined by the amplitude, frequency, and duration of the Ca^{2+} stimulus, which can then be translated into a cellular response (Schulman et al., 1992; Whitaker, 2006).

At fertilization, sperm-egg fusion generates a propagating Ca^{2+} wave from intracellular stores that induces egg activation (Whitaker and Steinhardt, 1982). This Ca^{2+} wave is involved in many essential early processes such as cortical granule (CG) exocytosis, cytoskeletal rearrangements, and cell-cycle progression (Abbott and Ducibella, 2001; Lorca et al., 1993; Stemmann et al., 2001; Tatone et al., 2002; Tatone et al., 1999; Tombes et al., 1991). In the mammalian egg, CG exocytosis begins about 5-10 minutes after insemination, but it takes approximately 45-60 minutes to be completed (Tahara et al., 1996). This is due to the duration of intracellular Ca^{2+} elevations necessary to activate downstream effector proteins, which have been demonstrated to positively regulate the level of CG exocytosis (Abbott and Ducibella, 2001). Continued Ca^{2+} oscillations are also required for metaphase II exit, where the anaphase promoting complex is activated, cyclin B is degraded and sister chromatids separate (Lorca et al., 1993; Markoulaki et al., 2003; Markoulaki et al., 2004; Nixon et al., 2002). Although both CG

exocytosis and metaphase II exit require Ca^{2+} oscillations, the amplitude and duration of Ca^{2+} differentially activate effector proteins to drive these cellular mechanisms.

At the single cell stage Ca^{2+} waves are present to initiate cleavage furrow positioning, generation of the contractile ring, and membrane additions as the furrow deepens, which ultimately leads to cytokinesis (Chang and Lu, 2000; Webb and Miller, 2000). A series of cell divisions then occur to generate the blastocyst, relying heavily on maternal stores of proteins and mRNAs since zygotic transcription does not occur until the midblastula transition (MBT).

As the embryo develops the cellular pathways become more complex and the need for both intracellular and intercellular Ca^{2+} is evident. At gastrulation a process known as convergence and extension occurs, where cells migrate toward the midline dorsally and intercalate through an anteriorward elongation (Bakkers et al., 2004; Keller and Danilchik, 1988; Myers et al., 2002). This process determines the anterior-posterior axis of the embryo and is largely dependent on Ca^{2+} and "non-canonical" Wnt (ncWnt) family members (Wallingford et al., 2001). ncWnts act in a β-catenin independent manner and function to release Ca^{2+} stores from the ER through phospholipase C to activate effector proteins, such as CaMK-II and PKC, causing cells to undergo cytoskeletal reorganization and shape changes to maintain proper polarity during migration. Well characterized non-canonical Wnts, Wnt5 and Wnt11, are necessary for proper cell movements during gastrulation. Suppression of Wnt5, Wnt11, or CaMK-II (Tombes lab unpublished data) during embryogenesis leads to anterior-posterior axis defects, including compressed somites and an undulated notochord (Kuhl et al., 2001; Roszko et al., 2009; Sheldahl et al., 2003).

Continued Ca^{2+} elevations are found during the segmentation period where Ca^{2+} is necessary to form somites, eyes, and establish organ left-right asymmetry (Brady and Hilfer,

1982; Creton et al., 1998; Shimeld, 2004; Webb and Miller, 2006). Recent work in the Tombes lab has identified three zebrafish CaMK-II genes required for left-right asymmetry, where CaMK-II acts as the downstream target of PKD2 Ca^{2+} in the Kupffer's vesicle (KV), thus generating sided expression of downstream targets. Zebrafish embryos that were injected with f-aequorin, a calcium-sensitive bioluminescent protein, and imaged have four main intercellular calcium pulses (Shimomura et al., 1990). There is a tail bud pulse at 90% epiboly, a brain pulse at bud stage, a trunk pulse at 6 somites, and an eye pulse at 10 somites. Each intercellular Ca^{2+} pulse is generated in a region where the formation of major structures is about to occur (Creton et al., 1998; Webb and Miller, 2000). Similar Ca^{2+} pulses are thought to exist in other species. Chick embryos treated with the Ca^{2+} ionophore, A23187, form somites, however, verapamil a Ca^{2+} channel antagonist inhibits segmentation (Chernoff and Hilfer, 1982).

Once the body plan of the embryo is established, localized Ca^{2+} elevations facilitate the development of organs, such as the heart and kidney. Although Ca^{2+} is well established in the heart as an important second messenger during cardiac contractions, researchers are now demonstrating that Ca^{2+} is also essential in rudimentary heart development. Zebrafish embryos injected with BAPTA develop a linear heart that is unable to pump blood and has an enlarged pericardial sac (Creton et al., 1998). Suppression of CaMK-II in zebrafish yields a similar phenotype whereby the heart fails to undergo looping and blood circulation is reduced (Rothschild et al., 2009). Ca^{2+} is also important in kidney development and homeostasis. Suppression of PKD2, a nonselective Ca^{2+} channel, induces kidney cysts in zebrafish and mice, and mutations in PKD2 leads to Autosomal Dominant Polycystic Kidney disease (ADPKD) (Lu et al., 2001; Obara et al., 2006; Piontek et al., 2004; Schottenfeld et al., 2007; Wilson, 2004a; Wilson, 2008). The target of PKD2 Ca^{2+} in the kidney remains to be elucidated. In addition,

Annexin IV, a Ca^{2+}-dependent phospholipid binding protein, has been shown to be important in *Xenopus* pronephros development, where suppression causes an enlarged and shortened pronephric tubule (Seville et al., 2002).

Embryonic development is dependent on Ca^{2+} and Ca^{2+}-dependent proteins to activate intracellular pathways. Alterations in Ca^{2+} signaling can lead to varied conditions such as heterotaxia, ADPKD, and heart failure. Although many model systems have been used to study Ca^{2+} signaling, zebrafish have become an attractive and valuable vertebrate model due to the wide variety of suppression methods and imaging techniques. Identifying the effectors of Ca^{2+} will help scientists to better understand organ placement, find treatments for cystic kidney diseases, and understand the causes of heart disease.

Zebrafish (Brachydanio rerio) as a Model System:

Zebrafish have become a very attractive model system to study genetics and development. Zebrafish mutants mimic human syndromes allowing researchers to delve into the pathogenesis of diseases in hopes of generating viable treatments. Although many model systems are used in research, zebrafish are moving to the forefront due to the similarity in cellular signaling that occurs during embryogenesis.

The use of zebrafish as an experimental organism began in the late 1970s at the University of Oregon, where George Streisinger recognized the strength of this small vertebrate in understanding both development and genetics. Zebrafish are a freshwater fish, indigenous to the rivers and streams in India and can also be found in your local pet store. Due to its short generation time (3 months), external fertilization, large clutches, optical clarity, and rapid development, zebrafish have become a well-established system in biological studies (Kimmel et

al., 1995). Streisinger's lab cloned zebrafish (Streisinger et al., 1981) and developed several techniques to harness the zebrafish's experimental potential including: mutagenesis (Grunwald and Streisinger, 1992a; Grunwald and Streisinger, 1992b; Walker and Streisinger, 1983), genetic mapping (Streisinger et al., 1986), and creation of genetic mosaics (Streisinger et al., 1989).

Sequencing the zebrafish genome began in 2001 at the Sanger Institute in England and is approximately 80% complete as of 2010 (ensembl.org). Zebrafish have 25 chromosomes and are thought to have undergone a genome-wide duplication event approximately 250 million years ago. Overall approximately 20-30% of the duplicated genes were retained in the genome as transcriptionally active genes (Postlethwait et al., 2004).

Zebrafish are a valuable model system because one can take advantage of both forward (ENU treatment) and reverse genetic techniques (viral insertion, TILLING, zinc finger nucleases, and antisense morpholino oligonucleotides). Traditional mutagenesis utilizes ENU treatment of sperm, leading to a point mutation in the genome, and ultimately generating a developmental phenotype (Grunwald and Streisinger, 1992b; Solnica-Krezel et al., 1994). Positional cloning can be used to identify the site of the mutation therefore identifying a potential function for a specific gene (Solnica-Krezel et al., 1994). A second technique involves insertional mutagenesis, where a retroviral provirus is inserted into the genome causing a specific phenotype (Allende et al., 1996). Sequencing is then used to identify the insertion site, therefore identifying the gene responsible for the developmental defects. Targeting induced local lesion in genome (TILLING) is a newer technique that allows the identification of a mutation in a gene of interest (Wienholds et al., 2003). This technique generates mutants of a certain gene as opposed to linking phenotypes to mutation in unknown genes. The newest technique involves the use of zinc finger nucleases specifically designed against a sequence of interest allowing one to generate a

mutation in the gene of interest. (Doyon et al., 2008). The primary reverse genetic technique is the injection of antisense morpholino oligonucleotides (MO's) into the embryo prior to the eight-cell stage. MO's are designed against a gene of interest to either inhibit translation or inhibit proper splicing of exons. (Nasevicius and Ekker, 2000). This technique enables the investigator to suppress the expression of a gene and determine which cellular processes require that gene. The use of forward genetic techniques is well established but does have drawbacks where many mutant alleles are not null but hypomorphic. One can establish a knockdown phenotype using MO's, however "off target" effects can occur. In addition, MO's persist in the embryo for about 3dpf allowing an investigator to look at early developmental defects but not larval or adult phenotypes. Still, the ability of investigators to use both forward and reverse techniques makes this organism a very valuable model for studying vertebrate development.

In addition, zebrafish have become important in understanding the role Ca^{2+} plays during embryogenesis. Techniques have been established to capture and visualize Ca^{2+} waves, through microinjection of photoproteins, Ca^{2+} dyes, and genetically targeted fluorescent indicators (Ebert et al., 2005; Palmer and Tsien, 2006; Shimomura et al., 1990). Although zebrafish are not as complex as humans, many of the same cellular signaling pathways are used during early development. The transparency of the embryo, external development, and cell size allows the study of Ca^{2+} signaling *in vivo* leading to the identification of downstream effectors, such as CaMK-II and PKC. These effectors are the mediators between the Ca^{2+} stimulus and cellular response and may be the key to unlocking the mysteries of human syndromes.

$Ca^{2+/}$Calmodulin-Dependent Protein Kinase Type II: Structure and Function:

$Ca^{2+/}$calmodulin-dependent protein kinase type II (CaMK-II) is the multifunctional serine/threonine protein kinase that is encoded by four genes (α, β, γ, and δ), to generate over forty splice variants in metazoans. CaMK-II hetero-oligomerizes to form dodecamers (twelve monomers) and is activated once Ca^{2+}/calmodulin (CaM) binds causing a conformational change in the protein. The three domains that comprise each monomer include the catalytic, variable, and oligomerization domains. The first 315-amino acids encode the catalytic domain and include the CaM binding site, ATP binding pocket, and autoinhibitory arm (Schulman et al., 1992). The autoinhibitory arm maintains CaMK-II in the basal state and upon Ca^{2+}/CaM binding this subdomain moves away from the catalytic site (Colbran et al., 1989). Alternative splicing within the variable domain generates various splice variants that determine subcellular localization and alterations in CaM binding affinity. The size of the variable domain can range from 30 to 100 amino acids. The oligomerization domain, also known as the association domain, facilitates association into the correct dodecameric configuration (Tombes et al., 2003; Tombes and Krystal, 1997).

CaMK-II is unlike other CaM kinases in that it hetero-oligomerizes and autophosphorylates at Thr^{287} (Thr^{286} in α) to allow for Ca^{2+} independent activity. Autophosphorylation of this residue accomplishes the same task as Ca^{2+}/CaM binding by exposing the catalytic site. P-Thr^{287} CaMK-II remains 20-80% active, generating what is known as Ca^{2+}/CaM-autonomous activity. Only upon dephosphorylation of this residue will CaMK-II become inactive and the conformation shift back to the closed configuration (Rosenberg et al., 2005).

Alternative splicing within the variable domain generates subcellular-targeted CaMK-II that allows for varied access to substrates. Domains II and VII are considered the "linker" domains between the catalytic and association domains and are present in all CaMK-IIs. Domain I increases the binding affinity for CaM, thus creating a more sensitive enzyme as well as influencing the ability of the enzyme to autophosphorylate (Bayer et al., 2002; Brocke et al., 1999). An alternative promoter within domain II of α CaMK-II generates αKAP, a catalytically inactive CaMK-II. A hydrophobic leader sequence targets catalytically active CaMK-IIs to membranes (Bayer et al., 1998). Domain III encodes a nuclear targeting sequence and preferentially targets the holoenzyme to the nucleus (Srinivasan et al., 1994; Tombes et al., 2003). The functions for the proline-rich exons IV and V are unknown at present, however it is noteworthy that the two exons are usually found together and not alone. Domain VI functions to antagonize the nuclear localization sequence, domain III, in γ CaMK-II. Domain VIII/IX can be encoded by a single exon, similar to domain IV/V, and is also proline rich. Domain X codes for SH3 binding domains, targeting the holoenzyme to membranes (Tombes et al., 2003).

Originally identified as a neuronal specific protein, CaMK-II has now been found in virtually every tissue type in mammals, phosphorylating a number of substrates to influence a variety of cellular mechanisms (Tombes et al., 2003). CaMK-II phosphorylates AMPA receptors in the brain generating long-term potentiation. Homozygous mice lacking neural specific α CaMK-II fail to develop long-term potentiation (Silva et al., 1992). Other neuronal substrates include proteins important at the postsynaptic density such as SHANK, SynGAP, and spinophilin (Dosemeci and Jaffe, ; Oh et al., 2004). Fewer nonneuronal substrates of CaMK-II are known. In the heart CaMK-II phosphorylates ryanodine receptors to release Ca^{2+} stores for the ER and phosphorylates phospholamban to promote the reuptake of Ca^{2+} into the ER by the sarco-

endoplasmic reticulum Ca^{2+} ATPase (SERCA) (Maier and Bers, 2002). Hypertrophy and heart failure have been linked to alterations in CaMK-II activity. Other nonneuronal substrates include caldesmon, CREB, EGFR, Vimentin, and HDAC4 (Feinmesser et al., 1999; Little et al., 2007; Stefanovic et al., 2005; Wang and Yang, 2000; Wu and McMurray, 2001).

CaMK-II has also been implicated in many cellular mechanisms, however identifying substrates has remained a challenge (Bayer and Schulman, 2001; Soderling, 2000). The Tombes lab has linked CaMK-II to cell-cycle progression, cell motility, neurite outgrowth, heart morphogenesis, and establishment of left-right asymmetry (Easley et al., 2006; Easley et al., 2008; Faison et al., 2002; Francescatto et al., 2010; Morris et al., 1998; Rothschild et al., 2009; Seward et al., 2008; Tombes et al., 1995). Other functions of CaMK-II include ion channel regulation, transcription, and secretion (Hudmon and Schulman, 2002a; Hudmon and Schulman, 2002b; Schulman et al., 1992).

Suppressing CaMK-II expression in well-established model systems will increase our understanding of most Ca^{2+}-dependent cellular pathways that lead to developmental disorders and adult syndromes in humans. Mouse CaMK-II knockouts are embryonic lethal and therefore cannot be used to study later CaMK-II functions *in vivo*. Zebrafish are an ideal vertebrate organism to study CaMK-II function given the many knockdown techniques, external fertilization, and transparent embryos. The purpose of this dissertation has been to identify all CaMK-II genes in zebrafish and then characterize their roles during zebrafish development.

Chapter 2: Differential Expression of CaMK-II Genes During Early Zebrafish Embryogenesis

ABSTRACT

CaMK-II is a highly conserved Ca^{2+}/calmodulin-dependent protein kinase expressed throughout the lifespan of all vertebrates. During early development, CaMK-II regulates cell cycle progression and "non-canonical" Wnt-dependent convergent extension. In the zebrafish, *Danio rerio*, CaMK-II activity rises within 2 hr after fertilization. At the time of somite formation, zygotic expression from six genes (*camk2a1, camk2b1, camk2b2, camk2g1, camk2g2, camk2d1, camk2d2*) results in a second phase of increased activity. Zebrafish CaMK-II genes are 92-95% identical to each other and to their human counterparts in the non-variable regions. During the first three days of development, alternative splicing in the variable region yields at least 26 splice variants, many of which are unique. Whole-mount *in situ* hybridization reveals that *camk2g1* and *camk2b2* comprise the majority of maternal expression. All seven genes are expressed strongly in ventral regions at the 18-somite stage. Later, *camk2a1KAP* is expressed in anterior somites and heart, while *camk2a1* is expressed primarily in the forebrain. *Camk2b1* is expressed in somites, mid- and forebrain, gut, retina, and pectoral fins. *Camk2b2* expression is high in the brain and pectoral fins and transiently expressed in the heart at 36hpf. *Camk2g1* appears strongly along the midline and then in brain, gut, and pectoral fins. *Camk2g2* is expressed early in the

midbrain and trunk and exhibits the earliest retinal expression. *Camk2d1* is elevated early at somite boundaries, then epidermal tissue, while *camk2d2* is expressed in discrete anterior locations, steadily increasing along either side of the dorsal midline and then throughout the brain, including the retina. Suppression of each gene using antisense morpholino oligonucleotides reflects the aforementioned mRNA expression pattern, yielding defects in somite, eye, fin, heart and anterior-posterior axis development. These findings reveal a complex pattern of CaMK-II gene expression consistent with pleiotropic roles during development.

INTRODUCTION

Although Ca^{2+}/calmodulin-dependent protein kinase type II (CaMK-II) is best known for its role in the central nervous system, CaMK-II has now been identified in every tissue throughout the life cycle. Interestingly, CaMK-II comprises 1% of all protein in the hippocampus in mice, demonstrating the importance of this protein in synaptic plasticity and long-term potentiation (Burgin et al., 1990; Mayford et al., 1996). However, CaMK-II is also important in gametogenesis, and at fertilization where it promotes meiotic resumption in frog and mouse oocytes (Johnson et al., 1998; Lorca et al., 1993; Winston and Maro, 1995). During development, CaMK-II is activated by members of the "non-canonical" Wnt family of glycoproteins, such as Wnt5, to promote cell movement during gastrulation (Kuhl et al., 2001; Sheldahl et al., 2003).

CaMK-II variability is primarily achieved through alternative exon usage in the central variable domain, yielding over 40 splice variants from the four CaMK-II genes (Hudmon and Schulman, 2002b; Tombes et al., 2003). Some of these variants are specifically targeted to the nucleus, the plasma membrane, the actin cytoskeleton, and post-synaptic densities (Caran et al., 2001; Heist and Schulman, 1998; Shen and Meyer, 1999; Srinivasan et al., 1994; Takeuchi et al., 2000; Urquidi and Ashcroft, 1995). Differential expression of CaMK-II genes occurs throughout the adult vertebrate body (Tobimatsu and Fujisawa, 1989), during embryogenesis, and are most commonly expressed in the developing central nervous system (Bayer et al., 1999) and in the developing cardiac system (Baltas et al., 1995; Edman and Schulman, 1994; Hagemann et al., 2001; Hoch et al., 2000; Singer et al., 1997). β CaMK-II is required for mouse embryonic

development (Karls et al., 1992), but α CaMK-II is not expressed until after birth (Brocke et al., 1995).

CaMK-II is unique from other CaM-dependent proteins because it is able to distinguish Ca^{2+} signals by frequency and amplitude through oligomerization and autophosphorylation, allowing the enzyme to remain active in the absence of Ca^{2+}/CaM (Tombes et al., 2003). In addition all subunits do not need to be activated by CaM for the enzyme to phosphorylate substrates and influence cellular mechanisms. These properties, along with subcellular targeting, identify CaMK-II as a key protein in translating Ca^{2+} stimuli into diverse cellular responses.

Although many studies have identified functions for CaMK-II, developmental studies have been challenging since many CaMK-II mouse knockouts are embryonic lethal. Zebrafish are a valuable system to study *in vivo* protein suppression due to their external fertilization, rapid development, and the varied knockdown methods for suppressing the expression of specific genes. In fact, zebrafish rely on diffusion for oxygen during the first five days of development, allowing the embryo to remain alive in the absence of blood flow (Yelon, 2001). This makes zebrafish an attractive model system to study the developmental role of CaMK-II *in vivo*.

Although, δ CaMK-II had been identified in a previous study (Strausberg et al., 2002), a total of seven zebrafish CaMK-II genes and eight open reading frames (ORFs) have now been identified in this project as transcriptionaly active during the first 3 days of development. KN-93, a calmodulin binding antagonist (Tombes et al., 1995), was used to suppress zebrafish CaMK-II activity and determine potential functions of CaMK-II. In addition, translation blocking antisense morpholino oligonucleotides were designed against the eight ORFs to determine the requirement for each during development. Each MO caused unique defects that demonstrate the requirement for CaMK-II in axis patterning, organogenesis, and left-right patterning. These are the first

studies to comprehensively evaluate all CaMK-IIs during development and demonstrate the importance of this signaling molecule in the development of vertebrate embryos. The findings in this chapter set the stage for all subsequent studies.

MATERIALS AND METHODS

Zebrafish care and maintenance

Wild type fish were obtained from the Zebrafish International Resource Center and maintained at 28.5ºC. Embryos were obtained through natural crosses, raised at 28.5ºC and staged as previously described (Kimmel et al., 1995).

Whole cell lysate preparation

Embryos were dechorionated and then lysed in 30 mM HEPES, pH 7.4, 20 mM $MgCl_2$, 80 mM β-glycerol phosphate, 5 mM EGTA, 0.1 μM okadaic acid (Life Technologies Invitrogen, Carlsbad, CA), 0.01 mg/ml each chymostatin, leupeptin, aprotinin, pepstatin, and soybean trypsin inhibitor (Sigma Chemical Co.), sonicated for 5 sec on ice, and centrifuged at 12,000xg for 15min at 4ºC. This buffer has been optimized for maximal recovery into this supernatant (Tombes et al., 1999; Tombes and Peppers, 1995). Protein concentrations were determined using the BCA assay (Pierce Chemicals).

CaMK-II activity assay

Total CaMK-II activity was assessed by measuring phosphate incorporation into autocamtide-2, a peptide modeled after the autophosphorylation site of CaMK-II (KKALRRQETVDAL). Reactions were carried out on 1-2μg protein from cell lysates in a total volume of 25μl containing final concentrations of 20 mM HEPES (pH 7.4), 0.1 mM dithiothreitol, 15 mM magnesium acetate, 20 mM β-glycerophosphate, 10 mM NaF, 0.5 μM

PKA inhibitor peptide, 0.1 μM okadaic acid, 10 μM [γ-^{32}P]-ATP (0.5 mCi per assay), 35 μM autocamtide-2, and either 1 mM EGTA (-Ca^{2+}) or 1 μM bovine calmodulin plus 2.0 mM $CaCl_2$ (+Ca^{2+}). After 10 min at 32ºC, 20 μl was pipetted onto P81 phosphocellulose paper squares (Whatman) that were air dried for 1 min and washed five times in 500 ml 1% phosphoric acid. Dried paper squares were quantitated by Cerenkhov counting in the absence of scintillation fluid. These assay conditions were optimized for compatibility with the buffer in which cell lysates were prepared (Tombes et al., 1999; Tombes and Peppers, 1995). Activity detected by AIP, the autoinhibitory peptide (Biomol) whose sequence is KKALRRQEAVDAL, was measured. Using partially purified CaMK-II from 6-day zebrafish embryos, we determined that this peptide could half maximally inhibit at 10 μM and was 90% effective at 25 μM, which are values very similar to that seen with partially purified mouse CaMK-II (Tombes and Peppers, 1995).

Genomic identification

Sequences were obtained by searching GenBank and Sanger Institute genomic databases using a BLAST (Basic Local Align Search Tool) search for zebrafish CaMK-II homologs. Seven CaMK-II genes were identified and are listed with accession number and GenInfo sequnce identification numbers (gi). They include camk2a1 (chromosome 21, NM_001017741, g1: 82524730); camk2b1 (chromosome 5, XM_685461, gi: 68437880); camk2b2 (chromosome 10, NM_, camk2g1 (chromosome 12, BC096785, gi: 66911241); camk2g2 (chromosome 13, XM_689010, gi: 68437880); camk2d1 (chromosome 7, BC077143, gi: 50417146) and camk2d2 (chromosome 1, NM_001002542, gi: 50540149).

RT-PCR and sequencing

Total RNA was prepared from dechorionated embryos at 1hpf, 24hpf, and 72hpf and cDNA was prepared as described (Lister et al., 2001). PCR primers, which bracketed the variable region, include three sense primers (TGGATCTGCCAACGCTCCACTGTGGC, TGGATATCACATCGCTCCACCGTCGC, TGGAGTCATCCTCTACATCCTGCTGG), which encode WICQRSTVA, WISHRSTV, and GVILVILL respectively, and three antisense primers (CCTCATGTGCACCTGATTGGAGA, CACAGTTTGTGGATGGCCAGGGCC, GTACCGAGCAGCTGATTGAAGCC), which encode PHVHLIGE, QFVDGQG, and VTEQLIEA. These primers were used in various combinations in order to achieve the greatest coverage of all potential CaMK-II sequences. CaMK-II PCR products were cloned into the TOPO/TA vector (Invitrogen) and clones were screened by PCR, purified, and then sequenced. Over 100 clones were screened in this fashion.

Whole mount in situ hybridization

Digoxigenin-labeled anti-sense riboprobes (0.5-1.5kb) were synthesized using T3 or T7 RNA polymerase (orientation dependent) from TOPO/TA vector-based cDNAs and then incubated with fixed, staged embryos as described (Dutton et al., 2001). Individual probes derived from cDNAs encoding the splice variants, αKAP, $\beta1_e$, $\beta2_G$, $\gamma1_G$, $\gamma2_L$, $\delta1_G$, and $\delta2_E$ were used to localize all transcripts from each gene. The αKAP probe was synthesized from a purchased clone (Open Biosystems) whereas other probes were synthesized from TOPO/TA clones. Anti-digoxigenin and alkaline phosphatase conjugated secondary antibodies were used and developed with NBT/BCIP as substrate. Sense probes showed no signal. In some cases,

stained embryos were embedded in NEG-50 frozen sectioning medium (Richard-Allan Scientific), frozen to -20ºC and 30µm sections obtained using an HM-550 cryostat (Richard-Allan Scientific). Sections were rehydrated in 50% glycerol and photographed with a Nikon Cool-Pix 990 color camera on an Olympus IX-70 phase contrast microscope. Whole-mount specimens were photographed with an Olympus DP70 digital camera on an Olympus SZX12 stereo microscope.

Immunolocalization

Wild-type and KN-93 treated embryos were fixed in 4% PFA for four hours at room temperature and then washed several times with 1XPBT. Embryos were blocked in 10% goat serum in 1x PBT for one hour at room temperature and then incubated in a 1:1000 dilution of mouse anti-acetylated alpha tubulin (Sigma) overnight at room temperature in block. Embryos were incubated with goat-anti-mouse Alexa-568 (Molecular Probes) for four hours at room temperature and imaged on a LSM 510 laser scanning confocal microscope (Zeiss) .

KN-93 Treatment

20-30 embryos were incubated continuously in 10 µM KN-93 in 3mls of system water from cleavage stages in 6 well dishes.

Morpholino Oligonucleotide Injections

Morpholino antisense oligonucleotides (MO's) were designed to disrupt translation by complementary base pairing to the predicted or known translational start sites of full length zebrafish or mammalian CaMK-II cDNAs. MO's were purchased from Gene Tools (Philomath

OR) and are shown for each gene in the 5'-3' direction with the sequence corresponding to the start codon underlined and mRNA nucleotide positions indicated.

camk2a1: GCCATCCTGGAAGCGTGTGCGCCTC-3'; nts -20 to +5,

camk2a1KAP: GGCATAGCGGTGGTCTGCTCTCCAC; nts -20 to +5,

camk2b1: GGCCATGTCTTCCCGTCTCGGACTC; nts -19 to +6,

camk2b2: GCGTGCAGGTTGTGGTTGCCATGTC; nts -3 to +19),

camk2g1: AATTGTAGCCATGTTGTGTGTGCGT; nts -13 to +12),

camk2g2: AATTGTAGCCATGTTGCGCTTTACG; nts -13 to +12),

camk2d1: CAGGTTGTTGAAGCCATGCTGAAAG; nts -8 to +17),

camk2d2: CAGATGGTCAGAGCCATTGTGATG; nts -7 to +17).

Mismatch: CAATGCTCACAGCGATTGTCATG

Morpholino stocks (1mM) were stored in aliquots at -80°C. Prior to injection, aliquots were heated to 65°C for 5 min, cooled to room temperature and then diluted in Danieau buffer (Westerfield, 1993). The dose-dependent effectiveness of each MO at suppressing CaMK-II expression was assessed by CaMK-II peptide assay, as described (Rothschild et al., 2007).

RESULTS

CaMK-II Activity Increases in Two Phases During Early Development

CaMK-II activity can be measured using a well-established CaMK-II specific assay, where the incorporation of radioactive ^{32}P into a synthetic peptide, autocamtide-2, is measured. The autocamtide-2 peptide is modeled after the autophosphorylation site of CaMK-II, KKALRRQETVDAL. Whole embryo lysates were prepared from various time points during the first three days of zebrafish development and a biphasic activity pattern was identified. At all stages, activity was Ca^{2+}/calmodulin dependent and could be inhibited by 20 μM AIP, a peptide that mimics the autoinhibitory domain found in all CaMK-IIs and that has previously been used to inhibit sea urchin CaMK-II (Baitinger et al., 1990). No activity was detected at the 1 cell stage, which was surprising given the evidence for CaMK-II in early meiotic events in other model systems. Activity began increasing immediately after the 1-2 cell stage coincident with known Ca^{2+} elevations in the early embryo (Jaffe, 1995). CaMK-II activity levels remained stable from 4-12hpf, but then increased again at 24hpf, about five-fold (Figure 2.1). At 24hpf the zebrafish embryo heart begins beating, the notochord vacuoles inflate, and the embryo is able to respond to touch stimulus, demonstrating the increase in complexity of the embryo and the need for greater concentrations of the multifunctional CaMK-II. At 3dpf total CaMK-II activity continues to increase, approximately 100-fold compared to the 1-cell embryo, and continues rising until 6dpf where activity levels off. At 6dpf the zebrafish is in the larval stage of development and can free swim, feed, and respond to external stimuli. The specific activity of 6-day embryos is comparable with that found in mouse embryonic cells (Tombes et al., 1995).

Identification of Zebrafish CaMK-II Genes

The identification of zebrafish CaMK-II genes was determined using best fit BLAST searches using known mammalian sequences (Tombes et al., 2003). There are four known CaMK-II genes in mammals and birds, and a single gene in *Drosophila* and *C. elegans*, however due to a genome wide duplication event in the teleost lineage (Postlethwait et al., 2004) there are seven catalytically active CaMK-II genes and one catalytically inactive, membrane targeting gene. The seven genes are shown with their predicted and aligned protein sequences (Figure 2.2). Alternative sequences from the variable domain are omitted from this alignment as previously described (Tombes et al., 2003). Based on gene-specific residues and sequence similarity we concluded that there is one α gene (*camk2a1*), two β genes (*camk2b1* and camk2b2), two γ genes (*camk2g1* and *camk2g2*), and two δ genes (*camk2d1* and *camk2d2*). An alternative promoter within *camk2a1* generates αKAP, a catalytically inactive CaMK-II that oligomerizes with active CaMK-II to target the holoenzyme to the membrane via a hydrophobic N-terminal sequence (Bayer et al., 1998). Pairwise identity of amino acid sequences within all seven genes ranged from 80-96% and from 90-96% when compared to the corresponding human CaMK-II.

Identification of CaMK-II Splice Variants in Zebrafish

The presence of alternative splice variants in each CaMK-II gene was evaluated using RT-PCR (Tombes and Krystal, 1997). Redundant and gene-specific primers that flank the variable region were used to amplify oligo dT-primed or random hexamer-primed cDNA synthesized from RNA isolated from zebrafish embryos between 1 and 72hpf. PCR products were cloned and screened by sequence.

All eight CaMK-II ORFs expressed at least one mRNA during the first three days of development demonstrating their transcriptional activity. Twenty-six different splice variants from these seven genes were identified (Figure 2.3a). According to zebrafish genome conventions and those previously established for this gene family, each splice variant is identified by a Greek letter and number referring to the paralog followed by a letter subscript. The predicted amino acid sequence of each of these variants predicts alternative exon usage as previously described for human sequences (Tombes et al., 2003). All CaMK-II genes contain linker domains II and VII within the variable region and may encode for alternative domains I, III, IV, V, VI and VIII/IX.

Between one and eight variants were found from each gene. Eleven of the twenty-six variants are novel. Six variants contain domain I, which is thought to influence CaM binding affinity (Bayer et al., 2002; Brocke et al., 1999). Six of the variants contain domain III, a putative nuclear targeting domain. The functions of domains IV and V are not known while domain VI is thought to interfere with nuclear localization in γ CaMK-II. Four variants contain domain VIII/IX, which may influence cell-surface binding. The twenty-six variants fall into 13 categories of alternative exon utilization (Figure 2.3b). Category 4 encodes domains II, VI, VII and was the most common combination with 4 variants represented. We identified several maternal transcripts including α, $\beta 1_K$, $\gamma 1_C$, $\gamma 2_L$, $\gamma 2_O$, and $\gamma 2_P$. $\gamma 1_C$ had the highest contribution of maternal CaMK-II. Interestingly even though several CaMK-II splice variants are present as mRNA in the early cleavage embryo, it appears that the corresponding proteins may not be translated, as indicated by low embryonic activity. The predicted full-length, molecular weight of all 26 CaMK-II variants is between 54 and 60 kDa.

Embryonic Localization of CaMK-IIs During Early Development

In situ hybridizations were performed to identify the timing and tissue localization for each of the seven genes. Zebrafish embryos were fixed and stained at various developmental stages up to 3dpf. Expression at the 8-cell (1hpf) and 512-cell stage (2.5hpf) reflects maternal mRNA expression since zygotic expression does not commence until after the mid-blastula transition, which occurs at approximately high stage (3.5hpf). Somite stage embryos were evaluated at the 3-somite (11hpf) and 18-somite stage (18hpf). Each gene revealed unique spatial and temporal expression as summarized in Table 2.1. The majority of the CaMK-II expression occurred once zygotic expression commenced, as demonstrated by the activity assays (Figure 2.1).

α1 (*camk2a1*) transcripts are expressed maternally and then appear to be expressed in lower levels diffusely through the early embryo but then absent at dome and shield stages. At the 3-somite and 18-somite stages *camk2a1* is expressed ubiquitously until 48hpf where expression is confined to the forebrain region, heart, and somites. Heart and somite expression has been identified as *α1KAP* and not catalytically active *camk2a1* through RT-PCR and a *camk2a1* specific antisense riboprobe. At 72hpf *camk2a1* expression remains in the forebrain region and α1KAP expression persists in the heart and somites (Figure 2.4). Only one *camk2a1* and one a1KAP splice variant were cloned and both encode for the simplest splice variant, containing exons II and VII.

β1 (*camk2b1*) mRNA was detected maternally at the 8-cell and 512-cell stage and then persisted at low levels through the 3-somite stage. At 18 somites, the expression increases and is identifiable in ventral regions of the embryo and brain. Expression persists ventrally and in the somites at 24hpf and becomes more discrete in the brain and heart at 48hpf. By 72hpf,

expression was strong in mid- and forebrain regions and lightly in the gut, retina, trunk, and pectoral fins (Figure 2.5). Two of the three β1 splice variants contain a putative nuclear targeting sequence. Further analysis of manually dissected hearts at 48hpf identified the $\beta1_K$ variant as the predominant heart CaMK-II.

β2 (*camk2b2*) mRNA was identified at high levels at the 8 and 512 cell-stage identifying it as a maternally expressed gene. Expression persists through somitogenesis and is found in the somites at 24hpf. At 36hpf *camk2b2* mRNA is transiently expressed in the heart. Expression is also identifiable in the brain, pectoral fins, and somites. By 72hpf expression diminishes and β2 mRNA is detected weakly in the forebrain (Figure 2.6). This gene encodes four splice variants during the first three days of development, with one variant containing domain I.

The strongest maternal expression detected during early cleavage stages and gastrulation was encoded by γ1 (*camk2g1*) (Figure 2.7). Expression at the 512-cell stage identifies *camk2g1* in both the yolk syncitial layer and the entire blastocyst. At the 18-somite stage expression is evident in the somites, brain, and kidney. By 24hpf, expression is very strong in the ventral somites, spinal cord cell bodies, and brain. mRNA is evident in the hindbrain, fins, otic placode, ventral organs, and somites at 48 and 72hpf. Of the four *camk2g1* variants identified, one contains a putative nuclear localization sequence, whereas one contains domain I, and one contains the putative membrane targeting domains VIII/IX.

γ2 (*camk2g2*) expression was found early in cleavage stage embryos and is expressed ubiquitously throughout the embryo until the 18-somite stage, where expression is localized ventrally and in the brain. Expression becomes more discrete in the brain at 48hpf and 72hpf where γ2 is found strongly in the entire brain and lightly in the retina and pectoral fins (Figure

2.8). This gene encodes 8 splice variants during the first three days of development, which is the greatest number of variants encoded by any of the eight ORFs, with 3 maternal variants.

δ1 (*camk2d1*) expression was not evident during early cleavage stage embryos and was first visible at 18-somite stage in the somites (Figure 2.9). This result is consistent with results from RT-PCR where no transcripts were identified during early development. At 24hpf δ1 expression appears low in the brain but much higher in the hatching gland. At 48hpf mRNA expression decreased with light expression in the brain, which persisted through 72hpf. The two δ1 splice variants identified were simple cytosolic variants, utilizing few alternative exons.

δ2 mRNA expression (*camk2d2*) was undetectable until the 18-somite stage. At 24hpf expression is identified in the brain, specifically forebrain and hindbrain regions. This expression persists through 72hpf where strong expression is apparent in the brain and retina (Figure 2.10). Three non-nuclear variants were identified with one variant containing the putative membrane targeting domains, VIII/IX.

Frozen thin sections were also used to identify CaMK-II expression in the central nervous system of β1, γ1, γ2, and δ2 at 72hpf. Locations at cross-sections are identified (A-F) in Figures 2.4- 2.9. All four genes were expressed in the retinal epithelia with δ2 and γ1 expressed in ganglion cell and amacrine layers. β1 and γ1 were intensely co-expressed in a cortical rim in the midbrain, whereas δ2 was expressed in a thin intense layer in the hindbrain. In addition, γ1 was expressed in the otic placode, while δ2 was expressed in more dorsal region of the hindbrain (Figure 2.11).

KN-93, a CaMK-II Inhibitor, Causes Developmental Defects in Zebrafish Embryos

KN-93, a calmodulin binding antagonist, maintains CaMK-II in the basal state, even in the presence of CaM (Tombes et al., 1995). Treatment with KN-93 causes cell cycle arrest and apoptosis in cell culture (Tombes et al., 1995), inhibits sperm flagellar motility in coral (Morita et al., 2009) and ascidians (Nomura et al., 2004), and has been shown to block meiotic progression in mouse oocytes (Madgwick et al., 2005). Treatment with an inactive analog, KN-92, has no affect on CaMK-II activation or cell behavior (Tombes et al., 1995). Zebrafish embryos were treated with increasing concentrations of KN-93 beginning at cleavage stages and imaged at 3dpf (Figure 2.12a). Blood pooling, upward tail curvature, shortened pectoral fins, reduced circulation, and failure to hatch from the chorion are evident by 3dpf. CaMK-II activity decreases with a half-maximal inhibitory concentration of 4μM (Figure 2.12b). In addition, KN-93 treatment caused a disorganization of axonal projections from spinal cord cell bodies as demonstrated by confocal z-stack renderings of embryos immunolabeled with an anti-acetylated α-tubulin antibody (Figure 2.13a,b).

Morphant Phenotypes Mirror CaMK-II mRNA Expression Patterns

Gene-specific translation blocking morpholino oligonucleotides were designed against each of the seven catalytically active CaMK-IIs and αKAP (Table 2.2). These eight MO's were titrated to determine the minimum concentration required to yield a reproducible phenotype (Figure 2.13). Morphants were imaged at 48hpf and assessed for gross morphological defects at 3dpf (Figure 2.13 and Table 2.3).

Suppression of each CaMK-II gene generated mostly unique and some overlapping phenotypes. *Camk2b2* and *camk2g1* mRNAs are expressed at high levels compared to the other CaMK-II genes prior to the MBT and throughout development. Suppression of these two genes

caused a myriad of defects including embryonic lethality. 1.25 ng of *camk2g1* morpholino caused convergent extension defects, alteration in the establishment of left-right asymmetry, somite compression, atrial enlargement, hydrocephaly, pericardial edema, cloacal occlusions, pronephric cysts, and coloboma. *Camk2g1* morphants did not live past 3dpf. *Camk2b2* knockdowns using 2pg of morpholino also suppressed the establishment of left-right asymmetry and caused the development of hydrocephaly. However suppression of *camk2b2* also induced heart looping defects, bradycardia, decreased circulation, somite defects, and diminished pectoral fin development. These defects match the expression of *camk2b2* in the heart at 36hpf, when the heart begins to undergo looping, and *camk2g1* at the shield when convergence and extension occurs. Therefore the time and location of expression of each gene is consistent with the phenotypes.

Higher concentrations of *camk2a, camk2b1, camk2g2, camk2d1,* and *camk2d2* morpholinos were necessary to observe knockdown phenotypes. This was not because of lower Tm or GC content. Suppression of *camk2b1* caused mild convergent extension and notochord defects, suppression of *camk2g2* caused hydrocephaly, *camk2d1* and *camk2d2* knockdowns only caused mild brain necrosis. Although these CaMK-II genes are expressed throughout embryonic development, each gene has a specific function. Some of these functions may overlap which could explain the lack of phenotype in *camk2g2* morphants when there are so many splice variants (8) expressed throughout the embryo. In addition, CaMK-II is known to function in the CNS and therefore knockdown of zebrafish CaMK-II genes may cause brain defects that cannot be defined simply by looking at gross morphology. The suppression of all seven catalytically active CaMK-II genes does cause a reduction in overall CaMK-II activity. However suppression of *camk2b2* and *camk2g1* caused the largest reduction (Figure 2.14).

DISCUSSION

In this study, CaMK-II expression was comprehensively monitored from fertilization through early development in the zebrafish. Our findings are consistent with other studies, which have implicated CaMK-II during events around the time of gastrulation and then in the developing circulatory and central nervous systems. This study also raises possibilities for the involvement of specific CaMK-IIs in the formation of the anteroposterior axis, somites, retinal epithelia, gut, and other tissues. The numerous CaMK-II variants encoded during this time period in a spatially and temporally regulated manner support complex transcriptional and post-transcriptional gene regulation and imply multiple roles for members of this protein kinase family.

Like other genes in teleost fish, CaMK-II genes have been duplicated. At least three quarters of the duplicated CaMK-II genes have been retained and are transcriptionally active. In contrast, only 20-30% of all duplicated zebrafish genes are retained (Postlethwait et al., 2004). The seven CaMK-II genes encode between one (α1) and eight (γ2) splice variants. By both RT-PCR and in situ hybridization, several of these genes are expressed maternally, including mRNAs from the α1, β1, β2, γ1 and γ2 CaMK-II genes. Maternal CaMK-IIs are not just the simple variants, but utilize alternative domains implicated in CaM binding or in targeting to the nucleus or membrane.

Surprisingly, no CaMK-II enzymatic activity was detected at fertilization, in contrast to the significant activity found in other species (Baitinger et al., 1990; Johnson et al., 1998;

Stevens et al., 1999; Winston and Maro, 1995). This is surprising since zebrafish eggs are fertilized at metaphase II (Becker and Hart, 1996), where CaMK-II has been implicated in enabling the release from meiosis II arrest (Johnson et al., 1998; Lorca et al., 1993; Winston and Maro, 1995). Within the first two hours of development, however, active CaMK-II is detected at the time when developmentally important Ca^{2+} transients are known to occur (Creton, 2004; Creton et al., 1998; Gilland et al., 1999). Activity assays and in situ localization support complex CaMK-II expression patterns as a result of maternal mRNA and zygotic gene expression.

At least six of the seven zebrafish CaMK-II genes are expressed in the developing nervous system, supporting the importance of this gene family in central nervous system development (Hudmon and Schulman, 2002b). In the mouse, the CaMK-II gene is expressed exclusively postnatally in the hippocampus and frontal cortex (Bayer et al., 1999; Burgin et al., 1990). Only one α CaMK-II gene has been uncovered so far in the zebrafish, so it is possible that another α CaMK-II gene may be expressed in the adult zebrafish brain. For this reason, we have numbered each zebrafish CaMK-II gene with a numerical postscript even though, in the case of α1, only one paralog has so far been identified from either the searches of zebrafish genome databases or from splice variant sequences.

Manually dissected 36 and 48hpf hearts expressed *a1KAP, camk2b1* and *camk2b2*, with the *camk2b1* variant containing a putative nuclear localization sequence and *camk2b2* a cytosolic variant. A non-catalytic splice variant of the gene, αKAP, has been found in mammalian cardiac muscle (Singh et al., 2005; Sugai et al., 1996), where it oligomerizes with and targets active β CaMK-II to membranes, such as the sarcoplasmic reticulum (Sugai et al., 1996; Takeuchi and Fujisawa, 1997). In situ locations reflect this non-catalytic variant; where it could hetero-oligomerize with *camk2b2* to influence excitation-contraction coupling.

Multiphasic expression was most apparent with β1 and γ1 CaMK-II, as described above and summarized in Table I. β1 was expressed within the first day in all somites, was lost along the trunk at 48hpf, but re-appeared strongly in the brain, gut, retina, and pectoral fins at 72hpf. γ1 mRNA was prevalent in cleavage-stage embryos and then along either side of the midline at 24hpf, was significantly decreased at 48hpf, and then reappeared in brain, gut, and pectoral fins. These patterns of expression suggest that these two CaMK-II genes are controlled by one set of transcriptional regulatory influences at 24hpf and another set at 72hpf. The additional influences of mechanisms that control alternative splicing during development is not known for CaMK-II genes, but could be initially assessed by quantitative analysis of the relative levels of each splice variant through development and/or detailed analysis of cis-regulatory elements.

Retinal expression of CaMK-II has previously been reported in the synaptic and pigment epithelial layers (Bronstein et al., 1988), but these and other studies have primarily implicated α CaMK-II (Laabich et al., 2000; Liu and Cooper, 1996). Our studies indicate that four CaMK-II genes are expressed in the retina; the only CaMK-IIs not expressed in the developing retina are encoded from the α1 and the δ1 genes. Among the retinal layers, our results indicate that each of the four CaMK-II genes encodes its own unique pattern of retinal expression.

Zebrafish CaMK-II localization is consistent with its involvement in non-canonical Wnt pathways (Kuhl et al., 2000a; Kuhl et al., 2000b; Sheldahl et al., 2003). Non-canonical Wnts induce convergent extension movements during and after gastrulation (Tada et al., 2002). In zebrafish, defects in convergent extension movements are observed with the Wnt5 pipetail mutant (*ppt*) (Kilian et al., 2003) and its receptor, frizzled 2 (Sumanas et al., 2001). Pharmacological disruption of Ca^{2+} dynamics during the discrete developmental window (6-8hpf) associated with gastrulation also leads to defects in axis formation (Creton, 2004). Wnt5

has been implicated in the specification of myoblasts (Anakwe et al., 2003) and retinal cells (Yu et al., 2004) and activates CaMK-II (Kuhl et al., 2000a). Wnts 4, 5a, and 11 also influence the midline assembly of organ precursors, including liver, gut, pancreas, and heart, all of which require mesoderm migration (Kim et al., 2005; Pandur et al., 2002). The reported elevation of CaMK-II activity on the ventral side of the embryo (Kuhl et al., 2000a) is consistent with our observation that five of the seven zebrafish genes express ventrally at early stages of development. In general, the co-incidence of CaMK-II expression with members of the Wnt family supports the possibility that CaMK-II diversity reflects variations in its responsiveness to members of the Wnt family.

Convergent extension is typically accomplished through either directed migration, cell shape changes, or cell rearrangements (Wallingford et al., 2001; Wallingford et al., 2002). These post-transcriptional mechanisms are likely the result of alterations in the cytoskeleton through discrete targets. Transient Ca^{2+} elevations have been proposed to promote focal complex disassembly and detachment from the extracellular matrix at the periphery of motile cells (Conklin et al., 2005; Marks and Maxfield, 1990). CaMK-II has been implicated in cell motility in mammalian cells (Lundberg et al., 1998; Pfleiderer et al., 2004) and CaMK-II has been detected in extracts of isolated pseudopods by mass spectrometry (Lin et al., 2004). A role for CaMK-II in convergent extension is, therefore, likely through its direct action on the cytoskeleton. In support of this, of the five maternal CaMK-II transcripts detected during early development, four are extranuclear.

Why are there so many CaMK-II splice variants expressed during embryogenesis? One fourth of the zebrafish embryo CaMK-IIs identified in this study have nuclear targeting sequences. Nuclear targeted CaMK-IIs are known to act directly on transcription factors, such as

CREB (Matthews et al., 1994; Ramirez et al., 1997; Shimomura et al., 1996; Sun et al., 1996). Other CaMK-IIs that we have identified have variable spacers, which may enable them to respond differently to exposure to Ca^{2+} and CaM. Others have newly discovered domains, which may enable them to interact with binding partners, substrates, or organelles in a manner that supports their specific functions. This study has laid the groundwork for assessing the role of specific CaMK-IIs in discrete developmental functions.

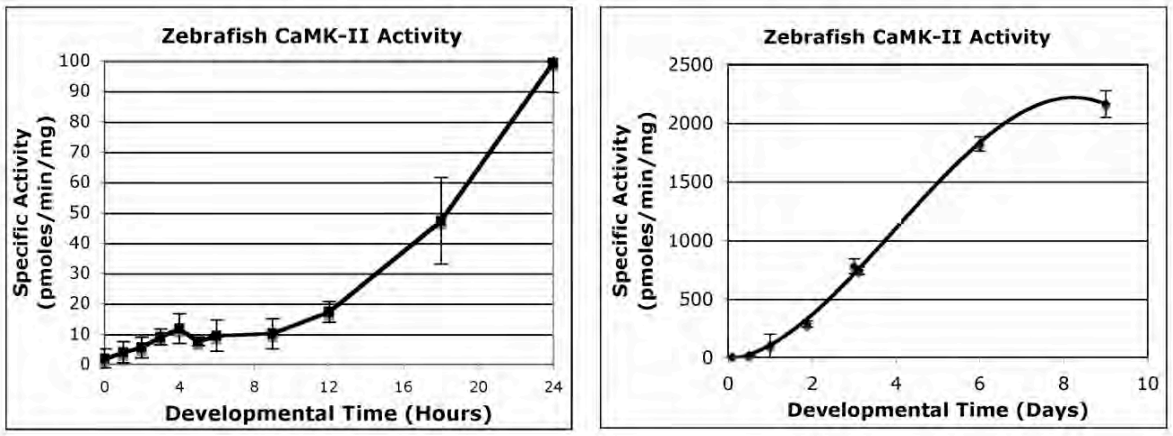

Figure 2.1. Developmental kinetics of CaMK-II enzymatic activity. Ca^{2+}-dependent CaMK-II-specific activity was measured in whole embryo lysates using the autocamtide-2 peptide-based assay and plotted during the first 24 hr (left) and the first 10 days (right). Values shown here were completely dependent on Ca^{2+}/CaM and were also sensitive to 20μM AIP, a CaMK-II specific autoinhibitory peptide.

Figure 2.2. Zebrafish CaMK-II genes. Seven zebrafish CaMK-II genes are shown as their predicted amino acid sequence lacking alternative variable domains. The catalytic domain comprises the first 315 and the oligomerization domain the last 135 amino acids. The variable region extends from amino acids 317 to 345 and corresponds to exons encoding conserved linker domains II and VII (Tombes et al., 2003).

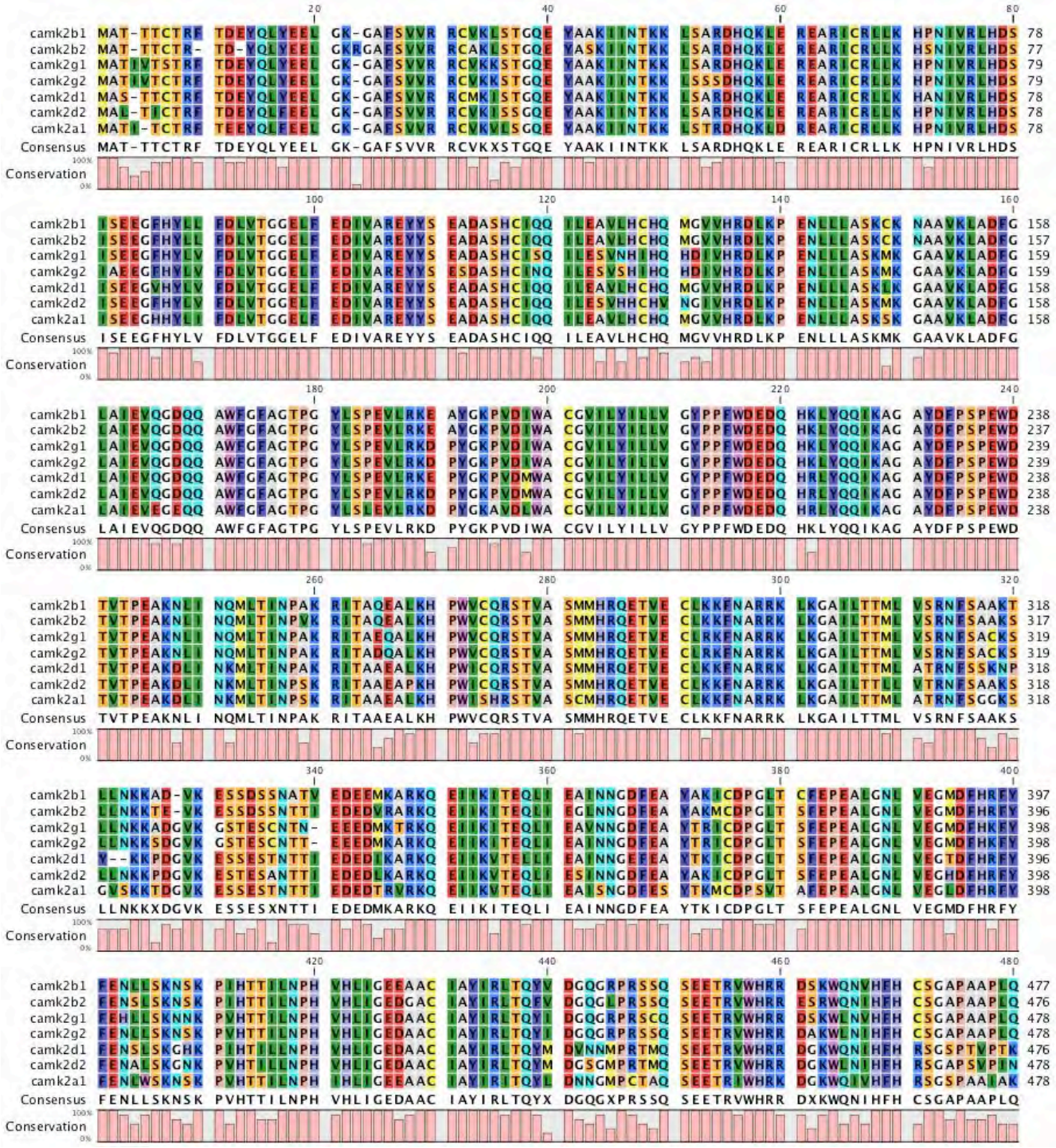
camk2b1 MAT-TTCTRF TDEYQLYEEL GK-GAFSVVR RCVKLSTGQE YAAKIINTKK LSARDHQKLE REARICRLLK HPNIVRLHDS 78
camk2b2 MAT-TTCTR- TD-YQLYEEL GKRGAFSVVR RCAKLSTGQE YASKIINTKK LSARDHQKLE REARICRLLK HSNIVRLHDS 77
camk2g1 MATIVTSTRF TDEYQLYEEL GK-GAFSVVR RCVKKSTGQE YAAKIINTKK LSARDHQKLE REARICRLLK HPNIVRLHDS 79
camk2g2 MATIVTCTRF TDEYQLYEEL GK-GAFSVVR RCVKKSTGQE YAAKIINTKK LSSSDHQKLE REARICRLLK HPNIVRLHDS 79
camk2d1 MAS-TTCTRF TDEYQLYEEL GK-GAFSVVR RCMKISTGQE YAAKIINTKK LSARDHQKLE REARICRLLK HANIVRLHDS 78
camk2d2 MAL-TTCTRF TDEYQLFEEL GK-GAFSVVR RCVKISSGQE YAAKIINTKK LSARDHQKLE REARICRLLK HPNIVRLHDS 78
camk2a1 MATI-TCTRF TEEYQLFEEL GK-GAFSVVR RCVKVLSGQE YAAKIINTKK LSTRDHQKLD REARICRLLK HPNIVRLHDS 78
Consensus MAT-TTCTRF TDEYQLYEEL GK-GAFSVVR RCVKXSTGQE YAAKIINTKK LSARDHQKLE REARICRLLK HPNIVRLHDS
Conservation
camk2b1 ISEEGFHYLV FDLVTGGELF EDIVAREYYS EADASHCIQQ ILEAVLHCHQ MGVVHRDLKP ENLLLASKCK NAAVKLADFG 158
camk2b2 ISEEGFHYLL FDLVTGGELF EDIVAREYYS EADASHCIQQ ILEAVLHCHQ MGVVHRDLKP ENLLLASKCK NAAVKLADFG 157
camk2g1 ISEEGFHYLV FDLVTGGELF EDIVAREYYS EADASHCISQ ILESVNHIHQ HDIVHRDLKP ENLLLASKMK GAAVKLADFG 159
camk2g2 IAEEGFHYLV FDLVTGGELF EDIVAREYYS ESDASHCINQ ILESVSHIHQ HDIVHRDLKP ENLLLASKMK GAAVKLADFG 159
camk2d1 ISEEGVHYLV FDLVTGGELF EDIVAREYYS EADASHCIQQ ILEAVLHCHQ MGVVHRDLKP ENLLLASKLK GAAVKLADFG 158
camk2d2 ISEEGFHYLV FDLVTGGELF EDIVAREYYS EADASHCIQQ ILESVHHCHV NGIVHRDLKP ENLLLASKMK GAAVKLADFG 158
camk2a1 ISEEGHHYLI FDLVTGGELF EDIVAREYYS EADASHCIQQ ILEAVLHCHQ MGVVHRDLKP ENLLLASKSK GAAVKLADFG 158
Consensus ISEEGFHYLV FDLVTGGELF EDIVAREYYS EADASHCIQQ ILEAVLHCHQ MGVVHRDLKP ENLLLASKMK GAAVKLADFG
Conservation
camk2b1 LAIEVQGDQQ AWFGFAGTPG YLSPEVLRKE AYGKPVDIWA CGVILYILLV GYPPFWDEDQ HKLYQQIKAG AYDFPSPEWD 238
camk2b2 LAIEVQGDQQ AWFGFAGTPG YLSPEVLRKE AYGKPVDIWA CGVILYILLV GYPPFWDEDQ HKLYQQIKAG AYDFPSPEWD 237
camk2g1 LAIEVQGDQQ AWFGFAGTPG YLSPEVLRKD PYGKPVDIWA CGVILYILLV GYPPFWDEDQ HKLYQQIKAG AYDFPSPEWD 239
camk2g2 LAIEVQGDQQ AWFGFAGTPG YLSPEVLRKD PYGKPVDIWA CGVILYILLV GYPPFWDEDQ HKLYQQIKAG AYDFPSPEWD 239
camk2d1 LAIEVQGDQQ AWFGFAGTPG YLSPEVLRKE PYGKPVDMWA CGVILYILLV GYPPFWDEDQ HRLYQQIKAG AYDFPSPEWD 238
camk2d2 LAIEVQGDQQ AWFGFAGTPG YLSPEVLRKD PYGKPVDMWA CGVILYILLV GYPPFWDEDQ HRLYQQIKAG AYDFPSPEWD 238
camk2a1 LAIEVEGEQQ AWFGFAGTPG YLSLEVLRKD PYGKAVDLWA CGVILYILLV GYPPFWDEDQ HRLYQQIKAG AYDFPSPEWD 238
Consensus LAIEVQGDQQ AWFGFAGTPG YLSPEVLRKD PYGKPVDIWA CGVILYILLV GYPPFWDEDQ HKLYQQIKAG AYDFPSPEWD
Conservation
camk2b1 TVTPEAKNLI NQMLTINPAK RITAQEALKH PWVCQRSTVA SMMHRQETVE CLKKFNARRK LKGAILTTML VSRNFSAAKT 318
camk2b2 TVTPEAKNLI NQMLTINPVK RITAQEALKH PWVCQRSTVA SMMHRQETVE CLKKFNARRK LKGAILTTML VSRNFSAAKS 317
camk2g1 TVTPEAKNLI NQMLTINPAK RITAEQALKH PWVCQRSTVA SMMHRQETVE CLRKFNARRK LKGAILTTML VSRNFSACKS 319
camk2g2 TVTPEAKNLI NQMLTINPAK RITADQALKH PWVCQRSTVA SMMHRQETVE CLRKFNARRK LKGAILTTML VSRNFSACKS 319
camk2d1 TVTPEAKDLI NKMLTINPAK RITAAEALKH PWICQRSTVA SMMHRQETVE CLKKFNARRK LKGAILTTML ATRNFSSKNP 318
camk2d2 TVTPEAKDLI NKMLTINPSK RITAAEAPKH PWICQRSTVA SMMHRQETVE CLKKFNARRK LKGAILTTLL VTRNFSAAKS 318
camk2a1 TVTPEAKDLI NKMLTINPSK RITAAEALKH PWISHRSTVA SCMHRQETVE CLKKFNARRK LKGAILTTML ATRNFSGGKS 318
Consensus TVTPEAKNLI NQMLTINPAK RITAAEALKH PWVCQRSTVA SMMHRQETVE CLKKFNARRK LKGAILTTML VSRNFSAAKS
Conservation
camk2b1 LLNKKAD-VK ESSDSSNATV EDEEMKARKQ EIIKITEQLI EAINNGDFEA YAKICDPGLT CFEPEALGNL VEGMDFHRFY 397
camk2b2 LLNKKTE-VK ESSDSSNTTI EDEDVRARKQ EIIKITEQLI EGLNNGDFEA YAKMCDPGLT SFEPEALGNL VEGMDFHRFY 396
camk2g1 LLNKKADGVK GSTESCNTN- EEEDMKTRKQ EIIKITEQLI EAVNNGDFEA YTRICDPGLT SFEPEALGNL VEGMDFHKFY 398
camk2g2 LLNKKSDGVK GSTESCNTT- EEEDMKARKQ EIIKITEQLI EAINNGDFEA YTRICDPGLT SFEPEALGNL VEGMDFHKFY 398
camk2d1 Y--KKPDGVK ESSESTNTTI EDEDIKARKQ EIIKVTELLI EAINNGEFEA YTKICDPGLT SFEPEALGNL VEGTDFHRFY 396
camk2d2 LLNKKPDGVK ESTESANTTI EDEDLKARKQ EIIKVTEQLI ESINNGDFEA YAKICDPGLT SFEPEALGNL VEGHDFHRFY 398
camk2a1 GVSKKTDGVK ESSESTNTTI EDEDTRVRKQ EIIKVTEQLI EAISNGDFES YTKMCDPSVT AFEPEALGNL VEGLDFHRFY 398
Consensus LLNKKXDGVK ESSESXNTTI EDEDMKARKQ EIIKITEQLI EAINNGDFEA YTKICDPGLT SFEPEALGNL VEGMDFHRFY
Conservation
camk2b1 FENLLSKNSK PIHTTILNPH VHLIGEEAAC IAYIRLTQYV DGQGRPRSSQ SEETRVWHRR DSKWQNVHFH CSGAPAAPLQ 477
camk2b2 FENSLSKNSK PIHTTILNPH VHLIGEDGAC IAYIRLTQFV DGQGLPRSSQ SEETRVWHRR ESRWQNIHFH CSGAPAAPLQ 476
camk2g1 FEHLLSKNNK PVHTTILNPH VHLIGEDAAC IAYIRLTQYI DGQGRPRSCQ SEETRVWHRR DSKWLNVHFH CSGAPAAPLQ 478
camk2g2 FENLLSKNSK PVHTTILNPH VHLIGEDAAC IAYIRLTQYI DGQGRPRSSQ SEETRVWHRR DAKWLNIHFH CSGAPAAPLQ 478
camk2d1 FENSLSKGHK PIHTILLNPH VHLIGEDAAC IAYIRLTQYM DVNNMPRTMQ SEETRVWHRR DGKWQNIHFH RSGSPTVPTK 476
camk2d2 FENALSKGNK PVHTILLNPH VHLIGEDAAC IAYIRLTQYM DGSGMPRTMQ SEETRVWHRR DGKWLNIHFH RSGAPSVPIN 478
camk2a1 FENLWSKNSK PVHTTILNPH IHLIGEEAAC IAYIRITQYL DNNGMPCTAQ SEETRIWHRK DGKWQIVHFH RSGSPAALAK 478
Consensus FENLLSKNSK PVHTTILNPH VHLIGEDAAC IAYIRLTQYX DGQGXPRSSQ SEETRVWHRR DXKWQNIHFH CSGAPAAPLQ
Conservation

Figure 2.3. CaMK-II splice variant exon utilization. Twenty different CaMK-II variants were identified by sequencing and are shown as their amino acid sequences in the central variable region aligned to demonstrate alternative exon utilization (A). Variants fall into eleven categories of exon utilization (B). Exons are named and boundaries set as previously determined (Tombes et al., 2003). Variants are named with dashes rather than subscripts in this figure for visibility.

A

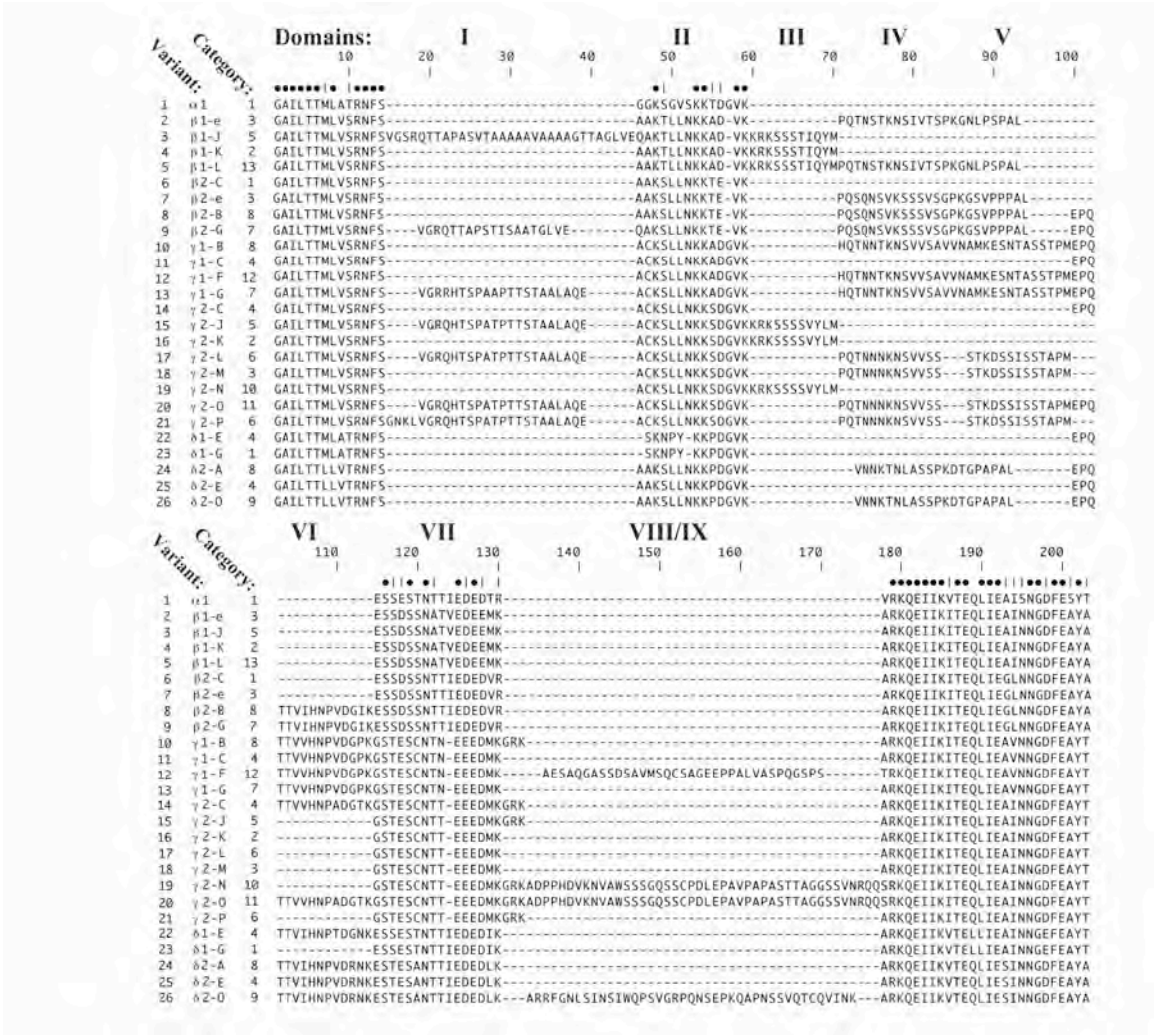

B

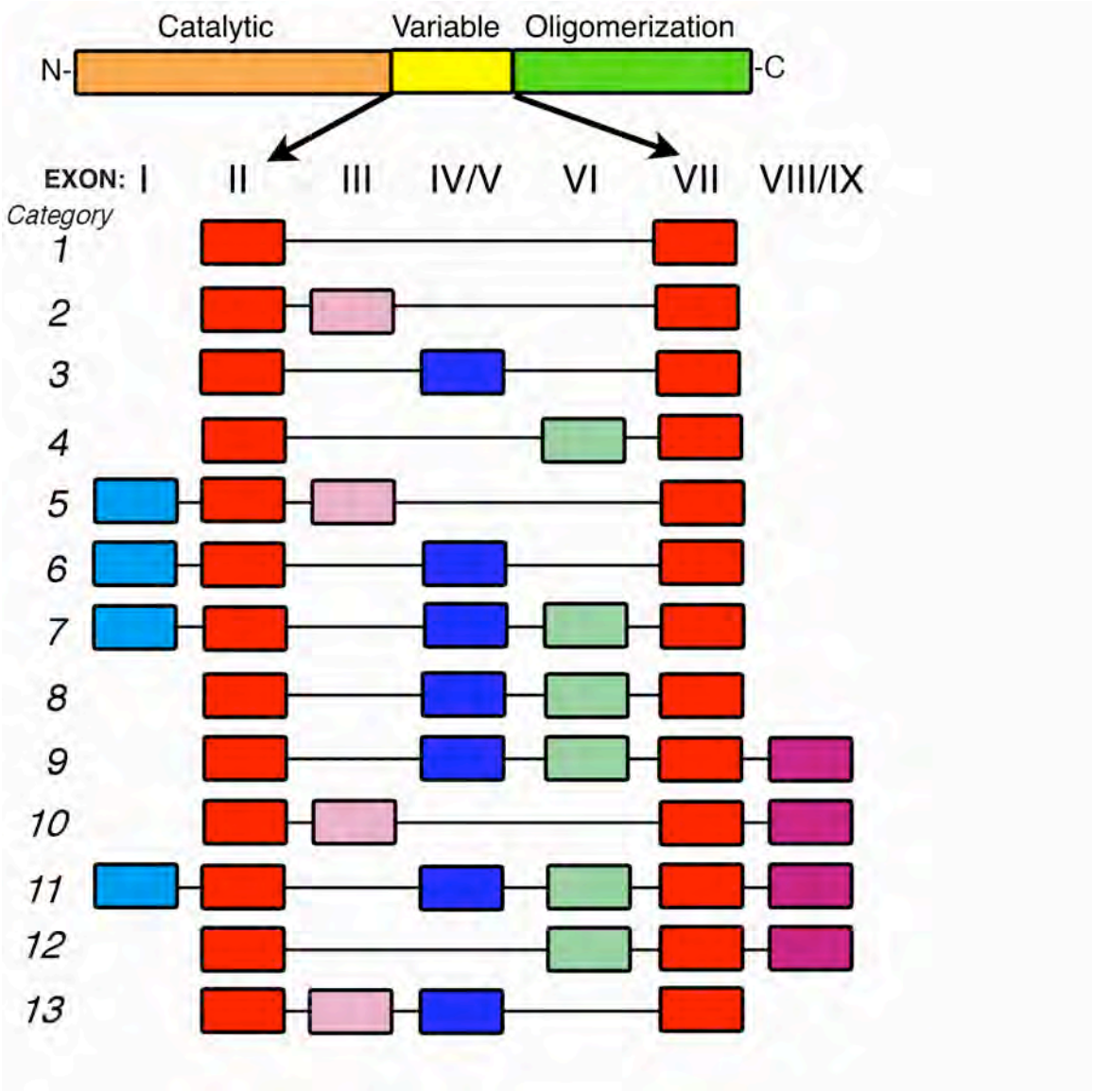
Catalytic
Variable
Oligomerization
N-
-C
EXON: I
II
III
IV/V
VI
VII
VIII/IX
Category
1
2
3
4
5
6
7
8
9
10
11
12
13

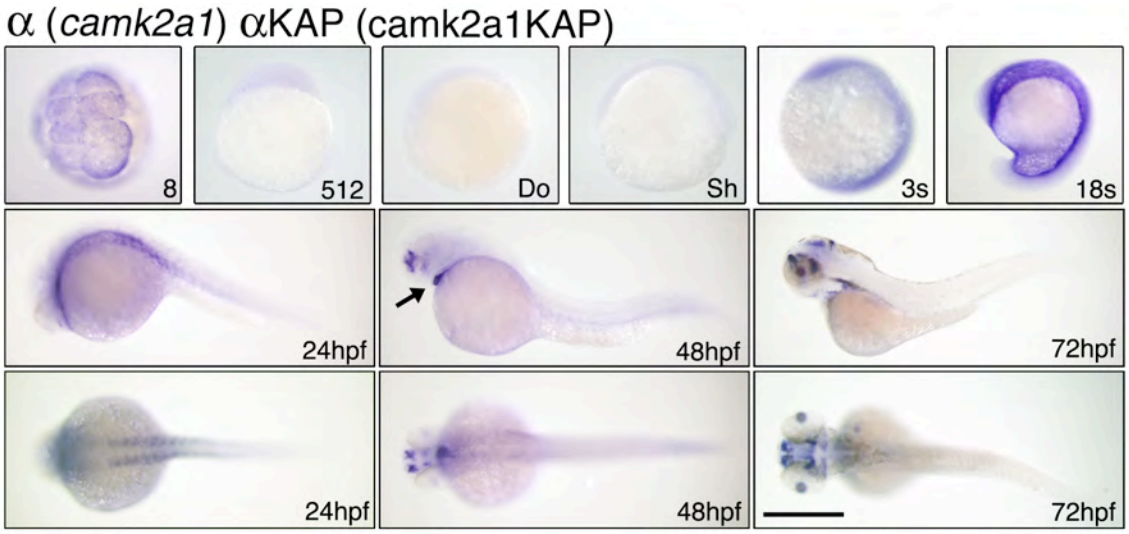

Figure 2.4. In situ localization of α1 and α1KAP CaMK-II mRNAs. CaMK-II expression was assessed by in situ hybridization with a probe for *camk2a1*KAP at the indicated stages. Stages analyzed include the 8-cell stage (8; 1hpf), the 512-cell stage (512; 2.5hpf), the dome stage (Do; 4hpf), the shield stage (Sh; 6hpf), the 3-somite stage (3s; 11hpf), and the 18-somite stage (18s; 18hpf). The 8-cell stage is an animal poll view; others are lateral except for dorsal views at 24, 48, and 72hpf. Arrow in 48hpf *camk2a1* indicates heart. Scale bar = 1 mm.

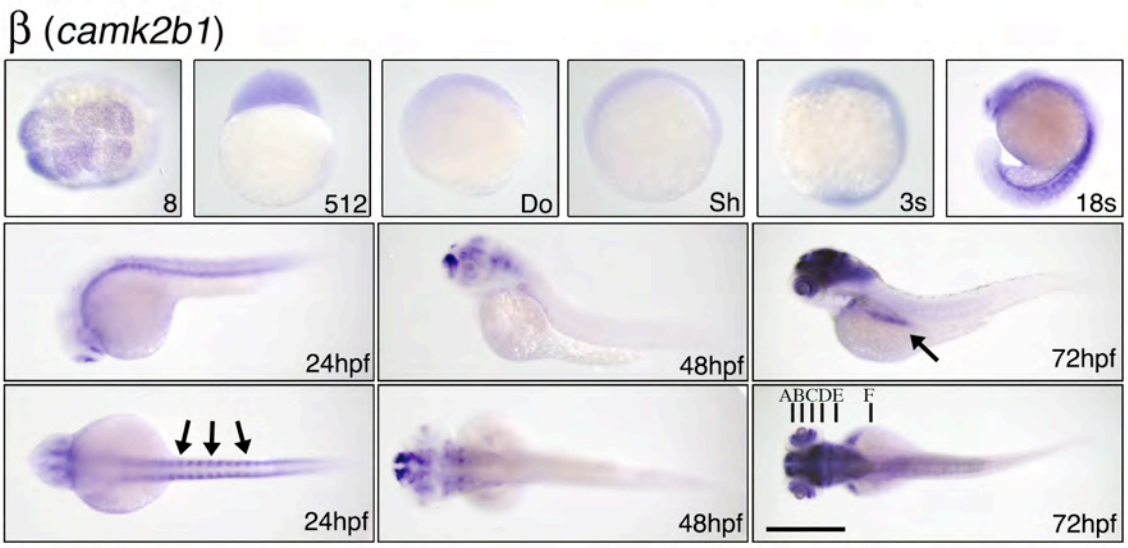

Figure 2.5. In situ localization of β1 CaMK-II mRNA. CaMK-II expression was assessed by in situ hybridization with a probe for camk2b1 at the indicated stages as in Figure 1.4. Arrows in camk2b1 at 24hpf indicate somites and at 72hpf gut. Letters locate cross-sections for Figure 2.11. Scale bar = 1 mm.

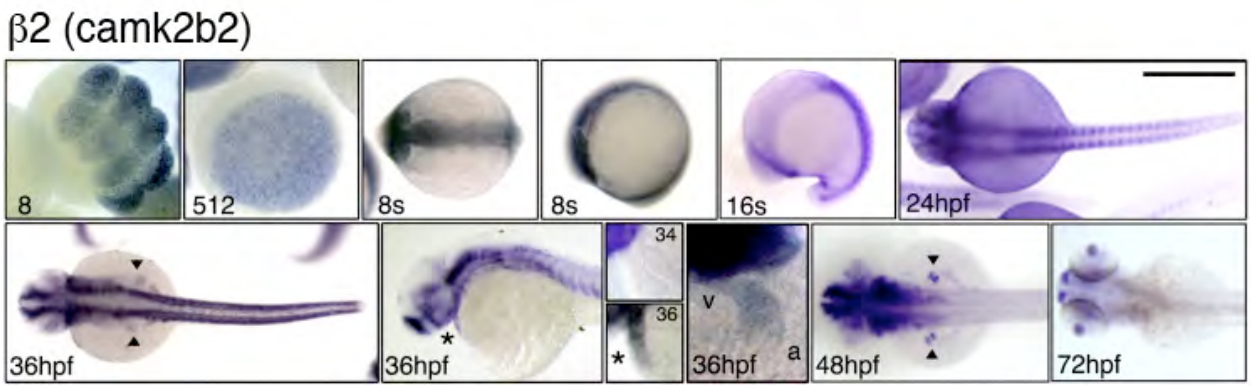

Figure 2.6. In situ localization of β2 CaMK-II mRNA. *Camk2b2* expression was assessed by in situ hybridization at the 8 and 512-cell, 8- and 16-somite and at indicated hours (24, 34, 36, 48 and 72) post fertilization (hpf). Anterior is to the left except for the head on view of the heart at 36 hpf. Arrow heads indicate fin buds, asterisks indicate heart, v = ventricle, a = atrium, scale bar = 1 mm.

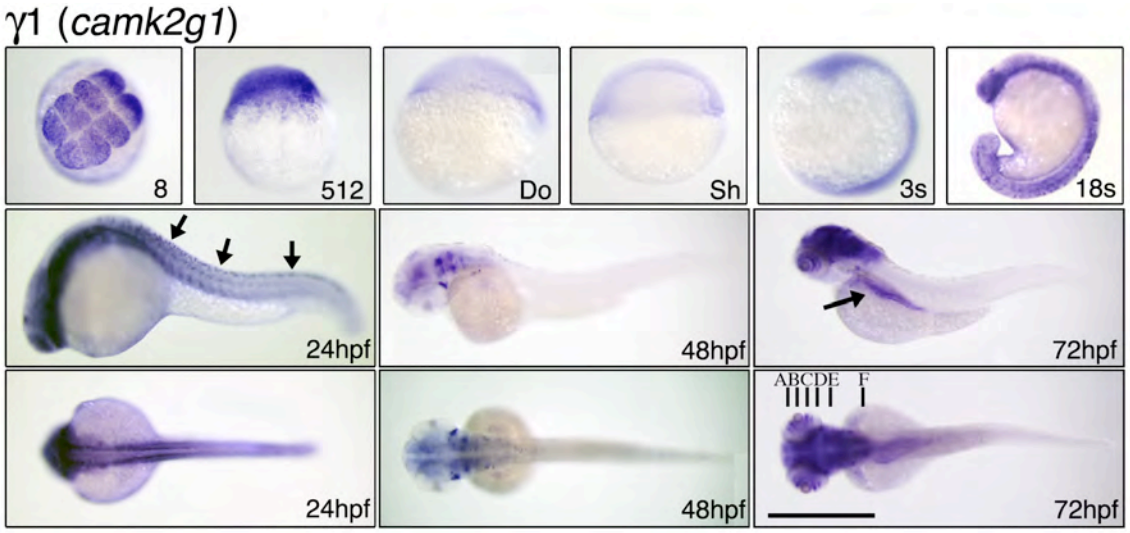

Figure 2.7. In situ localization of γ1 CaMK-II mRNA. CaMK-II expression was assessed by in situ hybridization with a probe for *camk2g1* at the indicated stages as in Figure 1.4. Arrows in *camk2g1* at 24hpf indicate dorsal cell bodies and at 72hpf gut. Letters locate cross-sections for Figure 2.11. Scale bar = 1 mm.

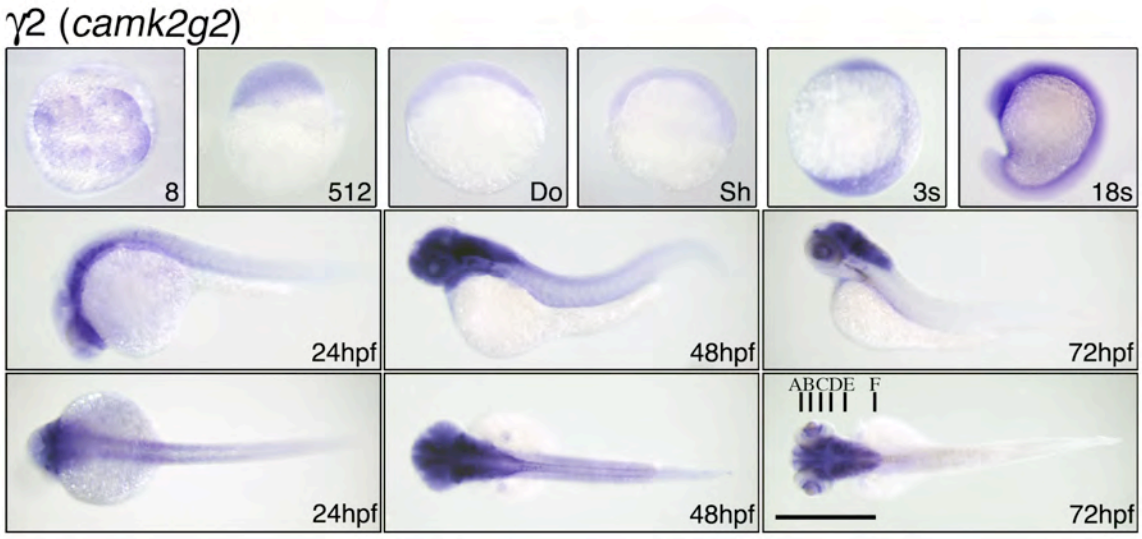

Figure 2.8. In situ localization of γ2 CaMK-II mRNA. CaMK-II expression was assessed by in situ hybridization with a probe for *camk2g2* at the indicated stages as in Figure 1.4. Letters locate cross-sections for Figure 2.11. Scale bar = 1 mm.

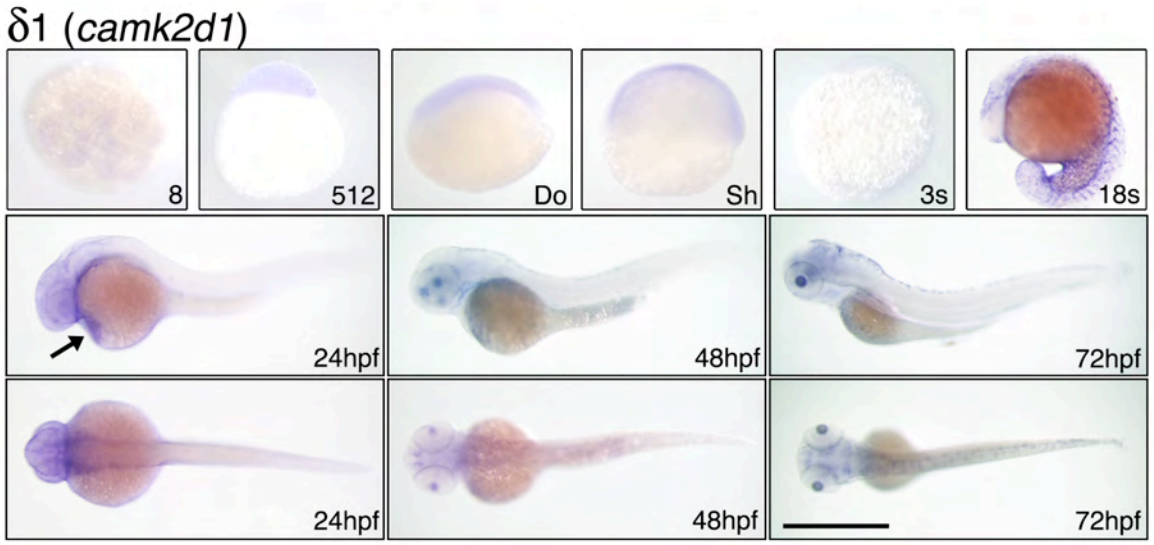

Figure 2.9. In situ localization of δ1 CaMK-II mRNA. CaMK-II expression was assessed by in situ hybridization with a probe for *camk2d1* indicated stages as in Figure 1.4. The 8-cell stage is an animal poll view; others are lateral except for dorsal views at 24, 48, and 72hpf. Arrows in *camk2d1* at 24hpf indicates hatching gland. Scale bar = 1 mm.

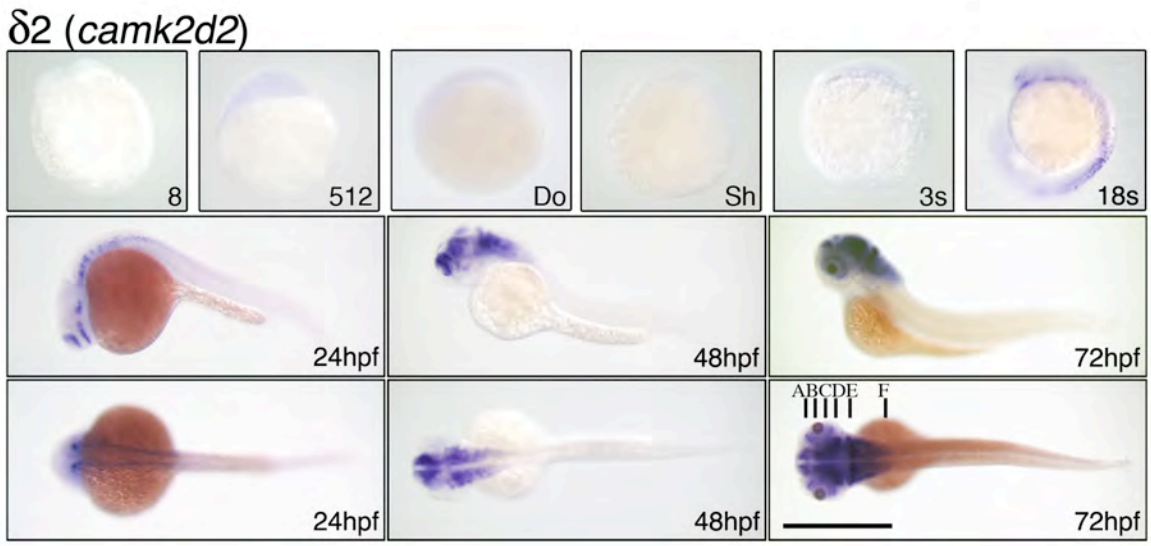

Figure 2.10. In situ localization of δ2 CaMK-II mRNA. CaMK-II expression was assessed by in situ hybridization with a probe for *camk2d1* and *camk2d2* at the indicated stages as in Figure 1.4. The 8-cell stage is an animal poll view; others are lateral except for dorsal views at 24, 48, and 72hpf. Letters locate cross-sections for Figure 2.11. Scale bar = 1 mm.

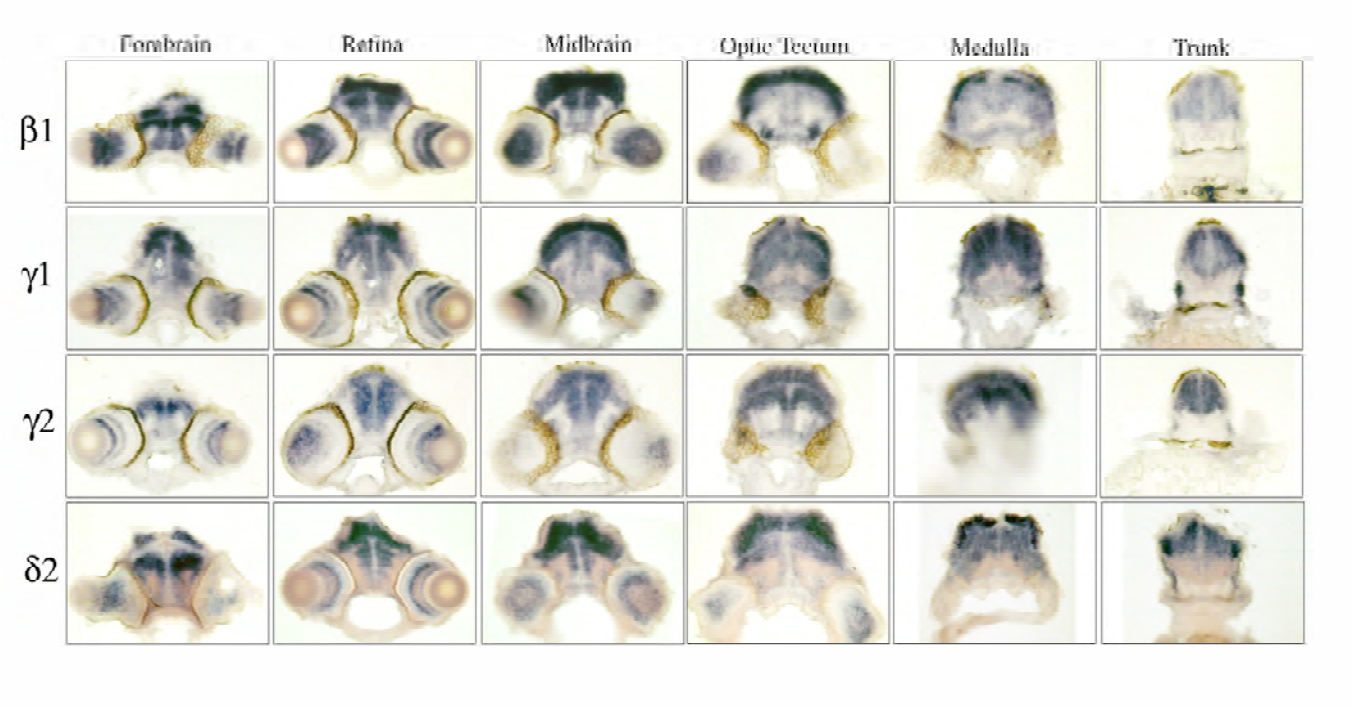

Figure 2.11. Cross-sectional localization of CaMK-II mRNAs. CaMK-II expression was localized at 72hpf by 30μm frozen thin sections of pre-stained embryos. Sections shown were acquired at the locations (A-F) indicated in Figures 2.5, 2.6, 2.8, and 2.10 along the anterior-posterior axis. Scale bar = 0.1 mm.

Table 2.1. Relative levels of expression of CaMK-II genes. Temporal and spatial locations of each gene were assessed and are summarized for all 7 genes during the first 3 days of zebrafish development.

	camk2a1	camk2b1	camk2b2	camk2g1	camk2g2	camk2d1	camk2d2
8-cell	+	+	+++	+++	+	-	-
512-cell	+	+	++	++	+	-	-
Dome	-	+	+	+	+	-	-
Shield	-	+	+	+	+	-	-
3-somites	+	+	++	+	+	-	-
18-somites	++	+	++	++	+	+	-
24hpf trunk	+	++	+++	+++	+	-	+
24hpf Epidermis	-	-	-	-	-	+	-
24hpf Brain	-	+	+	++	+	-	+
24hpf Hatching	-	+	-	-	-	+	-
48hpf Heart	++	++	++	-	-	-	-
48hpf Forebrain	+	+	++	-	++	-	++
48hpf Midbrain	-	+	++	+	+++	-	++
48hpf Retinal	-	-	-	-	++	-	-
72hpf Retinal	-	++	-	+	+	-	++
72hpf Forebrain	+	++++	+	++	+	-	+++
72hpf Midbrain	-	++++	-	+++	++	-	++
72hpf Hindbrain	-	++	-	++	++	-	+++
72hpf Pectoral	-	+	-	+	-	-	-
72hpf Gut	-	+	-	++	-	-	-
72hpf Trunk	-	+	-	-	-	+	-
Otic Vesicle	-	-	-	+++	++	-	-
Kidney	-	-	-	+++	-	-	-

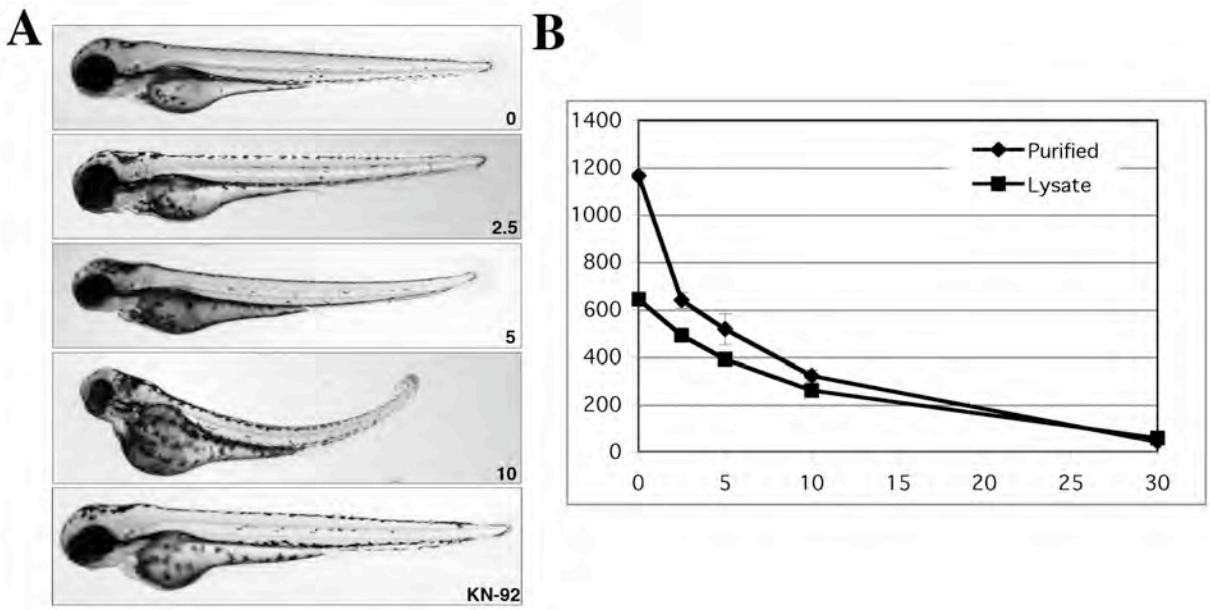

Figure 2.12. CaMK-II Inhibition by KN-93 Causes Developmental Defects. A. Embryos treated with increasing concentrations of KN-93 or the inactive analog KN-62 imaged at 3dpf. B. CaMK-II activity decreases in both 3 dpf purified zebrafish CaMK-II and 3dpf whole embryo lysates with increasing concentrations of KN-93.

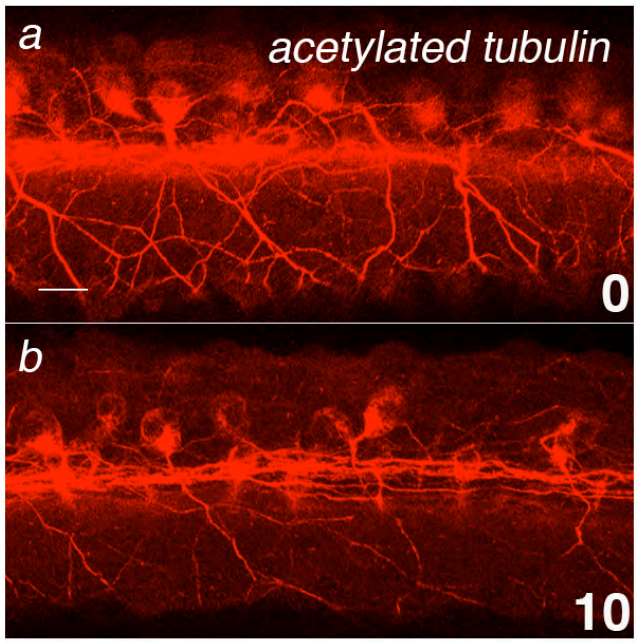

Figure 2.12. KN-93 Treatment Inhibits Proper CNS development. KN-93 treated embryos were assessed at 24hpf for proper spinal cord axonal development using an acetylated tubulin antibody. (a) Control embryos have several cell bodies that project axons towards the ventral axis of the embryo while (b) 10 μM KN-93 treated embryos have reduced axonal projections. Scale bar = 10 μm

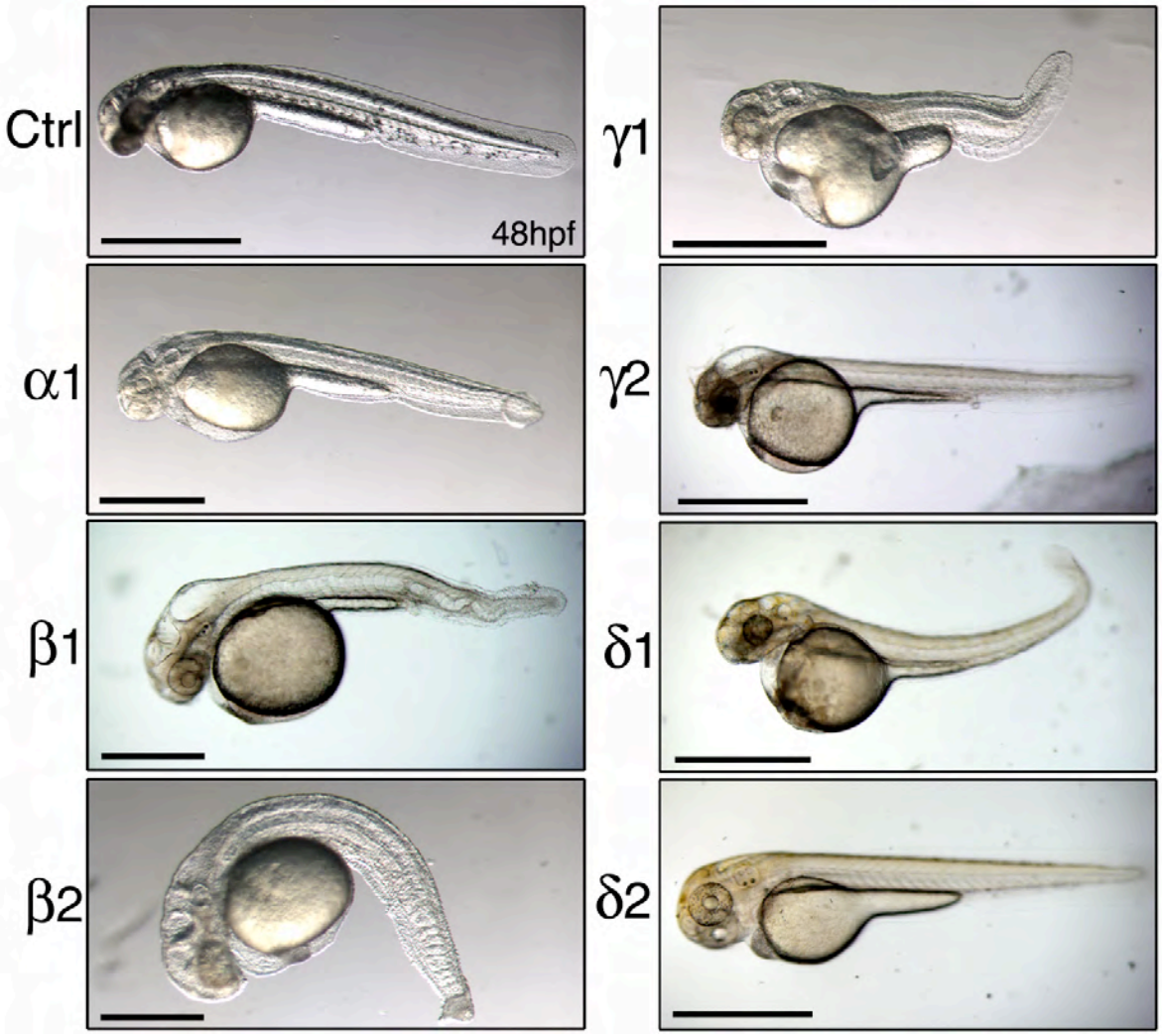

Figure 2.13. CaMK-II Morphant Phenotypes at 48hpf. Translation blocking antisense morpholino oligonucleotides designed against each gene were injected at the 1-4 cell stage and imaged at 48hpf. 5ng of control, α1, β1, γ2, δ1, and δ2 and 1.5ng of β2 and γ1 were injected at a constant volume of ~1nl. Scale bar = 1mm

Table 2.2. Morpholino Sequence Data. Morpholino sequences were aligned against all CaMK-II genes to identify possible cross-reactivity. Target gene is first column and MO is first row. Region of MO targeting is shown below for all CaMK-II genes with bold letters equating to designed translation blocking MO. All MO's are 25 bps but δ2 is 24 bps.

Target/MO	α1A(β2)	α1B	β1	β2	γ1	γ2	δ1	δ2	α1 KAP
α1	**0**	**0**	22	6	10	14	7	11	12
β1	8	20	**0**	5	12	12	12	13	17
β2	3	13	10	**0**	14	13	10	12	13
γ1	11	11	15	11	**0**	7	12	14	16
γ2	12	16	14	14	7	**0**	15	14	19
δ1	7	11	18	7	9	10	**0**	9	17
δ2	8	12	16	10	13	15	10	**0**	**14**
α1KAP	16	16	17	14	15	16	16	**10**	**0**
Cross-reacts w/	β2	–	–	-	-	-	-	–	

```
Camk2a1     AAGAGGCGCACACGCTTCCAGGATGGCAACCATCACCTGCACACGCT
Camk2a1KAP  AAGTGGAGAGCAGACCACCGCTATGCCCCTCACTATGCTTTCTGGGC
Camk2b1     TCCGAGTCCGAGACGGGAAGACATGGCCACGACTACATGTACGCGCT
Camk2b2     TCACAGCTGGAAGAGGACAGACATGGCAACCACAACCTGCACGCCGC
Camk2g1     CCTCCCCGCACGCACACACAACATGGCTACAATTGTAACCTCGACCA
Camk2g2     CGAAATCCTCGTAAAGCGCAACATGGCTACAATTGTAACCTGCACCA
Camk2d1     ATTGTTCTTCCTCACTTTCAGCATGGCTTCAACAACCTGCACCTGCA
Camk2d2     GCGCTGCCGATTCCCCATCACAATGGCTCTGACCATCTGCACCAGAT
```

Table 2.3. Summary of CaMK-II morphant phenotypes. CaMK-II morphants were assessed at 72hpf for morphological defects. All morpholinos were injected with 5ng of morpholino, accept *camk2g1* at 1.25ng, *camk2b2* and *a1KAP* at 2ng.

Gene	Morphant Phenotype
camk2a1	brain necrosis, hydrocephaly
camk2b1	hydrocephaly, notochord defects, convergent extension defects
camk2b2	hydrocephaly, bradycardia, heart morphogenesis defects, somite defects, reduced circulation, left-right asymmetry defects
camk2g1	hydrocephaly, heart morphogenesis defects, somite compression, convergent extension defects, coloboma, pronephric cysts, cloacal obstruction, left-right asymmetry defects,
camk2g2	hydrocephaly, brain necrosis
camk2d1	brain necrosis, failure hatch from chorion
camk2d2	brain necrosis
camk2aKap	left-right asymmetry defects, somite compression, bradycardia

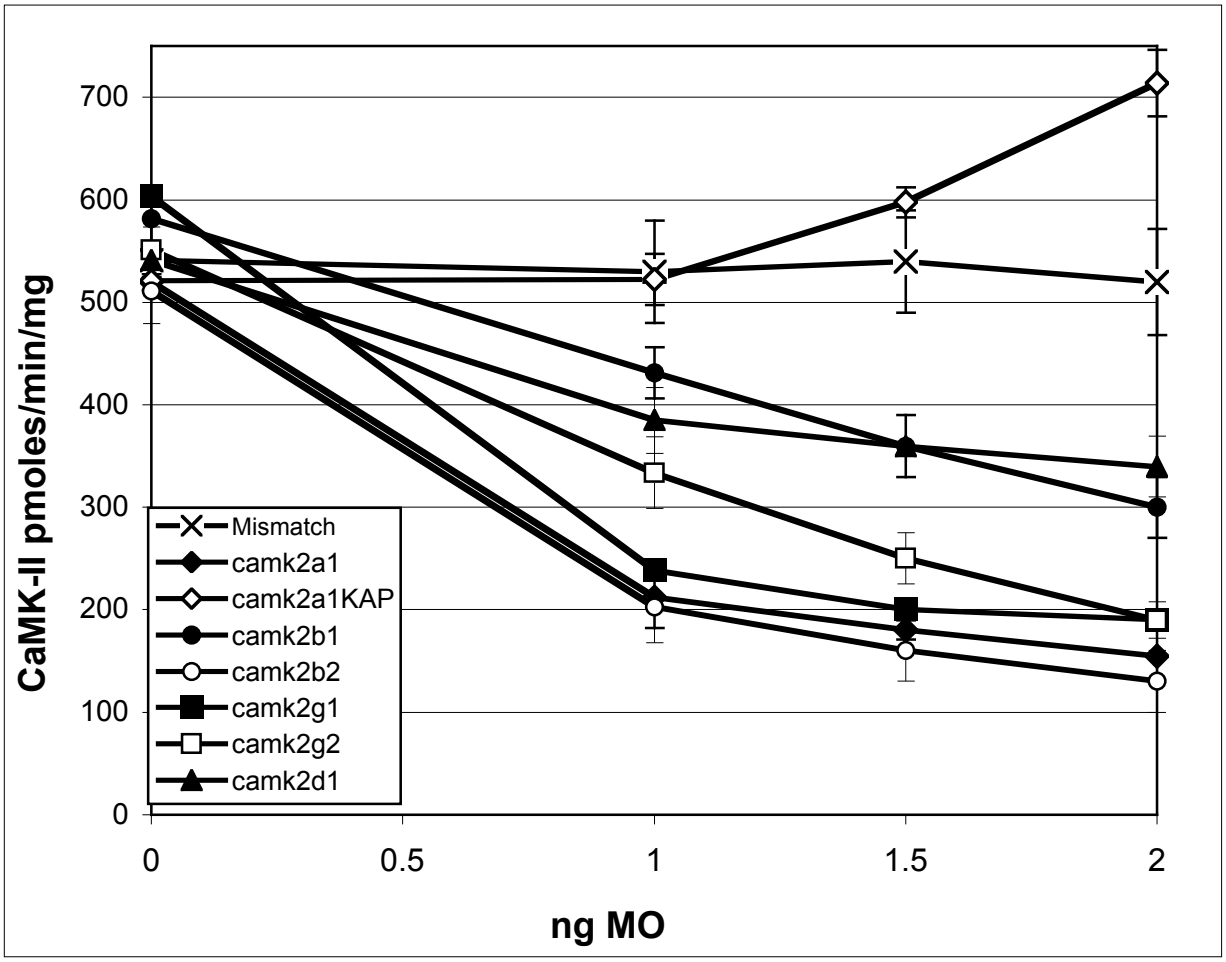

Figure 2.14. CaMK-II activity in 72hpf morphant embryos. Ca^{2+}-dependent CaMK-II-specific activity was measured using the autocamtide-2 peptide-based assay on 72hpf whole embryo lysates after injection of 1, 1.5, or 2ng of translation blocking MO for each gene.

Chapter 3: Tbx-5-Mediated Expression of CaMK-II is Necessary for Zebrafish Cardiac and Pectoral Fin Morphogenesis.

ABSTRACT

β2 CaMK-II was the first gene evaluated due to its distinctive suppression phenotype. This phenotype is reminiscent of that association with mutations in the T-box transcription factor, TBX5, that result in Holt–Oram syndrome (HOS), a human condition in which cardiac development is defective and forelimbs are stunted. Morphants of _2 CaMK-II (*camk2b2*), but not the _1 CaMK-II (*camk2b1*) paralog, exhibit bradycardia, elongated hearts and diminished pectoral fin development. Similarly, zebrafish *tbx5* morphants and mutants (*heartstrings*; *hst*) lack pectoral fins and exhibit a persistently elongated heart that does not undergo chamber looping. Tbx5 is expressed in the developing atrium, ventricle and in pectoral fin fields, but its genetic targets are still being uncovered. In this study, evidence is provided that Tbx5 induces the expression of a specific member of the CaMK-II family; this CaMK-II is necessary for proper heart and fin development. Normal cardiac phenotypes can be restored by ectopic expression of a human cytosolic CaMK-II in *tbx5* morphants. Like *tbx5*, *camk2b2* is expressed in the pectoral fin and looping heart, but this expression is diminished in both *tbx5* morphant and *hst* embryos. Conversely, the introduction of excess Tbx5 into zebrafish embryos and mouse fibroblasts doubles CaMK-II expression. We conclude that _ CaMK-II expression and activity are necessary for proper cardiac and limb morphogenesis. These findings not only identify a

morphogenic target for Ca^{2+} during heart development, but imply roles for CaMK-II in adult heart remodeling.

INTRODUCTION

Holt-Oram Syndrome

Holt-Oram syndrome (HOS) is a human autosomal-dominant disorder that affects 1 in 100,000 individuals and results in heart and limb abnormalities. This defect was mapped to the gene encoding the T-box transcription factor, TBX5, where haploinsufficiency causes foreshortened arms, sinus bradycardia, and septation defects (Basson et al., 1997; Basson et al., 1994). There are over 60 germline mutations in HOS patients, including nonsense, frameshift, and splice site mutations (Bohm et al., 2008). Many of these mutations result in a truncation that leads to a nonfunctioning protein. Tbx5 is composed of a DNA binding domain, known as the T-box motif, a transcriptional activator domain, and two nuclear localization signals (NLS) (Wilson and Conlon, 2002). Tbx5 is expressed in the heart and limb during embryonic development and becomes limited to the heart, liver, lung, prostate, and trachea of adults. Animal models of HOS mimic the developmental defects seen in patients and have allowed the identification of downstream transcriptional targets (Bruneau et al., 2001; Garrity et al., 2002; Rallis et al., 2003).

In zebrafish, Tbx5 is required for heart and pectoral fin development and is expressed in the pectoral fin bud, atrium and ventricle (Ahn Dae-gwon, 2002; Garrity et al., 2002). Tbx5 mutants (heartstrings; hst) and morphants fail to develop pectoral fins and exhibit cardiac elongation, diminished chamber development, and bradycardia (Garrity et al., 2002). *Hst* mutants fail to undergo the morphogenic process known as heart "looping," where the atrium and ventricle balloon and bend relative to each other (Yelon, 2001) *Tbx5* expression is required for early heart development and is known to induce the expression of a wide variety of genes implicated in heart and limb development, including *fgf10, sall4 and bmp6* (Harvey and Logan,

2006; Horb and Thomsen, 1999; Ng et al., 2002; Plageman and Yutzey, 2006; Rallis et al., 2003). It is also believed that Tbx5 acts in combination with other transcription factors, such as Gata4, Nkx2.5 and Tbx20 to influence the expression of downstream targets, including myocardial-specific genes *amhc*, *cmlc2* and *vmhc* (Lu et al., 2008; Naiche et al., 2005).

Ca^{2+} and Heart Morphogenesis

Ca^{2+} signals have also been implicated in the morphogenesis of the heart, as Ca^{2+} channel blockers, Ca^{2+} chelators, disruption of either Na^{+}/Ca^{2+} exchanger (NCX) or SERCA2, the sarcoplasmic reticulum (SR) Ca^{2+} ATPase, all interfere with cardiac looping. While T-box family members have been shown to influence vertebrate development through Wnts and FGFs, none of the known downstream targets of Tbx5 can explain this Ca^{2+} dependence.

A known target of embryonic Ca^{2+} signals is CaMK-II, an evolutionarily conserved serine/threonine protein kinase. During early development, CaMK-II is activated by Wnt family members and can rescue mutant phenotypes of certain non-canonical Wnts, whose role is to promote cell-movements during gastrulation (Kohn and Moon, 2005). Although non-canonical Wnts, Wnt11 and Wnt11-R, have been implicated in cardiac specification and/or morphogenesis, a role for CaMK-II in embryonic heart development has never been defined (Eisenberg and Eisenberg, 1999; Garriock et al., 2005; Pandur et al., 2002). CaMK-II has been implicated in adult cardiovascular disease and heart failure and has been proposed as a therapeutic target to minimize remodeling, arrhythmias and hypertrophy (Grueter et al., 2007; Yang et al., 2006; Zhang et al., 2005). Substrates or binding partners of CaMK-II known to influence cardiac function include phospholamban, L-type Ca^{2+} channels, and ryanodine receptors (Baltas et al., 1995; Grueter et al., 2006; Hudmon et al., 2005; Lee et al., 2006; Zalk et al., 2007). These

function to influence the level of intracellular calcium. An additional CaMK-II substrate is HDAC4, a member of the Class II histone deacetylases (Little et al., 2007). Phosphorylation of HDAC4 by CaMK-II causes HDAC4 to be shuttled out of the nucleus and remain in the cytosol (Backs et al., 2006). This causes the upregulation of hypertrophic heart markers, such as MEF2, which ultimately leads to cardiac hypertrophy (Zhang et al., 2003).

This study directly characterizes the function(s) of one of the seven CaMK-II genes expressed in zebrafish. These findings support a role for β2 CaMK-II in zebrafish heart and pectoral fin development downstream of Tbx5 and provide an explanation for the known Ca^{2+}-dependence of cardiac morphogenesis in a wide variety of species.

MATERIALS AND METHODS

Zebrafish strains and care

Wild type fish embryos (AB and WIK Strains) were obtained through natural matings, raised at 28.5°C, and staged as described (Kimmel et al., 1995). *Heartstrings* embryos were obtained through natural crosses of heterozygous *hst* parents. The *Tg(cmlc2:DsRed2)* line was generated by Tol2-mediated transgenesis. Briefly, 25 pg of a plasmid composed of Tol2 transposon ends flanking sequence from _ 210 to + 39 of the *cmlc2* promoter/5_-UTR, the DsRed2-Express open reading frame (Clontech), and the SV40 polyadenylation signal was co-injected with 25 pg of Tol2 transposase mRNA into embryos as described.

Whole mount in situ hybridization

Digoxigenin-labeled anti-sense riboprobes (0.5–1.5 kb) were synthesized using T3 or T7 RNA polymerase from cloned cDNAs, hybridized with fixed embryos and then developed using alkaline phosphatase-conjugated anti-digoxigenin antibodies as described above (Rothschild et al., 2007). Dual color fluorescent *in situ* hybridization was conducted using digoxigenin or fluorescein-labeled riboprobes and developed using peroxidase-conjugated anti-digoxigenin or anti-fluorescein antibodies (Roche, Basel Switzerland) with tyramide-fluorochrome (Cy3 or Alexa 488) derivatives (Perkin Elmer and Invitrogen) as described (Clay and Ramakrishnan, 2005). Fluorescent images were acquired using a NIKON C1 laser scanning confocal microscope. The zebrafish *cmlc2* (cardiac myosin light chain 2) probe was synthesized from cDNA (Open Biosystems, Birmingham, ALA), which had been transferred into the TOPO/TA vector. The *tbx5* probe was prepared as described (Garrity et al., 2002). The *nkx2.5*, *gata4* and

bmp4 probes were obtained and prepared as described (Chen and Fishman, 1996; Kelley et al., 1993; Martinez-Barbera et al., 1997; Peterkin et al., 2007).

Morpholino and cDNA injections

cDNAs and morpholino anti-sense oligonucleotides (MO's) were diluted in Danieau buffer (Westerfield, 1993) and injected at the 1 to 4-cell stage. MO's directed against *camk2b1* and *camk2b2* were designed by Gene Tools (Philomath OR) and injected at up to 5 ng per embryo. Two *camk2b2* MO's were used (A: AGCGTGTGCAGGTGATGGTTGCCAT) and (B: GCGTGCAGGTTGTGGTTGCCATGTC). *Tbx5* (CCTGTACGATGTCTACCGTGAGGC) and *tbx4* (CCAGAACGCAGTAATTTGTCCACTT) MO's were previously described (Ahn et al., 2002). cDNAs encoding human _C wild type (WT) CaMK-II and its constitutively active mutant ($Thr^{287}Asp$) (Caran et al., 2001) were inserted into the pFRM2.1 vector, which is under the control of the carp _-actin promoter (Eckfeldt et al., 2005) and is therefore universally expressed. Human _E CaMK-II matches less than half of the aligned nucleotides in either zebrafish *camk2b2* MO. A mouse Tbx5 cDNA (Open Biosystems) was subcloned into the pCDNA3 vector. cDNA constructs (10–40 pg per embryo) were injected separately or co-injected with MO's. A constant injection volume (~1 nl) was used per embryo and confirmed by volume analysis.

Transfections and immunoblots

Tbx5-pCDNA3 or pCDNA3 alone was either transfected into NIH/3T3 mouse embryonic fibroblasts using Lipofectamine 2000 (Invitrogen) as described (Caran et al., 2001) or injected into zebrafish embryos. Two days after transfection, cell or embryo lysates were prepared as

previously described (Rothschild et al., 2007). Equivalent amounts of soluble protein were immunoblotted as described (Lantsman and Tombes, 2005) using 1 _g/ml cB_1 antibody for _ CaMK-II (Invitrogen), a pan-specific CaMK-II antibody which recognizes _ CaMK-II (BD Biosciences) or an anti-actin peptide antibody (Sigma).

CaMK-II activity assay

Whole embryos were lysed and total CaMK-II activity was assessed by measuring phosphate incorporation into the substrate, autocamtide-2, as previously described (Rothschild et al., 2007).

Statistical analysis

Statistical analyses were performed using the paired *t*-test. For CaMK-II activity assays and blot analysis, values from at least four replicates were used. Statistically significant differences are denoted by an asterisk and *P* values indicated in figure legends. For zebrafish embryo morphological features or heart rates, *n* values varied between 147 and 285 individuals. Pectoral fins were assessed by integrating the *bmp4*-positive fin field area using digital image analysis.

RESULTS

Camk2b2 morphants resemble tbx5 morphants

The expression pattern of *camk2b2* mRNAs in both the developing heart and pectoral fins is reminiscent of a relatively limited number of genes including *tbx5* (Garrity et al., 2002). In addition, the *camk2b2* morphant phenotype was similar to the *hst* mutant (Garrity et al., 2002) and the *tbx5* morphant (Ahn et al., 2002), particularly with respect to heart morphology and function. Both *tbx5* and *camk2b2* morphants as well as KN-93 treated embryos exhibited an elongated, more slowly beating heart (Supplemental Movie 1 and 2) accompanied by pericardial edema (Figure 3.1a-c; Figure 3.2a,b). Heart rates were decreased from 160 to 20bpm, half-maximally at 4μM, which is the same concentration that half-maximally inhibits CaMK-II activity *in vitro* (Figure 2.13). The myocardial marker *cmlc2* (cardiac myosin light chain 2) remained strongly expressed in both *tbx5* and *camk2b2* morphants and KN-93 incubated embryos, but revealed an elongated myocardium that failed to undergo looping morphogenesis, as shown at 48 hpf (Figure 3.1f–h; Figure 3.2c,d). The elongated heart was also visible in *camk2b2* and *tbx5* morphants of *cmlc2*:DsRed transgenic embryos at 72 hpf (Figure 3.1k–m).

Like *tbx5* mutants and morphants, *camk2b2* morphants also displayed pectoral fin defects. Although still present, pectoral fins were always stunted and occasionally asymmetric in *camk2b2* morphants and KN-93 treated embryos (Figure 3.1q,v; Figure 3.2e,f). In *tbx5* morphants (Figure 3.1r, w) and mutants, pectoral fins were completely absent, indicative of an early and essential regulatory role for Tbx5 in initiating forelimb development. The phenotypic resemblance of the *tbx5* and *camk2b2* loss-of-function phenotypes suggested a genetic

relationship between these two genes.

Tbx5 morphant heart defects can be rescued by cytosolic CaMK-II

The suggested genetic linkage between *tbx5* and *camk2b2* was assessed by co-injecting morpholinos with a vector encoding GFP-linked human cytosolic $_C$ CaMK-II. This co-injection not only restored normal heart morphology and looping (Figure 3.1d,i,n) in *camk2b2* morphants, but also in *tbx5* morphants (Figure 3.1e ,j, o). The CaMK-II variant ($_C$) used in this rescue had both predicted insensitivity to the *camk2b2* MO and an alternative domain structure similar to zebrafish $_2C$ (Figure 1b), which is one of the four *camk2b2* variants detected by RT-PCR of isolated zebrafish heart mRNA (data not shown). GFP-tagged $_C$ CaMK-II exhibits normal Ca^{2+}/CaM-dependent catalytic activity and cytosolic localization (Caran et al., 2001) and was detected by fluorescent microscopy throughout embryos, including heart cells through at least the first four days of development (data not shown). Thus, restoration of CaMK-II activity via a human splice variant with similarity to an endogenous zebrafish *camk2b2* transcript was sufficient to ameliorate cardiac defects in *tbx5* morphants, as well as in *camk2b2* morphants.

Normal fin morphology, however, was only rescued by ectopic expression of CaMK-II in *camk2b2* morphants, not *tbx5* morphants (Figure 3.1s, x). In the wild type fin, *bmp4* expression was observed at the periphery (apical ectodermal ridge; AER) of the developing fin, as well as in mesenchymal cells at the center of the fin field (Figure 3.1p, inset). In *camk2b2* morphants, *bmp4* expression exists, but was limited to the mesenchymal area (Figure 3.1q, inset) of the truncated fins. The wild type mesenchymal and AER pattern of *bmp4* expression was restored, however, when morphant embryos were co-injected with CaMK-II (Figure 1s, inset). In contrast, neither fin development nor *bmp4*-expressing fin cells (Figure 3.1t, y) were observed in *tbx5*

morphants, regardless of the level of CaMK-II injected; *bmp4*-positive cells in the pectoral fin region are known to be absent in *tbx5* morphants (Garrity et al., 2002).

Both *tbx5* and *camk2b2* MO's decreased heart rates by 40–50% at both 48 hpf and 72 hpf (Figure 3.3a; Figure 3.2g), while both the mismatch MO and a MO directed against a related T-box gene, *tbx4* (Ahn et al., 2002), had no effect on heart rates. The similarity in the timing and magnitude of the *camk2b2* and *tbx5* morphant phenotypes provides further support for a common pathway. Heart rates of *tbx5* morphants were recovered to near normal levels and such rescues were dependent on the amount and activity state of co-injected CaMK-II (Figure 3.3b). For example, constitutively active ($T^{287}D$) CaMK-II (Ca^{2+}-independent) was most effective at low levels (20 pg), whereas wild type (WT) CaMK-II (Ca^{2+}-dependent) rescued heart rates in proportion to the amount injected. WT rescues were also more persistent beyond 72 hpf than those rescued with $T^{287}D$ CaMK-II, which showed some reversion to the morphant phenotype. This finding is consistent with Tbx5-dependent CaMK-II expression, not Ca^{2+} release.

Rescue experiments using 40 pg WT CaMK-II were summarized at 72 hpf (Figure 3.3c) by determining the presence of circulation or heart looping and by measuring the fin field area derived from *bmp4* expression, as shown in Figure 3.1. Only 10–20% of *camk2b2* or *tbx5* morphant embryos exhibited circulation and looping, but this could be restored to 50–80% of morphant embryos when co-injected with CaMK-II. The average fin field area in *camk2b2* morphants was approximately 30% of that in control embryos and was restored to 90% by CaMK-II co-injection. *Tbx5* morphants exhibited no visible fins or *bmp4*-positive cells with or without CaMK-II co-injection. Therefore, while CaMK-II expression is necessary and sufficient to recover *tbx5*-induced cardiac defects, it is necessary but not sufficient to recover fin defects.

As predicted for a role in cardiac morphogenesis, we demonstrate that *camk2b2* is

expressed in myocardial cells by co-localization with *cmlc2* using dual *in situ* hybridization (Figure 3.4). *Camk2b2* expression was more widespread in both atrium and ventricle than *cmlc2*, but this is reminiscent of *tbx5* expression, which is expressed in both myocardial and epicardial cells of the human heart (Hatcher et al., 2001).

Levels of early cardiac and pectoral fin markers are unaffected in *camk2b2* morphants

Both cardiac and paired limb progenitors derive from lateral plate mesoderm (LPM), where Nkx2.5, GATA4 and other transcription factors are expressed to influence heart and/or limb development (Chen and Fishman, 1996; Kelley et al., 1993; Martinez-Barbera et al., 1997; Peterkin et al., 2007; Waxman et al., 2008). We therefore evaluated the influence of *camk2b2* suppression on the expression levels of *gata4* and *nkx2.5* at the 8-somite stage. These important early markers were unaffected in *camk2b2* morphants (Figure 3.5 a–d) as previously shown for *tbx5* morphants (Garrity et al., 2002) indicating that the disruption in heart development occurs at later times and not during cardiac specification. At the 21s and 24 hpf stages, heart cone (Figure 5e,f) and heart tube (Figure 3.5g,h) formation were unaffected in *camk2b2* morphants as assessed using *cmlc2* expression. At 48 hpf, *bmp4* expression was detected in both control hearts (Figure 5i) and in the elongated *camk2b2* morphant hearts (Figure 3.5j). Representative thin sections reveal an elongated cellular morphology, particularly in the atrium of *camk2b2* morphant hearts (Figure 3.5k,l). In *camk2b2* morphant fins, *bmp4* was expressed in a more concentrated patch of cells (Figure 3.5n, arrows) than in control embryos, where *bmp4* was preferentially expressed in mesenchymal cells and at the AER of the developing fin (Figure 3.5m, arrows). Similarly, *tbx5* expression levels in *camk2b2* morphants remain unaltered (Figure 3.5p) when compared to control embryos (Figure 3.5o), consistent with a role for Tbx5 upstream and not downstream of

camk2b2.

Tbx5 mutant and morphants have reduced β CaMK-II expression

In further support of their relative genetic relationship, *tbx5* morphant and mutant embryos exhibit diminished cardiac and pectoral fin *camk2b2* expression and lower total CaMK-II activity levels (Figure 3.6). In *tbx5* (Figure 3.6c,d), but not *tbx4* morphants (Figure 3.6a,b), *camk2b2* expression was eliminated in the heart (*v, a*) and emerging pectoral fin fields (arrow heads), but not in the somites or brain. This loss of *camk2b2* expression was also observed in *hst* mutant embryos (Figure 3.6g,h), but not siblings that lacked the *hst* morphology (Figure 3.6e,f). In addition, CaMK-II enzymatic activity levels were measured in wild type, morphant and mutant embryos at 72 hpf (Figure 3.6i). Either of two separate *camk2b2* MO's (b2-A and b2-B) decreased CaMK-II activity by over 75% relative to uninjected or *tbx4* MO-injected embryos. Morphant embryos co-injected with human CaMK-II, which is insensitive to zebrafish MO's, exhibited a restoration of enzymatic activity proportional to the amount of cDNA injected. Both *tbx5* morphants (tbx5 MO) and the *hst* mutant (hst mut) embryos exhibited a 40–60% reduction in CaMK-II activity when compared to control morphants, *tbx4* morphants or non-mutant siblings. Although *camk2b2* expression is most likely subject to multiple transcriptional influences, these findings indicate that Tbx5 promotes a subset of *camk2b2* expression in the heart and fins.

Tbx5 enhances β CaMK-II expression across species

In order to directly assess whether Tbx5 promotes _ CaMK-II expression, a cDNA encoding mouse Tbx5 was transfected into NIH/3T3 cells. Tbx5 expression caused a two-fold increase in

_ CaMK-II protein levels, but neither altered levels of _ CaMK-II, the most prevalent CaMK-II in fibroblasts, or _-actin (Figure 3.7a). CaMK-II specific activity measurements, which normalize activity to total protein, also showed a significant Tbx5-dependent increase (Figure 3.7b). When mouse Tbx5, which is 98% identical to zebrafish Tbx5 within the T-box domain (Begemann and Ingham, 2000), was injected into embryos, a dose-dependent, but saturable, increase in CaMK-II specific activity was observed (Figure 7c). These results indicate that Tbx5 acts across species to promote the expression of the _(2) CaMK-II gene. Tbx5 is believed to bind to consensus sequence elements (TBE), defined as (A/G)GGTGT(C/G/T)(A/G) (Ghosh et al., 2001; Sun et al., 2004a). At least one putative TBE was found 200 nt upstream of the start codon in both zebrafish and mammalian _ CaMK-II genes, supporting the possibility that Tbx5 acts either alone or in conjunction with other T-box family members (Naiche et al., 2005) to promote the expression of this gene.

DISCUSSION

_2 CaMK-II is induced by Tbx5 and is necessary for cardiac and limb morphogenesis

We conclude that _ CaMK-II expression is dependent on the T-box transcription factor, Tbx5, and is necessary for the proper development of the heart and pectoral fins. This conclusion is based on five distinct lines of evidence including: 1) the coincident temporal and spatial expression of *camk2b2* and *tbx5* in heart and fins, 2) the similarity of *camk2b2* and *tbx5* morphant phenotypes, particularly in the heart, 3) the ability of cytosolic CaMK-II to rescue cardiac defects in *tbx5* morphants, 4) the sensitivity of CaMK-II expression to *tbx5* suppression, but not vice versa and 5) the induction of _ CaMK-II expression by ectopic Tbx5. While CaMK-II has been implicated in adult cardiac function and remodeling (Anderson, 2007; Yang et al., 2006; Zhang et al., 2005), this is the first report that supports a necessary role for CaMK-II in cardiac and forelimb development.

Camk2b2 is the only one of the seven transcriptionally active CaMK-II genes in zebrafish embryos whose embryonic expression pattern is consistent with a role in the maturation of the heart and pectoral fins. *Camk2b2* mRNAs are also expressed in the developing brain and somites, but *tbx5* suppression does not diminish *camk2b2* brain expression. Consistent with this finding and unlike *tbx5* mutants and morphants, *camk2b2* morphants have reduced head size and distorted trunks, in addition to their heart and fin defects. Ectopic human cytosolic _ CaMK-II reverses all of these developmental defects, which is consistent with cytosolic roles for all embryonic *camk2b2* variants. Although _2 CaMK-IIs could hetero-oligomerize with other CaMK-IIs, which may target the holoenzyme to other sub-cellular locations, this result demonstrates that CaMK-IIs exhibiting the same targeting domain structure can functionally

substitute for each other between genes and species.

Potential mechanisms of _2 CaMK-II action in heart and fin morphogenesis

Camk2b2 expression in the heart is coincident with heart looping, a process potentially influenced by cell migration, proliferation and apoptosis (Ahn et al., 2002; Garrity et al., 2002; Goetz et al., 2006; Yelon, 2001). Cardiac cone and tube morphology in *camk2b2* morphants is unaltered at 24 hpf, but the transition to a looped heart over the next 24 h is blocked. Non-canonical Wnt (ncWnt) family members, including Wnt5 (Slusarski et al., 1997) and Wnt11, but not canonical Wnt8 (Westfall et al., 2003b), induce Ca^{2+} elevations in zebrafish embryos and have been implicated in both convergent extension cell movements and in cardiac morphogenesis (Kohn and Moon, 2005; Kuhl et al., 2000a; Kuhl et al., 2000b; Sheldahl et al., 2003). These ncWnts are believed to activate CaMK-II (Kohn and Moon, 2005; Kuhl et al., 2000a; Kuhl et al., 2000b; Sheldahl et al., 2003) and defects in convergent extension in the Wnt5 *pipetail* mutant (*ppt*) (Kilian et al., 2003) and in knockdowns of its receptor, frizzled2 (Sumanas et al., 2001), can be partially rescued with ectopic CaMK-II (Westfall et al., 2003a). Wnt11, possibly acting in conjunction with the Na^{+}/Ca^{2+} exchanger, NCX, and/or SERCA2, the sarcoplasmic reticulum (SR) Ca^{2+} ATPase, may contribute to the Ca^{2+} release necessary to activate _2 CaMK-II.

Loss of either Tbx5 or CaMK-II disrupts cardiac morphogenesis, but does not diminish the expression of early genes that specify cardiac tissue, such as those encoding Gata4, Nkx2.5 and Bmp4. This is also consistent with studies that have demonstrated that the expression of these genes in *Xenopus* is insensitive to the CaMK-II inhibitor, KN-93 (Pandur et al., 2002). Although *tbx5* is expressed in lateral plate mesoderm (Ahn et al., 2002; Garrity et al., 2002) and

induces the expression of many early genes important for cardiac development, it is likely that Tbx5 collaborates with independently induced transcription factors (Brown et al., 2005; Clark et al., 2006; Naiche et al., 2005) to promote *camk2b2* expression in the looping heart or coalescing fin field. The expression of other Tbx5-dependent genes in the heart, such as connexin (Clark et al., 2006) are necessary to maintain the differentiated heart phenotype initially achieved through CaMK-II expression and activity.

In the developing fin, *camk2b2* is expressed subsequent to limb bud initiation, which occurs around 26 hpf (Grandel and Schulte-Merker, 1998), but simultaneous with creation of the apical fold at 36 hpf and continuing through 48 hpf, when mesenchymal cell migration is prevalent (Grandel and Schulte-Merker, 1998). This is also consistent with a role for CaMK-II in morphogenesis, not specification of fin cells. The inability of CaMK-II to rescue *tbx5* morphant fin defects is consistent with a requirement for additional critical Tbx5-dependent genes, such as FGFs and Wnts, in forelimb bud initiation (Harvey and Logan, 2006; Rallis et al., 2003; Takeuchi et al., 2003).

Specifically, CaMK-II could influence cardiac and limb morphogenesis through its known roles in cell cycle progression or cell migration. Both extrinsic physical forces and intrinsic cellular fates influence cardiac morphogenesis (Auman et al., 2007). The mechanism of CaMK-II action must be through transient or cyclical Ca^{2+}-dependent catalytic activity, since excessive constitutively active CaMK-II is incapable of rescuing mutant phenotypes. Both the natural cycle of contraction as well as morphogens must be considered as triggering the Ca^{2+} sources necessary to activate CaMK-II.

CaMK-II is known to promote progression of fibroblasts through the G1 phase of the cell cycle (Morris et al., 1998) possibly through its activity-dependent interaction with the TCF

transcriptional co-regulator, flightless-I (Seward et al., 2008). This is consistent with the reported cardiac cell cycle delay in G1 or early S-phase caused by Tbx5 depletion in *Xenopus* (Goetz et al., 2006). Both the depletion of Tbx5 and prolonged inhibition of CaMK-II lead to apoptosis (Goetz et al., 2006; Tombes et al., 1995). CaMK-II may influence morphogenesis through balanced effects on proliferation and apoptosis in embryonic cardiac and fin cells.

Alternatively, CaMK-II may influence morphogenesis by regulating directional cell migration as previously suggested for both heart (Schoenebeck and Yelon, 2007) and fin (Grandel and Schulte-Merker, 1998) development. Tbx5 has been implicated in proepicardial cell migration in the chick embryo (Hatcher et al., 2004) and CaMK-II is known to influence the migration of vascular smooth muscle cells (Lundberg et al., 1998; Pfleiderer et al., 2004) and fibroblasts (Easley et al., 2008). CaMK-II could also influence migration through direct phosphorylation of Tiam1, a guanine nucleotide exchange factor for Rac1 (Fleming et al., 1999; Fleming et al., 1998) or through its promotion of phosphotyrosine turnover of the focal adhesion proteins, paxillin and FAK (Easley et al., 2008). The tyrosine phosphatase, SHP-2, dephosphorylates FAK and paxillin, to promote focal adhesion turnover (Ren et al., 2004; Vadlamudi et al., 2002) and has been linked to human heart and limb development through SHP-2 mutations identified in Noonan or Leopard syndrome (Digilio et al., 2002; Poole and Jones, 2005; Tartaglia and Gelb, 2005; Tartaglia et al., 2001). Targeted mutations in SHP-2 based on actual Noonan and Leopard syndrome patients also yield a phenotype reminiscent of *heartstring* (Jopling et al., 2007). Altered directional cell migration could explain the observed phenotypes of stretched cardiac cells and disrupted fin cell dispersal observed in *camk2b2* morphants.

Finally, a mechanism by which cytosolic CaMK-II could influence the expression of genes required for morphogenesis comes from evidence that cytosolic CaMK-IIs influence the

localization of histone deacetylases (HDAC) in cardiomyocytes (Backs et al., 2006). HDAC1 and HDAC2 are both necessary for mouse cardiac morphogenesis (Montgomery et al., 2007), zebrafish HDAC1 morphants exhibit heart and fin defects (Pillai et al., 2004) and mouse HDAC1 and 2 knockouts result in the derepression of many genes, some of which are implicated in cell motility and cell structure (Montgomery et al., 2007). Therefore, cellular roles for CaMK-II in coordinating gene expression, migration, proliferation and apoptosis may all contribute to the morphogenesis of heart and limbs.

In summary, Tbx5 promotes the expression of *camk2b2* around 36 hpf in the heart as it is undergoing looping and in the fins at the time of mesenchymal cell migration. Although both *tbx5* and *camk2b2* expression persist beyond 48 hpf, the expression of *camk2b2* in the heart is more transient than fin expression, suggesting that the transcriptional co-regulators that collaborate with Tbx5 in heart and fins are subtly different. Once _2 CaMK-II is expressed, the source of activating Ca^{2+} and the binding partners or substrates through which CaMK-II influences heart and fin morphogenesis remain undefined.

Implications to human cardiac disease

A role for CaMK-II in embryonic morphogenesis, as described in this study, is consistent with its proposed function in maintenance of the adult heart. Excess cardiac CaMK-II in transgenic mice hyperactivates SERCA which, inhibits proper Ca^{2+} release and reuptake from the sarcoplasmic reticulum; resulting in cardiomyopathy and heart failure (Zhang et al., 2003). In fact, inhibition of CaMK-II activity represents a clinically relevant mechanism for suppressing the pathological remodeling of adult heart tissue (Zhang et al., 2005). Optimal levels of CaMK-II activity are therefore important for the morphogenesis, maintenance and function of both the

embryonic and adult heart. CaMK-II suppression provides a plausible explanation for both bradycardia and aberrant cardiac development observed in *tbx5* morphants (Garrity et al., 2002) and in individuals with Holt–Oram syndrome (Clark et al., 2006).

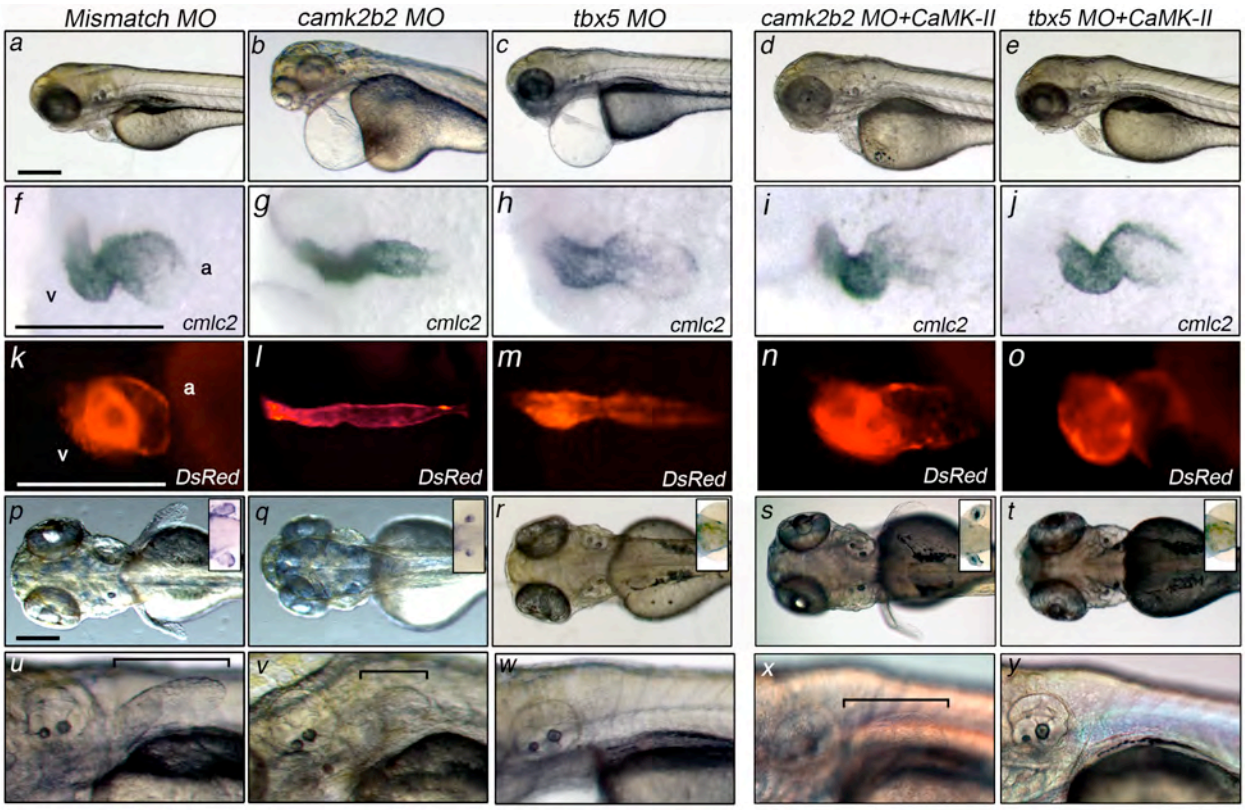

Figure 3.1. Tbx5 heart defects can be rescued by CaMK-II. Wild type or cmlc2:DsRed transgenic embryos (k–o) were injected with the mismatch MO (5 ng), *camk2b2* MO (2 ng) or *tbx5* MO (5 ng) with or without 40 pg wild type _E CaMK-II cDNA and imaged at 72 hpf (a–e; k–y) or subjected to *cmlc2 in situ* hybridization at 48 hpf (f–j). Scale bar = 0.5 mm and anterior is to the left. In f and k, a = atrium and v = ventricle. In p–t, insets reveal *bmp4 in situ* hybridization patterns in the pectoral fin area. In u–y, brackets indicate extent of pectoral fin length.

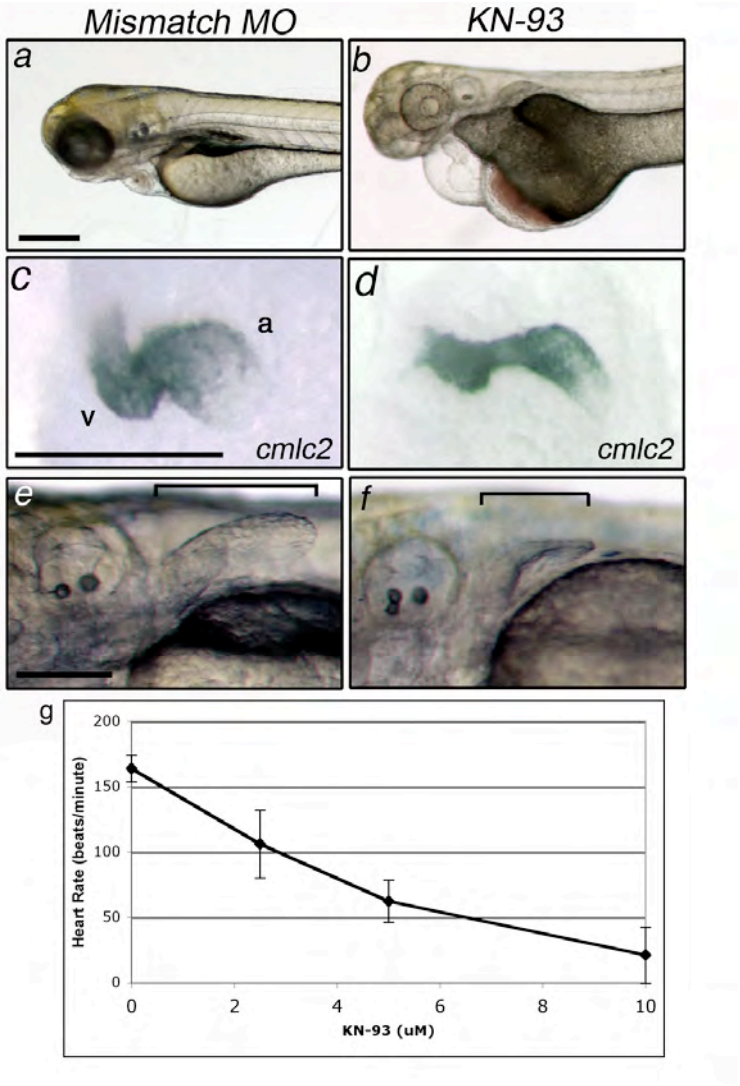

Figure 3.2. Pharmacological suppression of CaMK-II alters heart and fin development. Embryos treated with 10 μm KN-93 starting at cleavage stages were imaged at 72hpfpf to look at heart and fin development. KN-93 treated embryos had linear hearts as shown by DIC images at 72hpf (a,b) and *cmlc2* expression (c,d) at 48hpf. Fin development was also disrupted as shown by lateral views (e,f, bracket). Heart rates were assessed with increasing concentrations of KN-93 in 72hpf embryos. Scale bar=0.5mm.

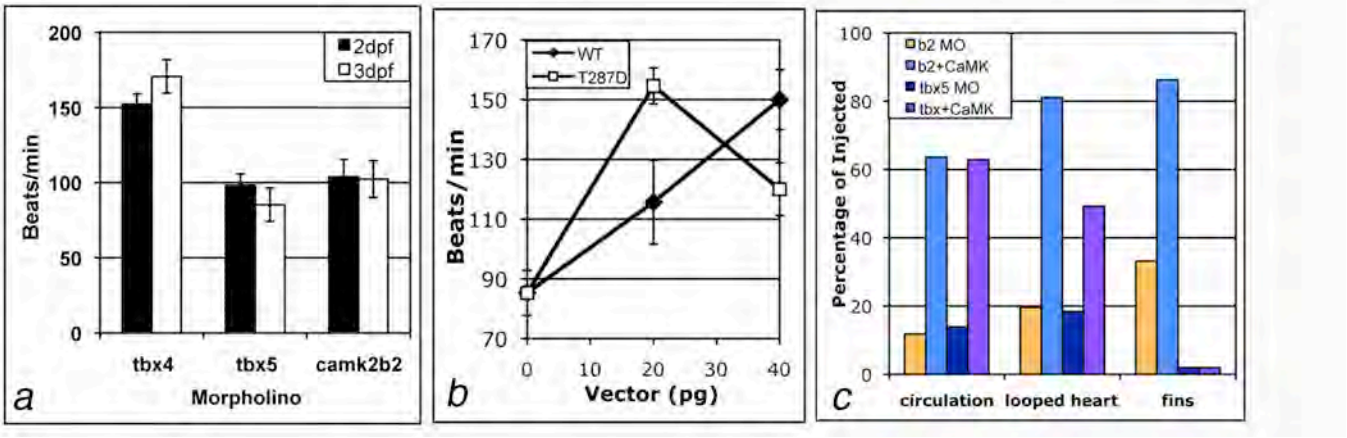

Figure 3.3. Summary of *camk2b2* and *tbx5* rescues. (a) Heart rates were averaged at 48 and 72 hpf after injection with 5 ng tbx4, 5 ng tbx5 or 2 ng *camk2b2* MO (beta2), n = 147–158 per condition. (b) Heart rates were averaged at 72 hpf after injection with 5 ng tbx5 MO plus the indicated pg of WT or $T^{287}D$ $_E$ CaMK-II cDNA, n = 56–62 per condition. (c) Summary: n = 88–187 per condition. Embryos injected with 2 ng of either *camk2b2* MO (b2) or 5 ng *tbx5* MO plus or minus 40 pg wild type $_E$ CaMK-II cDNA were scored at 72 hpf for the presence of absence of circulation or heart looping and shown as a percentage of all embryos. Fin field area was assessed at 72 hpf from *bmp4 in situ* hybridization and is presented as a percentage of the fin field area in *tbx4* morphant embryos.

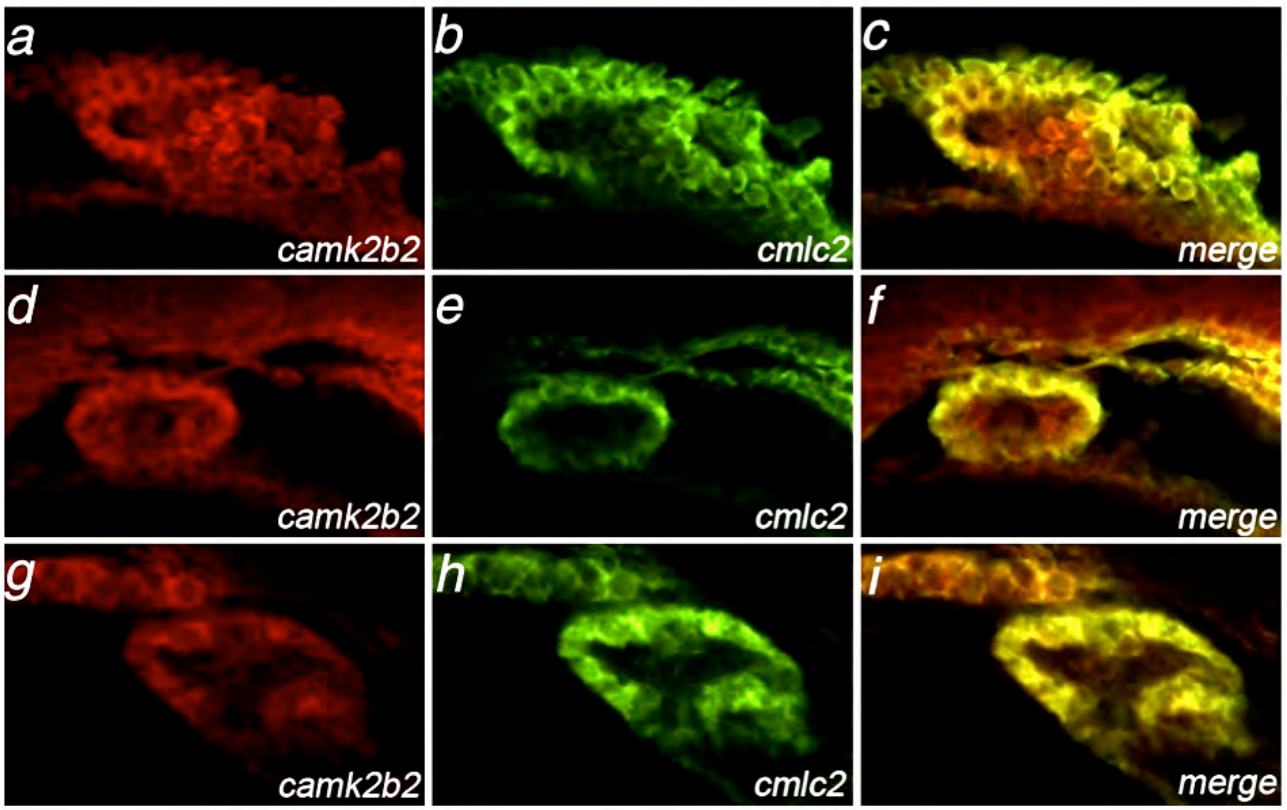

Figure 3.4. Co-localization of *camk2b2* with cmlc2. *Camk2b2* (Cy3, red) or *cmlc2* (Alexa 488, green) expression was assessed by in situ hybridization and confocal fluorescent microscopy and then merged in 36 hpf atrial (a–c), 36 hpf ventricular (d–f) and 48 hpf ventricular (g–i) samples.

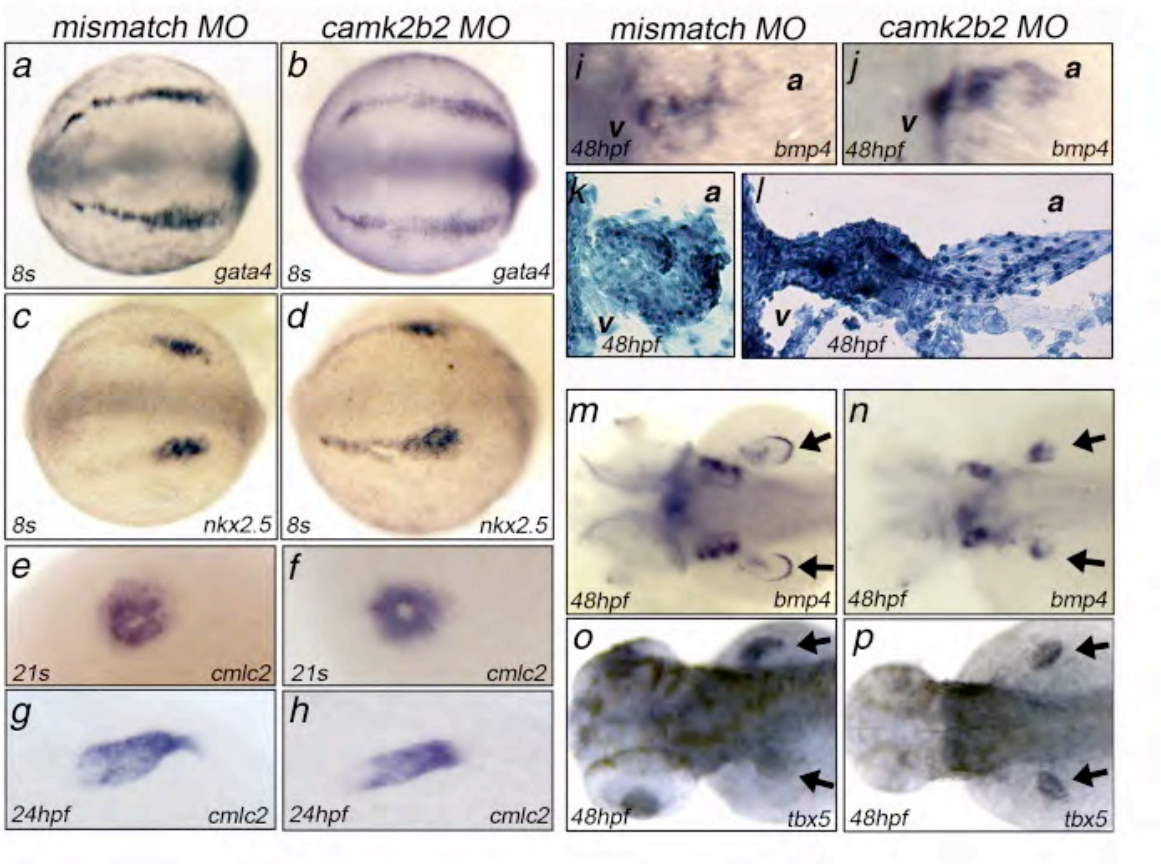

Figure 3.5. Early genes responsible for heart and fin specification are expressed in *camk2b2* morphants. *Gata4* and *nkx2.5* expression in the lateral plate mesoderm at the 8-somite stage (a–d), *cmlc2* at 21s (e, f) and 24 hpf (g, h), *bmp4* at 48 hpf (i, j, m, n) and *tbx5* at 48 hpf (o, p) were determined by in situ hybridization for embryos injected with 5 ng *camk2* mismatch MO or 2 ng *camk2b2* MO. Thin sections of cardiac tissue from mismatch or *camk2b2* morphants were stained with methylene blue (k, l). Anterior is to the left in all views.

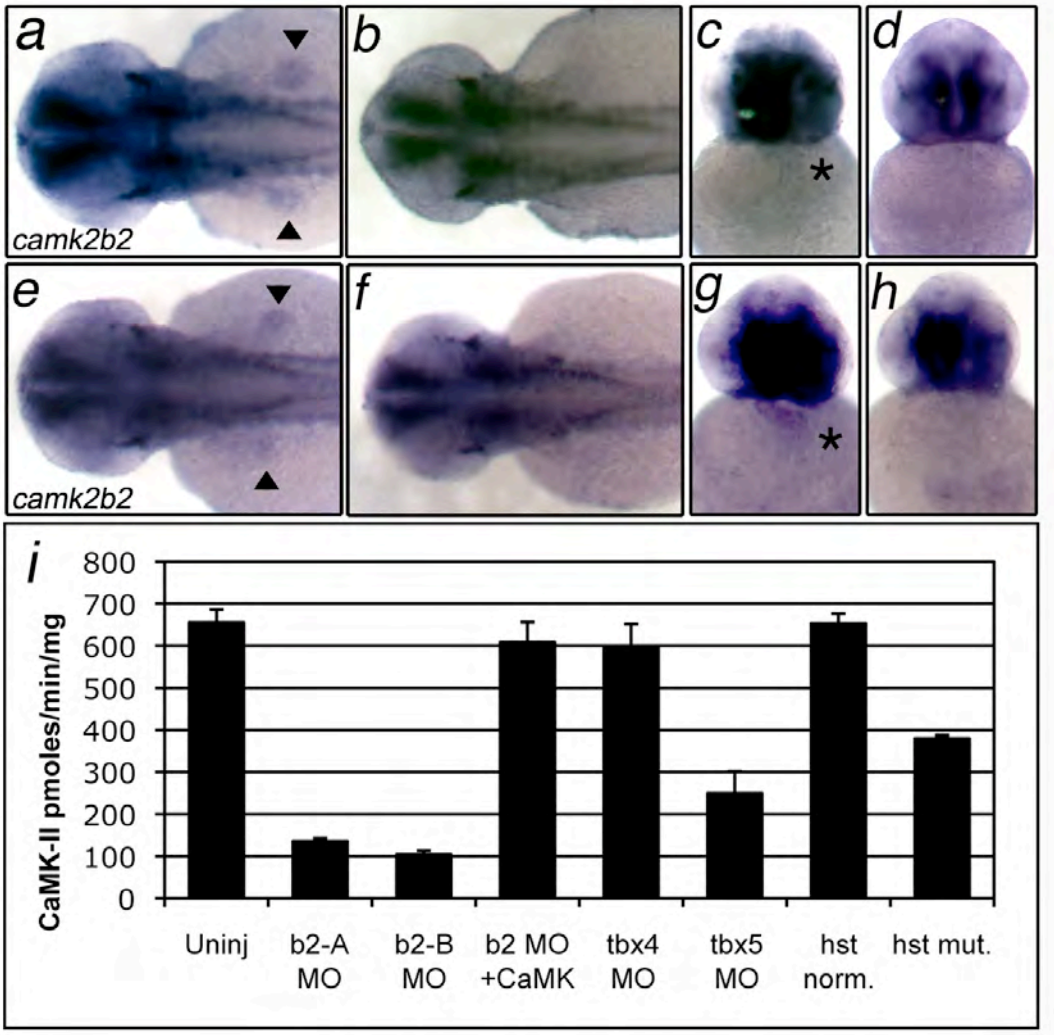

Figure 3.6. *Tbx5* morphants and mutants decrease CaMK-II levels. *Camk2b2 in situ* hybridization of 36 hpf embryos injected with 5 ng *tbx4* MO (a, b) or 5 ng *tbx5* MO (c, d) or uninjected hst siblings (e, f) and *hst* mutants (g, h) as determined phenotypically. Dorsal views (a, c, e, g) mark fins with arrow heads and head on views (b, d, f, h) mark atrium and ventricle. Scale bar = 0.2 mm. (i) CaMK-II activity was assessed at 72 hpf in at least 5 embryos per condition by CaMK-II peptide assay in the presence of Ca^{2+}/CaM. Conditions include uninjected embryos (Uninj), *camk2b2* MO A and MO B embryos at 2 ng (b2-A and b2-B), embryos co-injected with 2 ng *camk2b2* MO B and 40 pg wild type $_E$ CaMK-II cDNA (b2 MO + CaMK), *tbx4* and *tbx5* morphants (5 ng), *hst* embryos with (_/_) the hst phenotype (hst mut.) and siblings without (+/_; +/+) the *hst* phenotype (hst norm.)

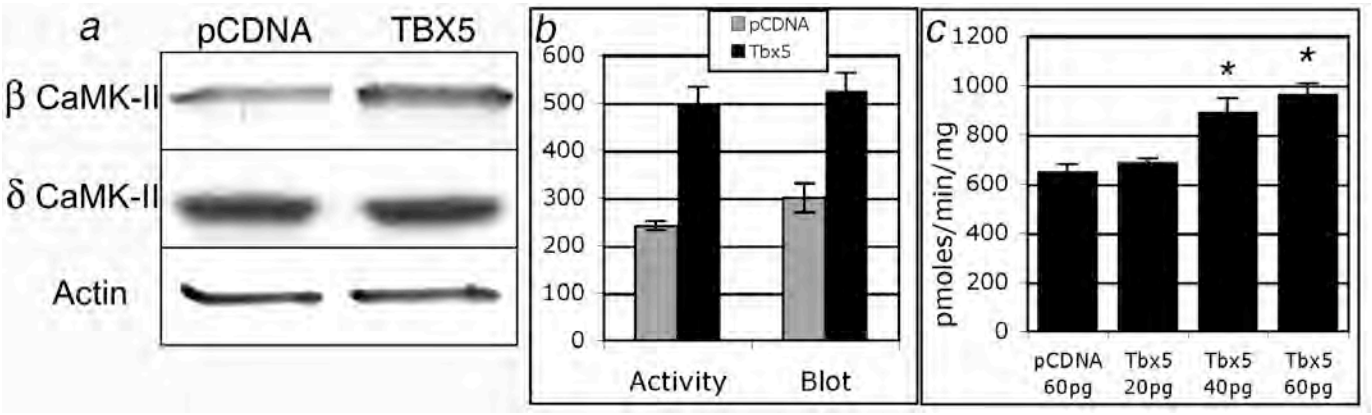

Figure 3.7. Tbx5 promotes _2 CaMK-II Expression. (a) _ CaMK-II, _ CaMK-II and actin immunoblots of 10 _g NIH/3T3 lysate from cells which had been transfected with Tbx5-pCDNA3 or empty pCDNA3 vector. (b) CaMK-II specific activity (in pmol/min/mg) and integrated blot densities (normalized) from NIH/3T3 cells were averaged from four separate transfections and are shown with standard deviations. (c) Zebrafish embryos were injected with the indicated amount of pCDNA3 or Tbx5-pCDNA3 and activity assays performed at 72 hpf. Asterisks indicate $P < 0.005$.

Supplemental Movies

Supplemental Movie 1 - Morphant phenotypes. A series of three short time lapse videos of embryonic hearts and circulation, 3 days post fertilization after injection with (a) 2 ng of control (mismatch) MO, (b) 1 ng camk2b2 MO and (c) 2 ng camk2b2 MO.

Supplemental Movie 2 - Morphant phenotypes. Two short time lapse videos of embryonic hearts 3 days post fertilization after injection with (a) 2.5 ng of camk2b2 MO and (b) 5 ng tbx5 MO.

Chapter 4: PKD2 Ca^{2+} Activates CaMK-II to Abrogate Cyst Formation in a Zebrafish Model of ADPKD

ABSTRACT:

γ1 CaMK-II was next analyzed since it is expressed at high levels during cleavage stages and has unique expression patterns during development. Interestingly, *camk2g1* is the only CaMK-II gene expressed in the developing embryonic kidney (pronephros). Ca^{2+} signaling is known to be important during kidney development and to maintain homeostasis in the nephron as an adult. Several kidney diseases have been linked to alterations in Ca^{2+} signaling including, autosomal dominant polycystic kidney disease (ADPKD), which affects 5-6 million people worldwide and is the most common monogenetic kidney disease. Mutations in two genes, PKD1 and PKD2, have been linked to ADPKD. PKD1 is a large transmembrane protein that forms a receptor channel complex with PKD2 to facilitate Ca^{2+} entry into the cytosol. These mutations cause alterations in Ca^{2+} signaling pathways leading to hyperproliferation, apoptosis, loss of cellular polarity, and ultimately the formation of massive fluid filled cysts. Understanding the downstream Ca^{2+} effectors could aid in finding viable treatments for patients with ADPKD. This study identifies CaMK-II as a target of PKD2 Ca^{2+} in the zebrafish pronephros. Suppression of *camk2g1* causes cloacal obstructions, which ultimately leads to the development of cysts. This *camk2g1* morphant phenotype mirrors suppression of *pkd2* in zebrafish embryos. Ectopic expression of constitutively active, not wild type, CaMK-II reverses cystic development, supporting a dependence on Ca^{2+} release, not CaMK-II expression in *pkd2* morphants. Furthermore, suppression of *pkd2* leads to decreased levels of active CaMK-II in the distal

pronephric duct and a 40% reduction in Ca^{2+}-independent activity in manually dissected pronephros. Actin organization and localization is disrupted in *camk2g1* morphants, while other markers of polarity are normal leading to the hypothesis that PKD2 Ca^{2+} activates CaMK-II to stabilize F-actin in the apical membrane of the zebrafish embryonic kidney.

INTRODUCTION

Autosomal Dominant Polycystic Kidney Disease

Autosomal Dominant Polycystic Kidney Disease (ADPKD) is the most common monogenetic kidney disease affecting 1 in 1,000 births and is typified by the development of massive kidney cysts. Approximately 10% of cases in the United States lead to end-stage renal disease (Wilson and Falkenstein, 1995). A systemic disorder, cysts also develop in the pancreas and liver, and cardiovascular defects arise including an increased risk for aortic aneurysms (Chapman et al., 1993; Gabow, 1993; Milutinovic et al., 1984; Wilson and Falkenstein, 1995). ADPKD is caused by mutations in two transmembrane proteins, PKD1 and PKD2 (Harris et al., 1995; Hughes et al., 1995; Igarashi and Somlo, 2002; Wilson, 2004a). PKD1 encodes polycystin-1, a large receptor-like integral membrane protein with an extracellular N-terminus that contains motifs for cell-cell and cell-matrix interactions, as well as a receptor for egg jelly homology domain (REJ) and a GPCR proteolytic site (GPS) (Wilson, 2004a). REJ is a glycoprotein responsible for the acrosome sperm reaction during sea urchin fertilization (Moy et al., 1996). The REJ domain is thought to be essential for proteolytic cleavage that occurs at the GPS (Qian et al., 2002). PKD2 encodes polycystin-2, a member of the TRP superfamily of nonselective Ca^{2+}-permeable ion channels (Clapham, 2003; Mochizuki et al., 1996). PKD2 functions at the plasma membrane, endoplasmic reticulum, and in the primary cilium to alter intracellular Ca^{2+} concentrations, activating effector proteins to drive cellular processes (Cai et al., 1999; Kottgen, 2007; Tsiokas, 2009; Tsiokas et al., 2007). Both PKD1 and PKD2 contain a coiled-coil domain in the intracellular C-terminus to allow for the formation of a receptor-channel complex

(Casuscelli et al., 2009; Qian et al., 1997). This complex is thought to play a major role in regulating levels of intracellular Ca^{2+}, where activation of PKD1 induces Ca^{2+} entry via PKD2 (Hanaoka et al., 2000; Vandorpe et al., 2001).

The identification of both *pkd1* and *pkd2* mutations in patients with ADPKD has yielded the hypothesis that the two genes are necessary and act in the same molecular pathway for the development of normal renal parenchyma. Interestingly, both a germ-line mutation and a somatic mutation are necessary to develop cystic kidneys, which has led to a two-hit model of cystogenesis (Kottgen, 2007; Pei et al., 1999). This theory explains why the severity of cyst development varies between patients with an identical allelic mutation. The complexity of this condition has currently hindered the ability to generate treatments for patients. Symptoms, such as high blood pressure, are managed with drugs and cystic development is watched closely but cannot be suppressed. Therefore, it is important for scientists to continue to identify downstream pathways that are essential in the maintenance of normal renal tissue, so pharmacological treatments can be generated that will abrogate the formation of cysts and cardiovascular defects

Animal models of ADPKD

Genetic manipulation strategies have been implemented in model systems to obtain insights into the molecular mechanism(s) of ADPKD. Homologs for both PKD1 and PKD2 have been identified in mice and zebrafish (Mangos et al., 2010; Obara et al., 2006; Roelfsema and Breuning, 1996; Wu et al., 1998). Mice homozygous for mutations in either *pkd1 or pkd2* usually die prior to E16.5 due to development of cysts in the kidney and pancreas, while heterozygous carriers generally develop cysts as adults (Lantinga-van Leeuwen et al., 2004; Lantinga-van Leeuwen et al., 2007; Lu et al., 1999; Lu et al., 1997; Wu et al., 1998). In addition mouse *pkd2*

knockouts develop cardiac abnormalities and *situs inversus*, a reversal of visceral organ placement (Pennekamp et al., 2002; Wu et al., 1998). Mice that have lowered expression of PKD1 also develop cystic kidneys demonstrating the requirement for a specific concentration of PKD1 to maintain normal renal development (Lantinga-van Leeuwen et al., 2004). Interestingly, a PKD rat model treated with a Ca^{2+} channel blocker increased cystic development, whereas a Ca^{2+} mimetic inhibited late stage cystic development (Gattone et al., 2009; Nagao et al., 2008). This suggests that the decrease in intracellular Ca^{2+} in PKD mutants causes the formation of kidney cysts.

Zebrafish develop a functioning pronephros by 48hpf, and can survive in the absence of blood flow for five days making this an idea system to study cystic diseases (Drummond, 2003; Drummond, 2005; Yelon, 2001). Suppression of *pkd2* in zebrafish results in hydrocephaly, loss of left-right asymmetry, a curved body, cloacal occlusions and pronephric cysts, while knockdown of *pkd1* causes tail curvature and pronephric cysts (Mangos et al., 2010; Obara et al., 2006; Schottenfeld et al., 2007). Similarly, injection of mRNA encoding *pkd2* that either lacks the coiled-coil domain or inhibits Ca^{2+} channel activity develops pronephric cysts in zebrafish (Feng et al., 2008). Interestingly the absence of the PKD1 C-terminal tail has been found to cause cyst development in lipid bilayers and Xenopus oocytes, while the overexpresion of the PKD1 C-terminal tail causes cysts in zebrafish embryos (Aguiari et al., 2003; Low et al., 2006; Vandorpe et al., 2001).

Animal models of polycystic kidney disease demonstrate the requirement for coordinated regulation of kidney development. Proliferation, apoptosis, polarity, migration, and cellular morphology are important processes that have to be balanced to form normal tissue. Absence of

intracellular Ca^{2+} disrupts this balance leading to cystic development. Identifying the downstream effector(s) will aid in identifying therapeutic targets for ADPKD.

Cellular mechanisms involved in ADPKD pathology:

Proliferation and apoptosis

A balance between proliferation and apoptosis is necessary to maintain a functioning kidney. Dissection of cystic kidneys revealed an increase in epithelial cell number around cysts (Grantham et al., 1987). Ca^{2+} channel dead PKD2 mutants proliferate faster and EGF-stimulated proliferation is increased in cells that lack PKD2 (Grimm et al., 2006). These results point to PKD2 as a negative regulator of cell proliferation. However, tubular epithelial cell apoptosis is also increased in animal models of ADPKD and in human kidneys of patients with ADPKD (Woo, 1995). Caspase inhibition has been shown to reduce cystic development in animal models of cystic kidney disease (Tao et al., 2005a; Tao et al., 2005b; Tao et al., 2008). It is believed that healthy kidney tissue undergoes apoptosis to allow for the cystic tissue to proliferate, demonstrating the requirement for both mechanisms in the development of ADPKD pathology.

Cilia

The localization of PKD1 and PKD2 to the primary cilium has generated compelling evidence that this complex may act as a flow sensor, where bending of the cilia is associated with an influx of Ca^{2+} into the cell (Praetorius and Spring, 2001; Praetorius and Spring, 2003; Yoder

et al., 2002). Mutations in ciliary assembly proteins, *ift88* and *kif3a*, fail to develop motile cilia and lack fluid flow causing the formation of kidney cysts in zebrafish and mice (Colantonio et al., 2009; Lin et al., 2003; Vasilyev et al., 2009). ADPKD cyst epithelia cells fail to initiate flow sensitive Ca^{2+} signaling pathways that are essential in maintaining kidney homeostasis (Nauli et al., 2003). ADPKD patients with mutations in PKD2 have reduced ER Ca^{2+} stores as well as an overall loss of intracellular Ca^{2+} (Hooper et al., 2005; Yamaguchi et al., 2006; Yamaguchi et al., 2004). In addition, calcium induced calcium release (CICR) from the ER, either through ER localized PKD2 or IP3R, normally causes a rise in intracellular Ca^{2+} thereby activating downstream pathways (Li et al., 2005). Although intracellular Ca^{2+} increases, the downstream effector proteins that help maintain normal function and prevent cyst formation have yet to be identified (Kottgen, 2007).

Polarity

Analysis of patients with ADPKD found that adult renal cells revert to a fetal epithelial organization, where the normally polarized proteins, EGFR and $Na^{+/}K^{+-}$ATPase, are mislocalized to the apical membrane (Burrow et al., 1999; Wilson et al., 2000). Cystic zebrafish mutants, such as *fleer* and *big league chew*, also mislocalize $Na^{+/}K^{+-}$ATPase to the apical membrane (Drummond et al., 1998). PKD2 is mislocalized from the basolateral membrane in *pkd2* morphants or embryos ectopically expressing *pkd2* mutations (Feng et al., 2008; Obara et al., 2006). Non-canonical Wnt signaling pathways also play a role in establishing apico-basolateral polarity; mice lacking Wnt9b lose planar cell polarity and develop cystic kidneys (Karner et al., 2009). Other core planar cell polarity proteins also lead to pronephric cysts when suppressed in zebrafish (Skouloudaki et al., 2009). It is reasonable to believe that a balance between cellular

proliferation, apoptosis and polarity maintain normal kidney homeostasis. A subtle disruption in this equilibrium could lead to cystogenesis in patients with ADPKD.

Summary

Although many studies demonstrate that PKD2 is important in regulating intracellular Ca^{2+} levels, few studies have identified the downstream effector. A recent study in the Tombes lab has identified CaMK-II as a downstream mediator of PKD2 Ca^{2+} in the Kupffer's Vesicle (KV), the ciliated organ necessary for establishment of left/right asymmetry. Knockdown of *pkd2* caused a reduction in and mislocalization of active CaMK-II around the KV resulting in randomization of *southpaw* expression in the lateral plate mesoderm (Francescatto et al., 2010). This work is the first to identify a Ca^{2+}-dependent protein downstream of PKD2.

Evidence is presented here that CaMK-II is the target of PKD2 Ca^{2+} in the developing zebrafish kidney. Active CaMK-II is found in the zebrafish pronephric duct beginning at 24hpf, peaks at 30hpf, and remains through 3dpf. Suppression of γ1 CaMK-II induces hydrocephaly, cloacal occlusions, pronephric cysts, loss of left-right asymmetry, and defects in ear development. Knockdown of PKD2 inactivates CaMK-II and ectopic expression of CaMK-II in *pkd2* morphant embryos partially reverses the cystic phenotype. CaMK-II is expressed and localized at the perfect time to be the ideal signaling molecule that decodes intracellular Ca^{2+} signals initiated by morphogenesis or physiological stimuli to maintain kidney homeostasis during development.

MATERIALS AND METHODS

Zebrafish strains and care

Wild type (AB and WIK), Tg(α1 subunit Na^+K^+ATPase:GFP) and Tg(β-actin:CAAX-GFP) fish embryos were obtained through natural matings, raised at 28.5°C as previously described (Kimmel et al., 1995).

Whole mount *in situ* hybridization

Digoxigenin-labeled anti-sense riboprobes (0.5–1.5 kb) were synthesized using T3 or T7 RNA polymerase from cloned cDNAs, hybridized with fixed embryos and then developed using alkaline phosphatase-conjugated anti-digoxigenin antibodies as described in chapter 2. The generation of *gata3, cdh17, wt1a*, and *ret1* were completed as previously described (Wingert and Davidson, 2008; Wingert et al., 2007). A plasmid encoding the *pax2a* cDNA was linearized using Not1 and transcribed with Sp6 RNA polymerase. A γ1c antisense probe was generated from 48hpf kidney cDNA, TOPO cloned, linearized with Not1 and transcribed using the T3 RNA polymerase. Fluorescent *in situ* hybridization was conducted as described in chapter 3. Fluorescent images were acquired using a NIKON C1 laser scanning confocal microscope.

CaMK-II antibodies

Immunolocalization using anti-phosphorylated (Thr^{287}) CaMK-II has previously been described by this laboratory (Easley et al., 2006). All zebrafish CaMK-IIs have a sequence of MHRQE[pT^{287}]VECLK in this region (Rothschild et al., 2009; Rothschild et al., 2007), which is very similar to the phosphopeptide antigen used to create this rabbit polyclonal antibody

(MHRQE[pT]VDCLK; Upstate/Millipore) and are therefore predicted to cross-react. The underlined glutamic acid (E) in zebrafish is the only (conservative) change (from the underlined aspartic acid (D)) in the epitope. This antibody has been shown to react with autophosphorylated (P-Thr^{287}) mammalian CaMK-II (Rich and Schulman, 1998). The pan-specific mouse monoclonal antibody (total CaMK-II) used in this study (BD Biosciences) was determined by immunoblot to be reactive with all ectopically expressed zebrafish CaMK-IIs tested so far including α1KAP, $\delta 1_G$ and $\beta 1_K$, although it was not sufficiently reactive to detect total CaMK-II in whole mount embryos until ~24hpf.

Pronephric dissection and flow sorting

For pronephric dissection Na^+/K^+-ATPase:GFP-transgenic embryos at 24, 48, and 72hpf were anesthetized and incubated in 10mM DTT for one hour in egg water. After several washes in egg water embryos were incubated in 5mg/ml collagenase for 3-6 hours at 28.5°C in DMEM. After gently pipetting embryos, the dissected pronephros were manually extracted under GFP epifluorescence illumination on a Nikon AZ100 stereoscope and placed into 1xPBS (Liu et al., 2007). Dissected pronephros were dissolved in Trizol Reagent (Invitrogen) to make RNA or harvested for CaMK-II activity assays as previously described in Chapter 2 (Rothschild et al., 2009; Rothschild et al., 2007). For flow sorted kidney cells, embryos were incubated in collagenase as described above for 6 hours then placed into 0.25% trypsin/EDTA for 30 minutes at 28.5°C. Embryos were filtered through mesh prior to sorting on a Becton-Dickinson FACS Aria II high-speed analyzer/sorter. Na^+/K^+-ATPase:GFP positive cells were dissolved in Trizol to generate RNA as stated above.

CaMK-II activity assay

Whole embryos were lysed or GFP pronephros were obtained and total CaMK-II activity was assessed by measuring phosphate incorporation into the substrate, autocamtide-2, as previously described (Rothschild et al., 2007).

Immunolocalization

Embryos were fixed in 4% paraformaldehyde (Phalloidin) in PBS and stored in methanol (P-CaMK-II, total CaMK-II, and acetylated tubulin) or fixed in Dent's fixative (80:20 Methanol:DMSO) (kidney specific alpha−1 subunit Na^+K^+-ATPase (α6F), atypical protein kinsae C (aPKC), and γtubulin). Embryos were incubated with rabbit anti-phospho-Thr^{287} (Millipore) (1:20), mouse anti-total CaMK-II (BD Biosciences) (1:20), mouse anti-acetylated α-tubulin antibody (Sigma Chemical Co.) (1:500), mouse anti-α6F (Developmental Studies Hybridoma Bank, University of Iowa) (1:10), rabbit anti-aPKC (Santa Cruz) (1:10), or mouse anti-γtubulin (Sigma Chemical Co.) (1:500) followed by either goat anti-mouse $Alexa^{488}$, goat anti-mouse $Alexa^{568}$, or goat anti-rabbit $Alexa^{568}$ (Invitrogen) (1:500). Embryos were permeabilized using NP-40 prior to the addition of Alexa-488 phalloidin (Invitrogen) (1:50). Embryos were imaged using confocal microscopy (Nikon C1 Plus two-laser) on a Nikon E-600 compound microscope using a 100X oil immersion objective.

mRNA generation

Vectors encoding cytosolically targeted wild type and constitutively active ($T^{287}D$) CaMK-II δ_E in pCDNA3 were linearized using AvrII and transcribed using the T7 mMessage kit (Ambion).

Immunoblot

Dissected pronephros were lysed and prepared as described above. Equivalent amounts of soluble protein were immunoblotted as described (Lantsman and Tombes, 2005) using 1 _g/ml P-CaMK-II antibody (Millipore), and a pan-specific CaMK-II antibody (BD Biosciences).

Morpholino and cDNA injections

The zebrafish pkd2 MO (5'-AGGACGAACGCGACTGGAGCTCATC-3') was previously described and was purchased from GeneTools (Philomath OR) (Sun et al., 2004b). The *camk2g1* MO was described in chapter 2. Morpholino stocks (1mM) were stored in aliquots at -80ºC. Prior to injection, aliquots were heated to 65ºC for 5 min, cooled to room temperature and then diluted in Danieau buffer. 4.5pg and 1pg of MO was injected into embryos at the 1-4 cell stage for pkd2 and *camk2g1*. A constant injection volume of 1nl was measured prior to injection. Co-injection of CaMK-II δ_E was described in chapter 3.

High speed video microscopy

Live embryos were imaged using differential interference contrast optics after transient anesthesia with 0.003% Tricaine (MS222, Sigma) and immobilization between coverslips. Ciliary motility was imaged in the kidney and otic vesicle of live, anesthetized embryos using a NIKON 60X water immersion Plan APO objective with DIC optics and 25 frames per second acquisitions. Lengths of cilia in fixed embryos were determined from anti-acetylated α-tubulin whole mounts using quantitative length algorithms in Nikon Elements version 3 experimental replicates for at least ten embryos per replicate. Statistical analyses were performed using the

paired t-test. Statistically significant differences are denoted by an asterisk and indicated P-values.

RESULTS

Activated CaMK-II localizes to the CNS, embryonic kidney and ear

To determine tissue localization of total and activated CaMK-II two well-characterized antibodies were used; the first detects all CaMK-II and is reactive with the C-terminal region, while the second recognizes phosphorylated T^{287}, the autophosphorylation site responsible for autonomous CaMK-II activity (Easley et al., 2006). The specificity of the antibody was established by overexpression of zebrafish CaMK-II in mPCT cell culture. CaMK-II activation was determined by P-CaMK-II and total CaMK-II immunoblots after autophosphorylation over time on ice. The resulting blot demonstrated that the level of total CaMK-II remained the same but the level of immunoreactivity with the P-CaMK-II antibody was proportional to autonomy (Francescatto et al., 2010).

Since CaMK-IIs are enriched in the central nervous system, it was not surprising that total CaMK-II was first detected in the brain and spinal cord. 30hpf zebrafish embryos express CaMK-II in the forebrain region and in both cells and axonal projections of the telencephalon as shown by co-localization with acetylated tubulin (Figure 4.1a-d). Interestingly, certain cell clusters have high levels of total CaMK-II but little active CaMK-II, identifying different activation states. Expression of highly active CaMK-II, but not acetylated tubulin, in axonal projections may demonstrate the need for CaMK-II in axonal pathfinding *in vivo*, given that acetylated tubulin is required for axon stabilization (Figure 4.1d). In addition, CaMK-II was also

identified in cell bodies of spinal cord sensory neurons (Figure 4.1e-g), but was absent from sensory axons (Figure 4.1h).

High levels of total CaMK-II and low levels of highly active CaMK-II were found in the muscle sarcomeres within the somites (Figure 4.1i-k). CaMK-II is important in muscle contractions through ryanodine receptor phosphorylation, which cause Ca^{2+} extrusions from the ER. This process requires CaMK-II to be activated and inactivated quickly to generate the cyclical release and reuptake of Ca^{2+} from the ER. This rapid activation and deactivation would limit the amount of highly active CaMK-II in these cells (Maier and Bers, 2002; Schneider and Rodney, 2004).

The identification of CaMK-II in the kidney (pronephros) and embryonic ear (otic vesicle) was unexpected. The pronephros is the larval kidney that functions to filter blood and remove waste. Active CaMK-II was identified on the apical face of cells lining the pronephric ducts (Figure 4.1j) and on all cortical sides of cells (Figure 4.1l). Total CaMK-II levels were low but visible, demonstrating a high level of Ca^{2+} independent activity within the pronephros (Figure 4.1i). In the otic vesicle, total CaMK-II was enriched in the cells from which emerge the kinocilium, an organelle necessary for otolith formation and hearing. Zebrafish otoliths are similar to mammalian otoconia, which are “stones” of the inner ear necessary for balance and hearing. Active CaMK-II was enriched at the base of the kinocilium and was also found throughout the cytosol. The identification of highly active CaMK-II in ciliated organs may point to a role for CaMK-II in preventing “ciliopathies” such as deafness and cystic kidney diseases (Fliegauf et al., 2007; Nigg and Raff, 2009).

Differential activation of CaMK-II along the zebrafish kidney

The zebrafish pronephros is the first kidney to form and function to filter blood through the larval stage of development. It is composed of two nephrons with two glomeruli fused at the midline. Pronephric tubules connect the glomeruli to pronephric ducts, which are used to excrete waste out the cloaca at the distal end of the pronephric duct. Pronephros development can be categorized into four stages. Specification begins at 12hpf and is followed by epithelialization of the pronephric duct between 16-24hpf. Nephron patterning occurs between 30 and 40hpf and angiogenesis begins at 40hpf (Drummond, 2002; Drummond, 2003). P-CaMK-II was assessed along the kidney during these established stages of pronephros development. Active CaMK-II is easily seen at 24hpf, at the end of the epithelialization stage, on the apical side of ciliated cells lining the pronephric duct and in a cortical pattern in the cloaca (Figure 4.2a). Active CaMK-II is found within cloacal cilia as demonstrated by co-localization with acetylated tubulin (Figure 4.2b,c, arrowhead), but is not found in ductal cilia. Active CaMK-II is targeted to the membrane in the cloaca as shown by co-localization with a membrane targeted CAAX:GFP expressing embryos (Figure 4.2c, arrow).

Activation peaks at 30hpf, at the beginning of nephron patterning, where P-CaMK-II is found in both apical and basolateral membranes of the proximal pronephric duct and at high levels in the distal pronephric duct and cloaca (Figure 4.2d-f).

The $\alpha 1$ subunit of Na^+K^+-ATPase is located in a discontinuous pattern along the pronephric ducts in transporting epithelial cells and is excluded from multiciliated cells. Active CaMK-II co-localizes in the basolateral membrane with some Na^+K^+-ATPase expressing cells. (Figure 4.2g-i) CaMK-II remains highly active but not diminished in the kidney through 72hpf, where expression is noticeable in the distal pronephric duct, cloaca, and cloacal cilia (data not

shown). Interestingly, there is a loss of active CaMK-II in a small segment towards the distal end of the pronephric duct, which is first noticeable at 24hpf and persists throughout embryonic development denoted as a gap in Figure 4.2j.

KN-93 reduces active CaMK-II in the kidney

The specificity of the P-CaMK-II antibody in immunolocalization was evaluated by incubating embryos in KN-93, a well-characterized CaMK-II inhibitor. KN-93 inhibits CaM from binding to CaMK-II, thus blocking activation and preventing Thr^{287} autophosphorylation. Embryos were continuously treated from cleavage stages with 10 μM KN-93, fixed at 30hpf, immunolabeled with P-CaMK-II, and imaged. KN-93 treatment visibly reduced the level of active CaMK-II in the distal pronephric duct and cloaca (Figure 4.3b,c). In addition, Na^+K^+-ATPase:GFP embryos were collagenase treated to excise kidneys at 3dpf (Figure 4.3d,e). The GFP positive pronephric ducts were harvested and assessed for total and P-CaMK-II by immunoblot. For comparison, 6dpf whole embryo lysates were evaluated. Both 3dpf kidney lysates and 6dpf embryo lysates show a strong band at approximately 60 kDa representing endogenous CaMK-II that is enriched in the kidney (Figure 4.3f). Furthermore, highly active CaMK-II was only evident in the kidney lysate (Figure 4.3g). These results support the specificity of the P-CaMK-II antibody for activated CaMK-II and suggest that not only is CaMK-II enriched in the kidney but that it is highly active (see Figure 4.10).

γ1 CaMK-II mRNA is expressed in the kidney

To determine which of the seven CaMK-II genes is present in the pronephric duct during zebrafish development Na^+/K^+-ATPase:GFP-transgenic pronephric ducts were either manually

sorted after collagenase treatment or trypsinized and sorted using a flow cytometer. Manually sorted pronephric duct cDNA was generated for 24, 48, and 72hpf embryos while flow sorted pronephric duct cDNA was generated for 48hpf embryos. Gene specific primers were used to amplify, TOPO clone, and sequence cDNAs to identify which CaMK-II genes and splice variants were present in the developing pronephros. $\gamma 1_C$ was the predominant variant in the zebrafish kidney, with no γ2, β1, or β2 CaMK-IIs identified in flow sorted cells. These primers have already been shown to amplify all seven genes (Chapter 2). $\gamma 1_C$ is a simple variant, encoding domains II, VI, and VII in the variable domain and is predicted to be cytosolic (Figure 2.3, Figure 2.4). A second variant, $\gamma 1_F$ was identified from manually dissected cDNAs, but absent from flow isolated cDNAs. $\gamma 1_F$ contains domains II, IV/V, VI, VII, VIII/IX in the variable domain. Domain VIII/IX is thought to contain membrane targeting sequences. The absence of this variant in flow sorted cells could be due to either mis-timing of expression of this variant and/or the presence of other tissue in the manually dissected pronephros that is absent in flow sorted cells.

To verify the expression of *camk2g1* in the pronephros, an antisense mRNA probe was generated against the $\gamma 1_C$ variant and whole mount in situ hybridization (WISH) experiments were performed for 18hpf, 28hpf and 72hpf embryos. Although CNS expression was predominant, expression in the pronephric duct region was identified at all three time points (Figure 4.4a-c, arrow). Pronephric duct expression was confirmed at 72hpf in cyrosections (Figure 4.4c', arrow). To verify these results, fluorescent in situ hybridization using the $\gamma 1_C$ probe was combined with immuno-staining of acetylated tubulin in 48hpf wild type embryos (Figure 4.4d). As shown above, acetylated tubulin was used as a marker for cilia in the pronephric duct lumen. In addition, double fluorescent in situ hybridization (DFISH) in 72hpf

wild type fish showed co-localization of *camk2g1* with *pax2a* (Figure 4.4e-g). Pax2a is the earliest marker of pronephros development and is expressed throughout the pronephric duct during embryogenesis. *Camk2g1* and *pax2a* co-localized in pronephric cells, while *camk2g1* was also evident in the ventral somites (Figure 4.4g, arrowhead). This mRNA expression pattern is consistent with the *camk2g1* gene encoding CaMK-II in the developing pronephros.

Suppression of γ1 CaMK-II causes cloacal occlusions and cyst formation

Camk2g1 expression was suppressed using the *camk2g1* translation-blocking antisense morpholino oligonucleotide (Table 2.3). Injection of 1 ng caused pericardial edema, hydrocephaly, cloacal occlusions and pronephric cysts (Figure 4.5a-f). Injection of higher concentrations (1.5-3 ng) yielded anterior-posterior axis defects, atrial enlargement, somite compression, and loss of left-right asymmetry (data not shown). Development of pronephric cysts could be viewed in whole mount at the level of the third somite, posterior to the pectoral fins (Figure 4.5c,d, arrowhead). Thin paraffin sections stained with hematoxylin and eosin confirmed that *camk2g1* suppression induced cyst formation (Figure 4.5g,h, asterisk). Cyst formation has also been observed in several mutants and morphants of proteins important in cilia and cloacal development. Therefore, cloacal development was assessed in 3dpf *camk2g1* morphants using whole mount DIC imaging (n=143) and 73% had visible cloacal occlusions (Figure 4.5e,f, arrow; Figure 4.6a). To determine if cilia development and assembly was disrupted, *camk2g1* morphant embryos were immunolabeled with an antibody against acetylated tubulin. Cilia were the proper length as compared to control embryos (control 8.9 μm $\pm$ 0.3 μm; g1 morphant 8.5 μm $\pm$ 0.8μm) (Figure 4.5k,l) and functioned normally in *camk2g1* morphants, as shown by ciliary beating at 3dpf in the pronephric duct (Supplemental Movie 2 and 3).

Pronephric cilia normally beat in a wave-like fashion, however cloacal cilia beat similar to shorter cilia of the KV or spinal cord (Supplemental Movie 4) (Kramer-Zucker et al., 2005). As shown above, highly active CaMK-II localizes to cloacal cilia and therefore may play a role in the development of cloacal occlusions in *camk2g1* morphants.

Development of the pronephros depends on the proper anterior migration of pronephric epithelial cells to form the convoluted proximal segment. This is visible as a hook-like structure in the anterior region of the pronephros, as shown by Na^+/K^+-ATPase antibody staining (Figure 4.5i, arrowhead). Previous research has shown that surgical obstruction of the distal segment blocked proximal migration, abolishing convolution (Vasilyev et al., 2009). To determine if suppression of *camk2g1* inhibited proper anterior convolution, Na^+/K^+-ATPase:GFP-transgenic and Na^+/K^+-ATPase antibody immunolabeled embryos were assessed at 3dpf for pronephric duct morphology. 87% of pronephric ducts failed to undergo convolution and remained straight and parallel (Figure 4.5j, Figure 4.6f). In addition, anterior migration can be determined by measuring the distance from the posterior ear to the anterior pronephric duct. In control embryos this distance is approximately 200μm at 3dpf. Suppression of *camk2g1* increased this distance to approximately 700um, implying a loss of anterior directed migration (Figure 4.6b).

Specification of the pronephros is not altered in *camk2g1* morphants

To determine if early specification or differentiation was altered in *camk2g1* morphants, in situ hybridizations were completed using known pronephric markers including, *pax2a, gata3, ret1, wt1a* and *cdh17* (Figure 4.7). Expression of pax2a, a paired box transcription factor, is evident in 14hpf control and morphant embryos (Figure 4.7a,b) demonstrating that even at high morpholino concentrations progenitor populations are intact (data not shown). At 24hpf, *pax2a*

expression persists in control and morphant embryos throughout the pronephros (Figure 4.7c,d). It is of note that darker expression occurs at the distal end possibly reflective of the cloacal obstruction (Figure 4.7c,d). Cadherin17 (*Cdh17*), expression was also analyzed at 24hpf, where it was expressed in all tubule and duct progenitors in both control and *camk2g1* morphants (Figure 4.7e,f). Since cloacal occlusion was evident using universally expressed markers of pronephros development, additional probes were used that are expressed in a subset of pronephric duct cells. To look more closely at the development of the cloaca *gata3* reveals expression in both control and *camk2g1* morphants (Figure 4.7g,h). *Ret1*, a receptor tyrosine kinase, appears in the collecting ducts (distal pronephric duct) of both control embryos and morphants (Figure 4.7i,j). Development of anterior structures is very important in generating the glomerulus, therefore *wt1a* was used to look at expression of podocyte lineage cells. Podocytes are thought to play a role in assembling the glomeruluar capillary tuft to enable filtration (Drummond, 2003). Although wt1a was expressed in *camk2g1* morphants, the field of expression appears expanded at 24hpf (Figure 4.7k,l). By 48hpf the two areas of wt1a expression migrate to the midline and fuse to form the glomerulus. Suppression of *camk2g1* inhibits the fusion of the wt1a fields, as two separate wt1a population of cells are evident (Figure 4.7m,n). This result is consistent with a possible reduction of cellular migration due to an obstructed pronephros.

Otolith development is defective in *camk2g1* morphants

Defects in cilia function and assembly cause a myriad of defects including the loss of left-right asymmetry, hydrocephaly, kidney cysts, and otolith development. Concentration dependent suppression of *camk2g1* generates similar phenotypes. Since P-CaMK-II is highly

active at the base of kinocilium in the embryonic ear at 30hpf, as shown above, *camk2g1* suppression was assessed to identify if activation of *camk2g1* was important in embryonic ear development. Kinocilia are one of two types of microtubule based cilia in the otic vesicle. There are two pairs of two to three motile kinocilia that beat to form the otoliths. The second type of cilia is short and immotile and is thought to play a sensory role in the embryonic ear.

As shown above (Figure 4.1), CaMK-II is also activated in the embryonic ear (otic vesicle) beginning at 24hpf and persisting at the base of the kinocilium until 30hpf (Figure 4.8a). Suppression of *camk2g1* and treatment with KN-93 both decreased P-CaMK-II levels in the otic vesicle (Figure 4.8b,c). To verify that embryonic ear development was not diminished due to a loss of specification or differentiation, the expression of *gata3* mRNA was evaluated. *Gata3* was expressed in the otic vesicle of control, *camkg1* morphant, and KN-93 treated embryos at 24hpf (Figure 4.8d-f). Ciliagenesis is important in the proper development of otoliths, as suppression of cilia assembly proteins leads to ectopic otolith formation (Colantonio et al., 2009). Therefore, embryos were immunolabeled with acetylated tubulin at 24hpf to evaluate kinocilia length (Figure 4.8g-i). No discernable difference was identified between control, *camk2g1* morphant, and KN-93 treated embryos (Figure 4.8j). However at 3dpf, *camk2g1* morphants that have ectopic otoliths show an alteration in number and location of kinocilia (data not shown).

Otic vesicle gross morphology was assessed at 3dpf in control, *camk2g1* morphant, and KN-93 treated embryos. More than 95% of control embryos had two otoliths, comprised of an anterior otolith and a larger posterior otolith (Figure 4.8k). Suppression of *camk2g1* (Figure 4.8l-l-n) and treatment with KN-93 (figure 4.8o,p) caused ectopic and abnormally shaped otoliths to develop. Often otoliths appeared smaller and fused (Figure 4.8q). Treatment with KN-93 after

26hpf did not alter otolith formation, pointing to an early requirement for active CaMK-II (data not shown). Otolith morphology analysis is summarized in Figure 4.8k.

To better understand the development of otoliths, high-speed video microscopy was used to view the tethered cilia beating and the $CaCO_3$ microcrystals aggregate to form the otoliths. Two sets of tethered cilia are present opposite each other in a 24hpf embryo. These tethered cilia can be easily visualized in control embryos (Supplemental movie 7 and 8). The cilia beat forming a localized vortex to aid in adding $CaCO_3$ microcrystals to the seeded otolith that form at the tip of the kinocilium (Supplemental movie 9). Suppression of cilia assembly proteins, *ift88* and *gas8*, caused ectopic otoliths to develop because the tethered cilia fail to beat (Colantonio et al., 2009). Suppression of *camk2g1* and KN-93 treatment does seem to alter tethered cilia beating and also appears to alter the stability of the central kinocilia (Supplemental movies 10-13). The tethered cilia seem to beat irregularly in some *camk2g1* morphants, which may cause the microcrystals that enter into the vortex to move irregularly as compared to control embryos. However, the $CaCO_3$ microcrystals continue to move in both *camk2g1* morphants and KN-93 treated embryos (Supplemental movies 14). The combination of the instability of the central kinocilia and the failure of the microcrystals to move correctly may explain the alterations in otolith development.

Ectopic expression of CaMK-II rescues cyst Development in *pkd2* morphants

CaMK-II activation is dependent on Ca^{2+} entry into the cytosol either through extracellular or intracellular sources. There are several Ca^{2+} channels in the ER, plasma membrane and cilia that could influence the activation of CaMK-II in the kidney. Previous work in the Tombes lab has demonstrated that knockdown of *pkd2* in zebrafish embryos caused a

reduction in active CaMK-II around the KV (Francescatto et al., 2010). Since PKD2 is a member of the TRP superfamily of nonselective Ca^{2+} permeable channels and is expressed in the kidney, it is plausible that CaMK-II acts downstream of PKD2 during kidney development.

4.5 ng of a *pkd2* translation blocking morpholino was injected alone or co-injected with either 40ng/ul of cytosolically targeted, GFP tagged wild type or constitutive active ($T^{287}D$) δ_E CaMK-II under the control of the β-actin promoter as described above. Embryos were assessed at 3dpf for cloacal occlusions, hydrocephaly, and tail curvature through DIC images (Figure 4.9a-c). Approximately 89% of PKD2 morphants developed obstructed pronephric ducts, 97% had hydrocephaly, and 96% exhibited tail curvature. Ectopic expression of constitutively active, but not wild type, CaMK-II reversed cloacal obstructions in 46% of embryos (Figure 4.9d-f). Hydrocephaly and tail curvature could not be rescued as well by overexpression of CaMK-II. GFP-CaMK-II expressing *pkd2* morphants were also assessed for anterior pronephric duct convolution at 72hpf in Na^+/K^+-ATPase:GFP embryos or Na^+/K^+-ATPase antibody immunolabeled embryos. 5% of *pkd2* morphants and 48% of constitutively active CaMK-II expressing morphants displayed proper convolution, respectively (Figure 4.9g-j). These results are summarized in Figure 4.9m.

To complement the rescue, the distance between the posterior otic vesicle and the anterior pronephric duct was measured, as described above. *Pkd2* morphant pronephric epithelia failed to migrate anteriorly, as previously reported (Vasilyev et al., 2009), causing a 600μm distance to form compared to 200μm in control embryos. Ectopic expression of cytosolically targeted constitutively active CaMK-II partially reduced the distance from the ear to the anterior pronephric duct to 350μm (Figure 4.9n). Although 52% of *pkd2* morphants co-injected with constitutively active CaMK-II did not show a complete rescue of proximal tubule convolution,

the pronephric epithelia appeared to migrate anteriorly, as demonstrated by measuring the distance between the proximal tubule and the posterior otic vesicle. The lack of a complete rescue could be due to the mosaic expression pattern that results from injection of a cDNA, where only a subset of pronephric epithelia expressed constitutively active CaMK-II. To address this issue, mRNA was generated and injected sequentially with 4.5ng of *pkd2* morpholino and assessed at 3dpf. Constitutively active CaMK-II mRNA was degraded rapidly and therefore was unable to rescue the cystic phenotype (data not shown). Together, these data suggest that CaMK-II may be the downstream effector of PKD2 Ca^{2+} in the zebrafish pronephric duct.

Activated CaMK-II is reduced in *camk2g1* and Pkd2 morphant embryos

To determine if PKD2 Ca^{2+} activates CaMK-II, the P-CaMK-II antibody was used in whole mount embryos and CaMK-II activity assays were completed on manually dissected pronephros. Since P-CaMK-II activity peaks at 30hpf in the kidney, control, *camk2g1* and *pkd2* morphants were fixed at 30hpf and levels of P-CaMK-II assessed in the distal pronephric duct. Control embryos had high levels of active CaMK-II in apical regions of the duct, lower levels in the basolateral membrane, and clusters of highly active CaMK-II were visible in the cytosol (Figure 4.10a). Suppression of *camk2g1* reduced the level of active CaMK-II in the apical membrane, with very little P-CaMK-II visible in the basolateral membrane and subcellular clusters (Figure 4.10b). Knockdown of *pkd2* caused a marked reduction of active CaMK-II in the apical membrane, with a loss of P-CaMK-II in basolateral membranes and clusters (Figure 4.10c). CaMK-II activity assays were also completed on excised pronephric ducts to determine if CaMK-II autonomy also decreased in *pkd2* morphants. In fact, CaMK-II autonomy was

decreased by approximately 40% in manually excised pronephric cells (Figure 4.10d). These results point to CaMK-II as the PKD2 Ca^{2+} target in the zebrafish kidney.

Actin polarity is altered in *camk2g1* morphants

Since CaMK-II is known to influence cytoskeletal organization and stabilization, cell polarity was evaluated in *camk2g1* morphants. To examine F-actin, embryos were fixed at 24hpf and immunolabeled with Alexa^{488} phalloidin. Control embryos maintained apical localization of F-actin in the cloaca, while F-actin was mislocalized to both apical and basolateral membranes in *camk2g1* morphants (Figure 4.11a,b). Cell morphology was also altered in the distal end of the cloaca, where *camk2g1* morphant cells failed to become columnar (Figure 4.11b). In the distal pronephric duct, F-actin appeared slightly disorganized compared to control embryos (Figure 4.11c,d). Similar to other cystic mutants and morphants, *camk2g1* knockdown also mislocalized Na^+/K^+-ATPase from the basolateral to apical membrane in the proximal pronephric duct (Figure 4.11i,j). *Camk2g1* morphants, however, showed proper apical polarity of γ-tubulin, a protein found in basal bodies, and of the apical membrane marker atypical protein kinase C, aPKC, in the cloaca and distal pronephric duct (Figure 4.11e-h). These results identify CaMK-II as an important protein in maintaining the F-actin cytoskeleton in the pronephros, where a loss of *camk2g1* leads to cloacal obstructions and ultimately cyst development.

DISCUSSION

This study identifies the first direct downstream target of kidney PKD2 Ca^{2+} and implies a role for CaMK-II in ADPKD pathology. Suppression of *camk2g1* induces cloacal occlusions, hydrocephaly and pronephric cysts similar to *pkd2* morphants. Activation of CaMK-II requires PKD2 Ca^{2+} for maintenance of normal renal epithelial cells in the zebrafish since *pkd2* morphants have a reduction in active CaMK-II. *Camk2g1* morphants have reduced anterior migration and abnormal actin polarity, pointing to these mechanisms as the principal cause of cystogenesis in *camk2g1* morphants.

Cloacal obstruction and CaMK-II

Development of the cloaca requires cellular proliferation, cell shape changes, and establishment of apico-basal polarity (Pyati et al., 2006; Vasilyev et al., 2009). Unlike proximal epithelial cells, cloacal cells do not migrate, however improper cloacal development has been shown to inhibit proximal pronephric epithelial migration (Vasilyev et al., 2009). The formation of the cloacal opening requires cells to undergo a cuboidal to columnar cell transformation (Pyati et al., 2006). *Camk2g1* morphant cloacal cells fail to undergo this morphological change and remain cuboidal. In addition, the actin cytoskeleton is altered where F-actin is found in both apical and basolateral membranes, as compared to apical in control embryos. In *Xenopu*s and *Drosophila* embryos apical constriction is necessary to alter cell morphology during gastrulation (Kam et al., 1991; Keller, 1981; Sweeton et al., 1991). Loss of this apical constriction leads to alterations in cell shape that inhibit proper tissue development (Daggett et al., 2007). F-actin organization is also lost in *arhgef11*, a Rho GEF, morphant embryos in which pronephric cysts

form by 48hpf (Panizzi et al., 2007). The lack of polarity inhibits the morphological changes necessary to generate the cloacal opening, thereby inducing the formation of pronephric cysts.

PKD1 is also known to interact with E-cadherin complexes, which contain β-catenin, generating the hypothesis that PKD1 influences β-catenin signaling (Geng et al., 2000; Wilson, 2001). Wnt ligand binding causes β-catenin to dissociate from E-cadherin complexes, then it is shuttled into the nucleus to influence transcription of TCF/LEF dependent genes (Moon et al., 2002; St Amand and Klymkowsky, 2001). Tiam1, a Rac GEF and known substrate of CaMK-II, is necessary to form and maintain cadherin-based adhesions (Malliri et al., 2004). In addition, primary ADPKD cell culture experiments demonstrated the importance of the E-cadherin/β-catenin complex, where a loss of adhesion alters renal epithelial function (Charron et al., 2000).

In addition to its role at adherins junctions, β-catenin is best studied in its role as a positive regulator of canonical Wnt transcription. Human and rodent cyst tissue upregulates the expression of c-myc, which is a β-catenin dependent gene, altering renal epithelial proliferation (Lanoix et al., 1996). Mouse models that overexpress c-myc develop kidney cysts throughout their life (Wilson, 2004a). In addition, CaMK-II has been shown to influence β-catenin transcription through an interaction with flightless-I (Fli-I), an actin binding and capping protein. Activation of CaMK-II inhibits Fli-I from translocating into the nucleus to inhibit TCF/LEF dependent transcription (Seward et al., 2008). However, suppression of Pkd2 or *camk2g1* does not appear to alter proliferation of zebrafish pronephric epithelial cells (Obara et al., 2006).

Recent research has determined that Fli-I also influences actin assembly through a Diaphenous related formin protein, mDia. mDia is the mammalian Diaphanous homolog1 and is thought to bind to Fli-I to enhance actin assembly (Higashi et al.). Therefore, it is possible CaMK-II forms a complex with Fli-I and mDia to regulate actin assembly in the zebrafish

pronephric duct. CaMK-II also binds to F-actin in P19 neurons, where inhibition of CaMK-II causes F-actin disorganization and reduced neurite outgrowth (Easley et al., 2006).

CaMK-II and pronephric epithelial cellular migration

Zebrafish pronephros development requires migration of the pronephric epithelia to form the embryonic kidney. Collective cell migration begins at 28.5hpf, coincident with highly active CaMK-II in the proximal pronephric duct, where pronephric epithelial cells undergo a proximal-directed migration toward the glomerulus. This migration occurs as a sheet, where apical cell connections are maintained and basal surfaces project lamellipodia at the leading edge under the cell in front. Cells that were migratory stained positive for phospho-FAK, demonstrating adhesion to the basement membrane and the requirement for focal adhesion turnover (Vasilyev et al., 2009). The inactivation of focal-adhesion complex proteins, such as PKD1 and tensin, leads to the development of cysts in mice (Lo et al., 1997; Wilson, 2004b). Suppression of *camk2g1* and *Pkd2* inhibited proper pronephric duct migration and anterior convolution, whereas *pkd2* morphants ectopically expressing constitutively active CaMK-II partially recovered cellular migration.

CaMK-II and PKD1 have been identified at focal adhesions (Easley et al., 2008; Wilson et al., 1999). PKD2 forms a receptor channel complex with PKD1, where PKD1 interacts with the extracellular matrix (ECM) and focal adhesion proteins (Wilson, 2004a; Wilson, 2008). ADPKD patients that have mutations in PKD1 have increased adhesiveness to the ECM and decreased motility, this is identical to studies where CaMK-II is acutely inhibited in mouse fibroblasts (Easley et al., 2008; Wilson et al., 1999). Focal adhesion turnover requires the dephosphorylation of tyrosine residues on paxillin and FAK (Mitra et al., 2005). PKD1 co-

localizes with paxillin in renal cell culture, demonstrating a possible link between PKD1 and CaMK-II at focal adhesions (Israeli et al., ; Wilson, 2001). CaMK-II also influences cell motility through the phosphorylation of Tiam1 to activate Rac and enable cells to secrete ECM proteins for adhesion and migration (Fleming et al., 1999). Therefore the lack of migration in proximal epithelial cells in Pkd2 and *camk2g1* morphants could be due to the inhibition of CaMK-II at focal adhesions.

Alternative CaMK-II substrates during kidney development

mDia also functions to inhibit PKD2 channel activity under resting potentials, where mDia remains in the autoinhibited conformation. Upon EGFR activation a conformation change occurs in mDia allowing for channel activation and Ca^{2+} entry into the cytosol of LLC-PK1 kidney epithelial cells (Bai et al., 2008). CaMK-II is known to phosphorylate proteins to alter intracellular Ca^{2+} concentrations, either directly or indirectly to influence cellular mechanisms. In the heart CaMK-II phosphorylates ryanodine receptors to release Ca^{2+} from the ER and phosphorylates phospholamban to initiate reuptake of Ca^{2+} back into the ER through SERCA (Maier, 2009). This process allows for excitation-contraction coupling in the heart. PKD2 has structural similarities to voltage-activated L-type Ca^{2+} channels, a known substrate of CaMK-II (Grueter et al., 2006; Mochizuki et al., 1996). Although CaMK-II has not been shown to phosphorylate PKD2, several CaMK-II consensus sites are located throughout the PKD2 sequence.

Histone deacetylases (HDAC) have become a therapeutic target in cancer treatment, where inhibition of HDACs allow transcription of genes normally downregulated. Recent research has demonstrated that HDAC5 may also be a viable target in treating ADPKD.

HDAC5, a class II histone deacetylase, is phosphorylated in a Ca^{2+}-dependent manner and then shuttled to the cytosol. As a result MEF2C target genes are activated, including missing in metastasis (MIM), which is involved in actin cytoskeletal dynamics. *Mef2c* knockout mice and MIM-deficient mice develop tubule dilations and cysts, while inhibition of HDAC5 in Pkd2-/- mice suppresses renal cyst formation (Xia et al.). Similarly, in the heart CaMK-II phosphorylates HDAC4, also a class II histone deacetylase, which retains HDAC4 in the cytosol to upregulate MEF2C target genes (Little et al., 2007; Zhang et al., 2007). These results identify CaMK-II as the possible effector protein activated by PKD2 Ca^{2+} to phosphorylate HDAC5 to maintain normal renal development.

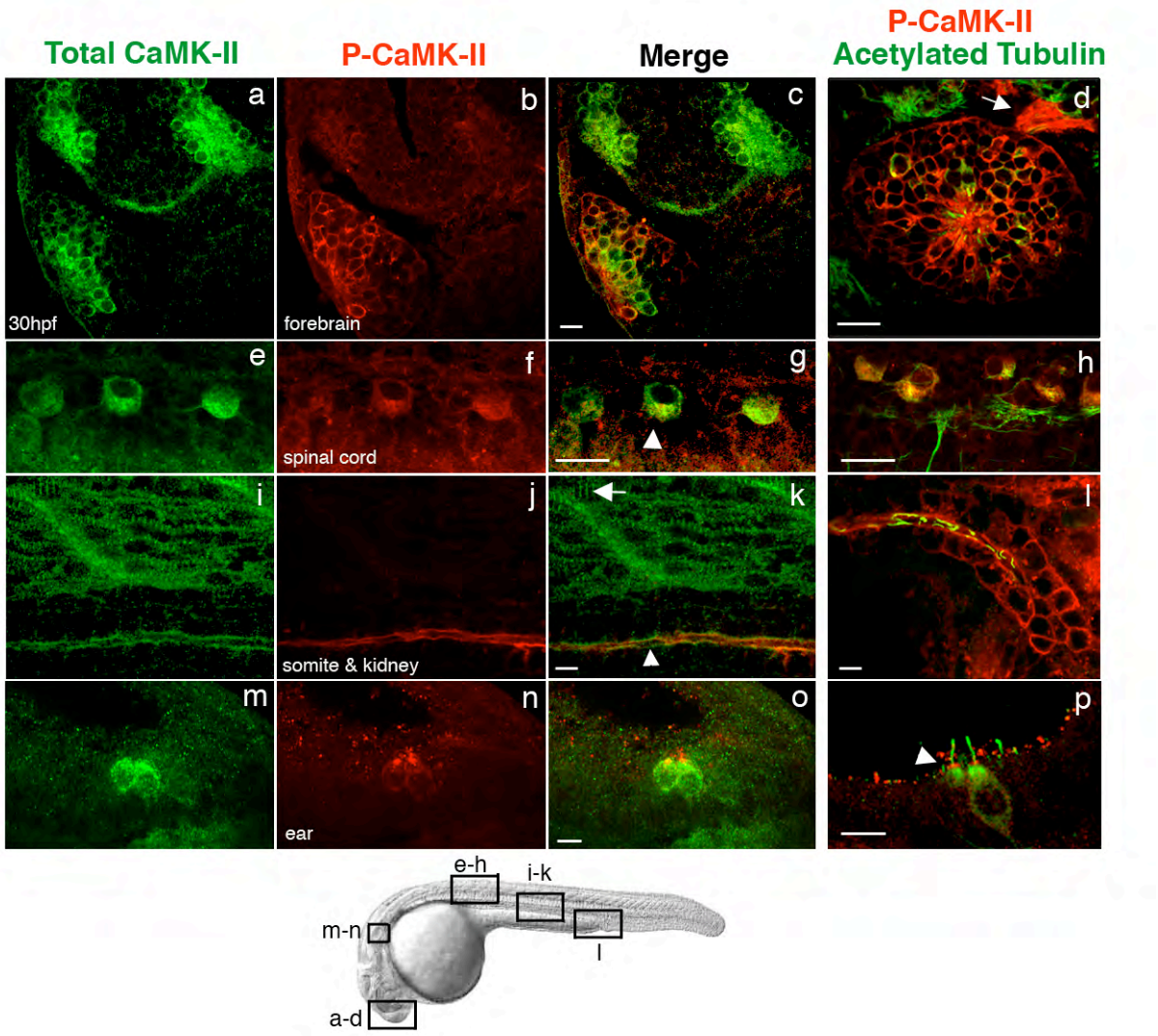

Figure 4.1. CaMK-II localizes to the CNS, somites, embryonic ear and kidney. Total CaMK-II (a,e,i,m) and P-CaMK-II (b,f,j,n) co-localize in the forebrain (a-c,), spinal cord cell bodies, (e-g, arrowhead in g), muscle sarcomeres and apical membranes of the kidney (i-k) and embryonic ear (m-o) at 30hpf. P-CaMK-II co-localizes with acetylated tubulin in some cells and axons in the forebrain (d) and in spinal cord cell bodies, but is undetectable from spinal cord axons (h). P-CaMK-II localizes cortically in cloacal cells but does not co-localize with pronephric duct cilia (l). Active CaMK-II is enriched at the base of the hair cell kinocilium (p, arrowhead), but is also cytosolically enriched in these cells. Scale bars= 10 μm.

Figure 4.2. Differential activation of CaMK-II in the kidney.

(a-c) Active CaMK-II is first evident at 24hpf in the pronephric ducts, cloaca and cilia. P-CaMK-II co-localizes with acetylated tubulin in cloacal cilia but is absent from pronephric duct cilia (b,c, arrowhead). Cortical localization of P-CaMK-II is confirmed by co-localization with membrane bound GFP (c, arrow).

(d-i) Activated kidney CaMK-II peaks at 30hpf. Proximal pronephric duct localization of P-CaMK-II is both apical and basolateral but also found in distinct cytosolic clusters (d,f, asterisk). High levels of apical P-CaMK-II are evident in the distal pronephric duct and cloaca (e,f).

(g-i) P-CaMK-II is found in transporting epithelial cells as demonstrated by co-localization with an antibody against the kidney specific $\alpha 1$ subunit of $Na^{+}K^{+}$-ATPase. (j) Active CaMK-II is absent from a small section of the intermediate pronephric duct from 24hpf-72hpf. Scale bar=10 μm.

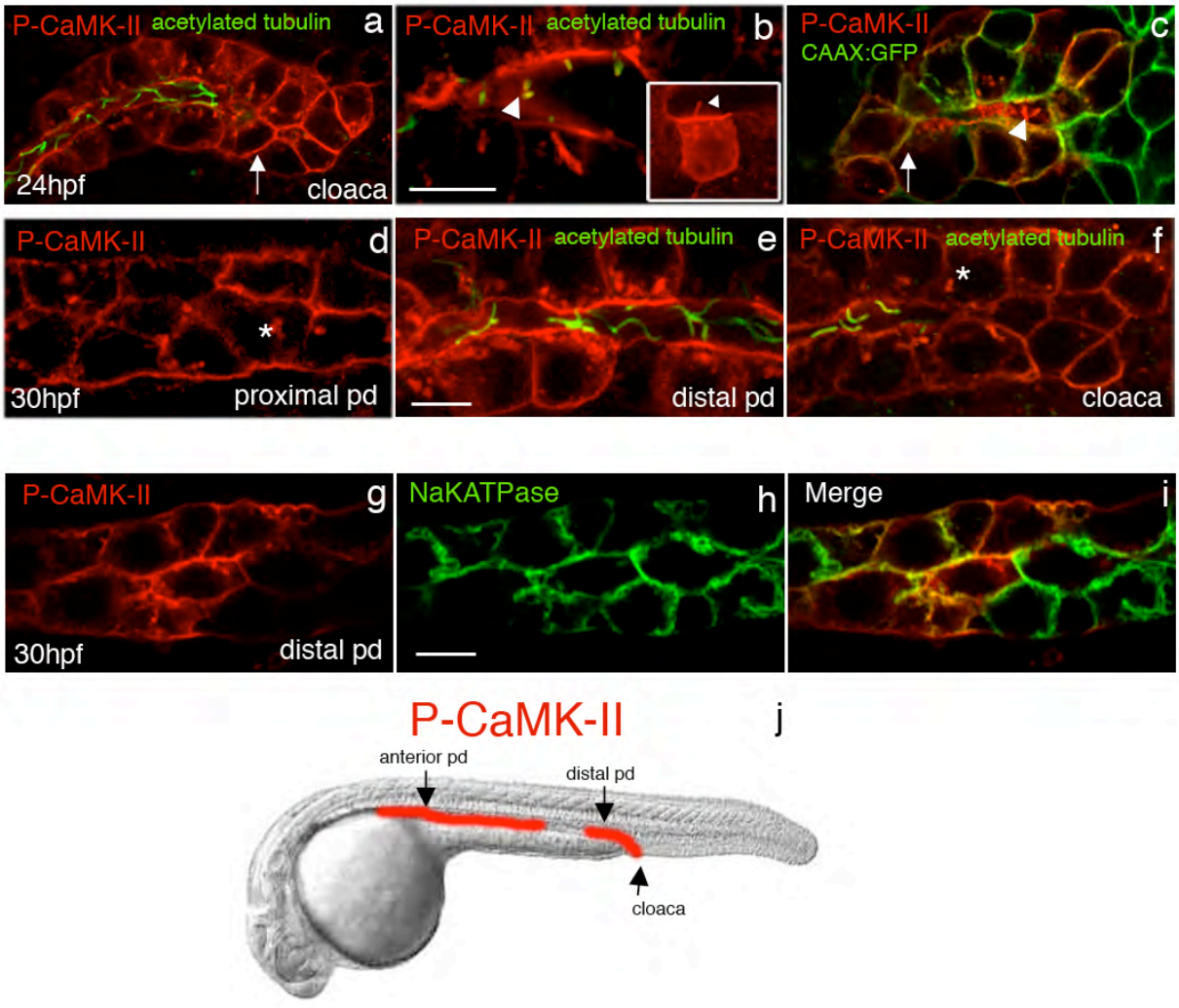
P-CaMK-II
acetylated tubulin
a
24hpf
cloaca
P-CaMK-II
acetylated tubulin
b
P-CaMK-II
CAAX:GFP
c
P-CaMK-II
d
30hpf
proximal pd
P-CaMK-II
acetylated tubulin
e
distal pd
P-CaMK-II
acetylated tubulin
f
cloaca
P-CaMK-II
g
30hpf
distal pd
NaKATPase
h
Merge
i
P-CaMK-II
j
anterior pd
distal pd
cloaca

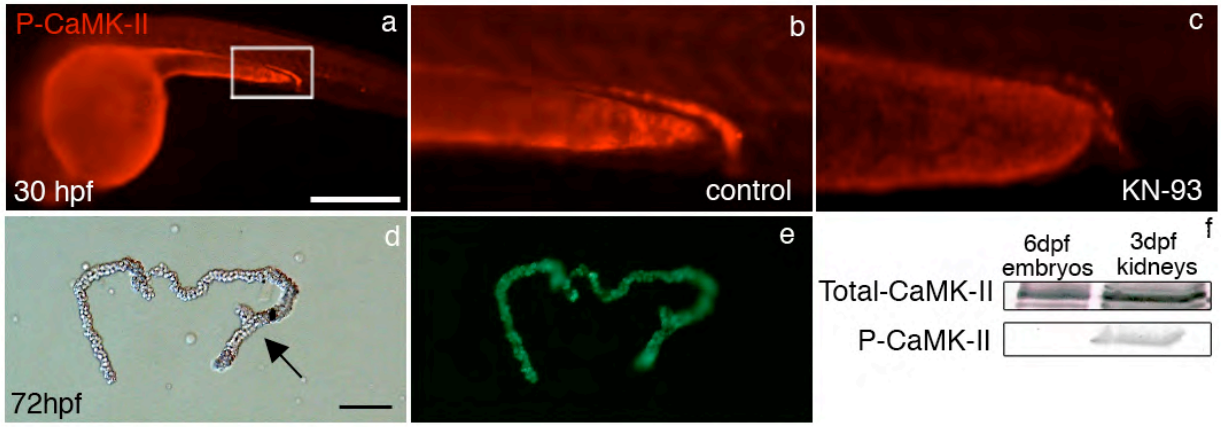

Figure 4.3. KN-93 inhibits activation of CaMK-II in the kidney. (a-c, Scale bar=0.5mm) Whole mount images of P-CaMK-II immunolabeled embryos treated with either DMSO control (a,b) or 10 μm KN-93 (c). 72hpf dissected Na^+K^+-ATPase:GFP positive pronephric duct (d,e; arrow is the cloaca, Scale bar=100 μm). Total-CaMK-II and P-CaMK-II immunoblot of 6dpf zebrafish compared to 72hpf dissected pronephros lysate using 4μg of protein (f,g).

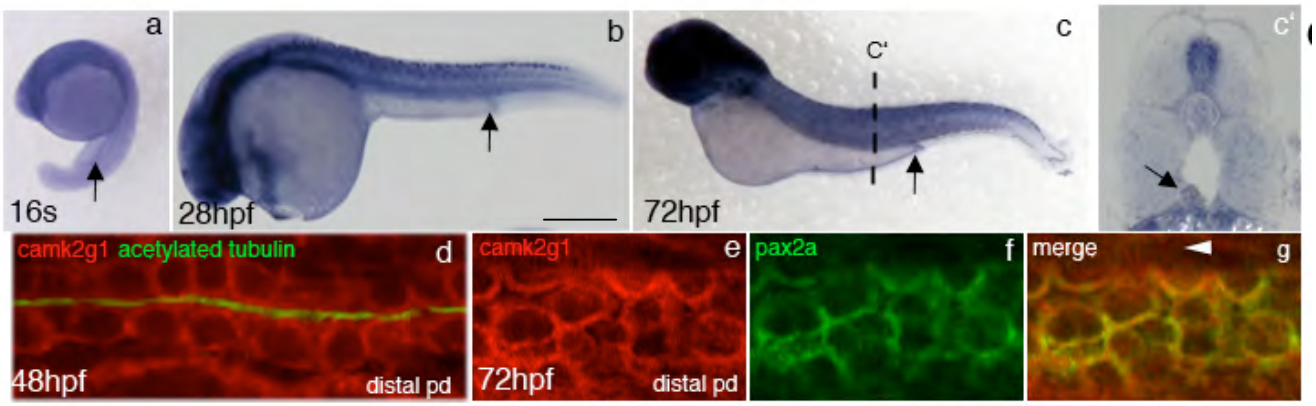

Figure 4.4. *Camk2g1* mRNA is expressed in the kidney. (a-c) WISH experiments were completed using $\gamma 1_C$ probe on 16s 28hpf, and 72hpf wild type embryos, (pronephros denoted by arrow in b,c,c') and (c') 72hpf embryos were cryosectioned. (d) FISH of 48hpf embryos with $\gamma 1_C$ probe followed by immunostaining with acetylated tubulin to demarcate pronephric tubule cilia. (e-g) Double FISH demonstrates that $\gamma 1_C$ mRNA (e, Cy3) and kidney marker, pax2a (f, Alexa 488) co-localize (g) in the distal pronephric duct. Scale bar = 0.5mm.

Figure 4.5. Suppression of *camk2g1* induces kidney cyst formation. Control (a,e,g,I,k) and *camk2g1* morphant (b-d,f,h,j,l) embryos at 72hpf. *Camk2g1* morphant embryos develop hydrocephaly (b, arrow; Scale bar=0.5 mm), pericardial edema (b, arrowhead), cysts (c,d, arrowhead; Scale bar=100 μm) and cloacal occlusions (e,f, arrow; Scale bar=100 μm) by 72hpf. Thin paraffin sections stained with hematoxylin and eosin identify cysts (g,h, asterisks). Improper proximal pronephric tubule convolution is assessed by α6F Na^+K^+ATPase immunolabeling at 72hpf (i,j; Scale bar=50 μm) Cilia are identified by acetylated tubulin immunolabeling at 24hpf (k,l; Scale bar=10μm).

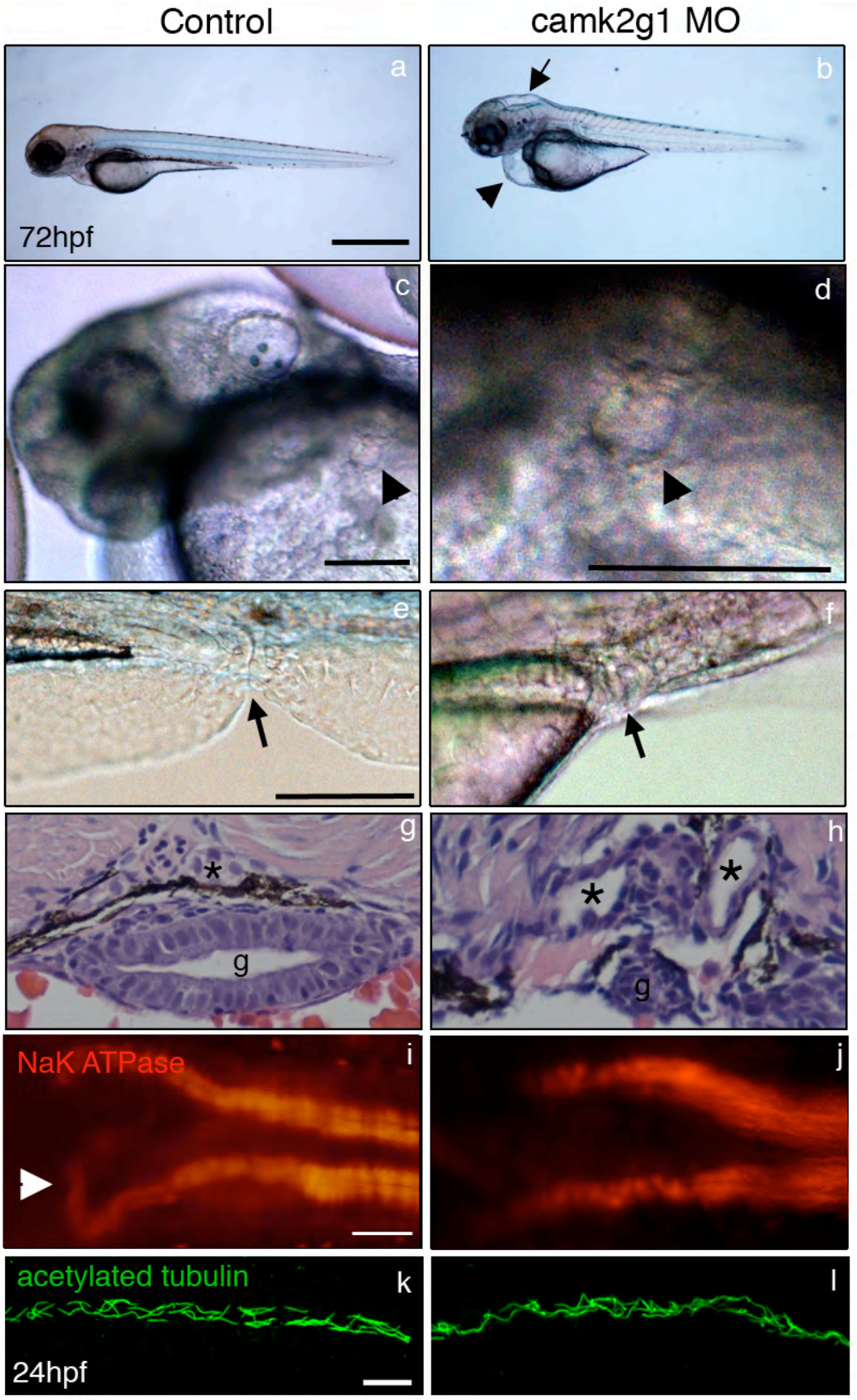
Control
camk2g1 MO
a
b
72hpf
c
d
e
f
g
h
g
g
NaK ATPase
i
j
acetylated tubulin
k
l
24hpf

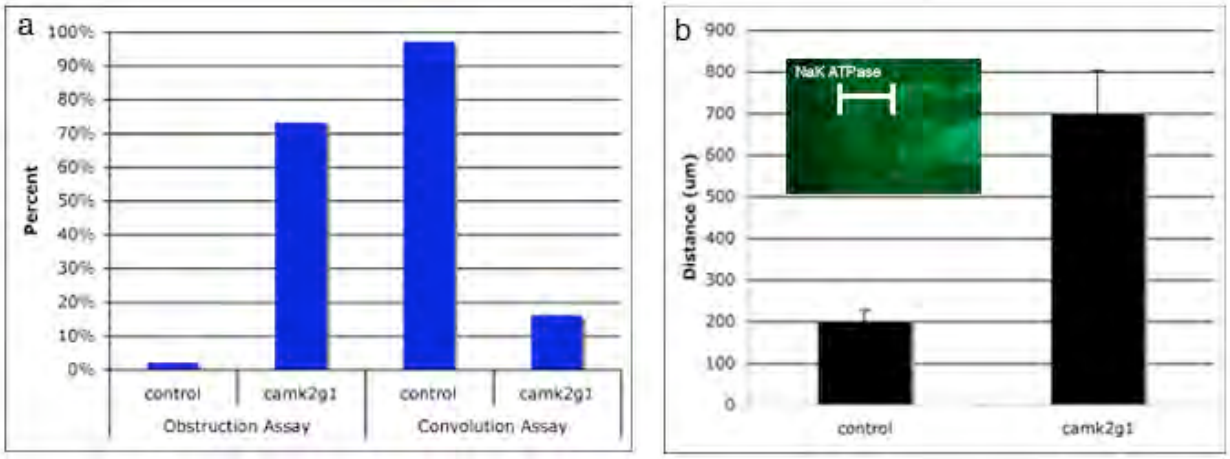

Figure 4.6. Anterior and posterior kidney defects in *camk2g1* morphants. Cloacal development was assessed to determine if a cloacal opening forms by 72hpf (a; Figure 4.5e,f). Anterior convolution was determined by the presence of a "hook" in the anterior pronephros (a; Figure 4.5i,j). Migration of the anterior pronephros was determined by the measurement from the posterior embryonic ear to the anterior pronephros (b; inset).

Figure 4.7. Pronephros specification is not altered in *camk2g1* morphants. WISH of control and *camk2g1* morphants using *pax2a* at 14 somites (dorsal view; a,b) *pax2a, cdh17, gata3, ret1,* at 24hpf (c-j; lateral view, anterior to the left) *wt1a* at 24hpf (k,l) and 48hpf (m,n; dorsal view). Pronephros depiction modified from (Wingert et al., 2007) to identify the region of expression for each probe G=glomerulus, PCT=proximal convoluted tubule, PD=pronephric duct, C=cloaca (o; dorsal view).

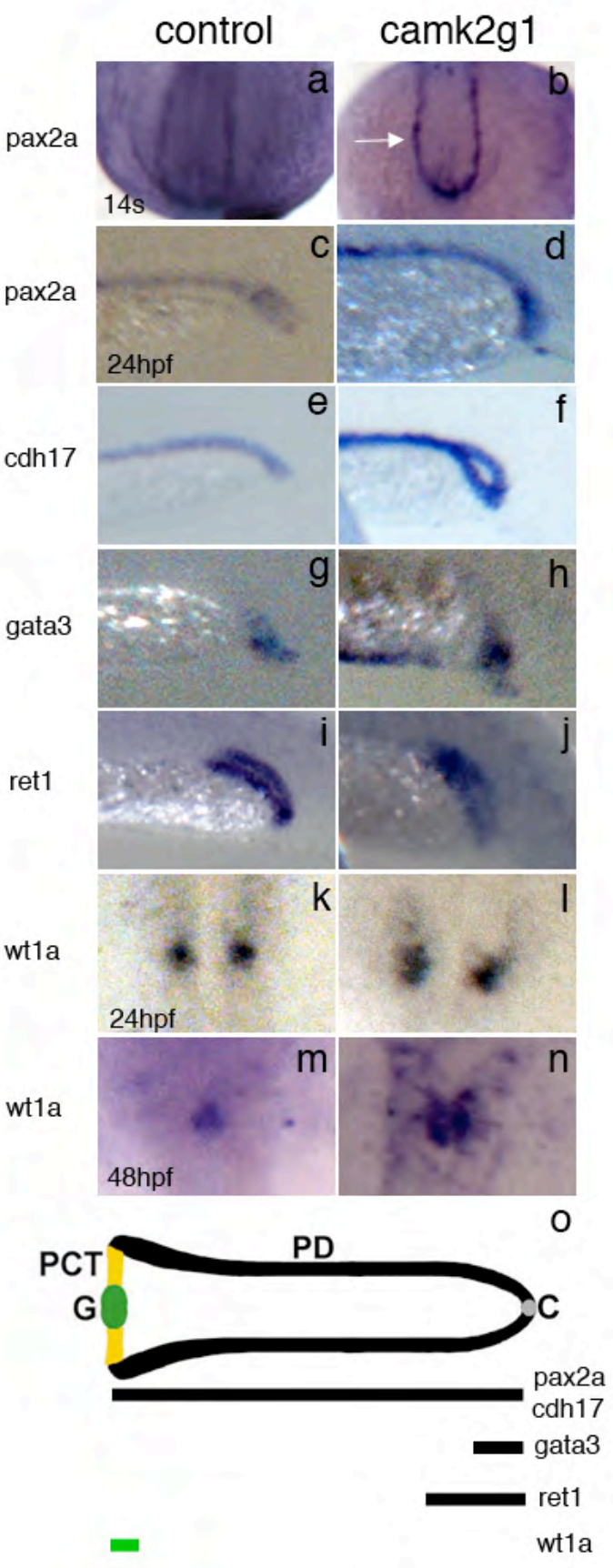
control
camk2g1
a
b
pax2a
14s
c
d
pax2a
24hpf
e
f
cdh17
g
h
gata3
i
j
ret1
k
l
wt1a
24hpf
m
n
wt1a
48hpf
o
PCT
PD
G
C
pax2a
cdh17
gata3
ret1
wt1a

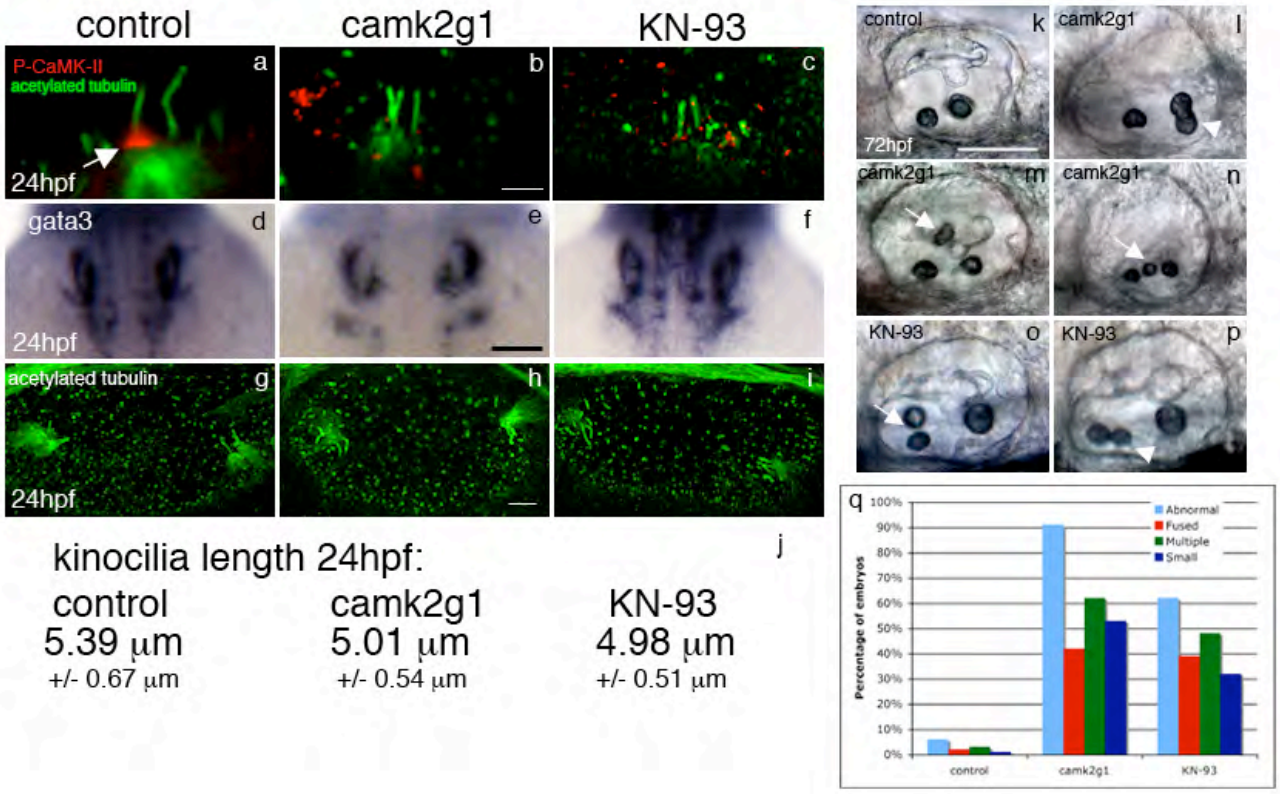

Figure 4.8. Otolith development is defective in *camk2g1* morphants. Activated CaMK-II is reduced in *camk2g1* morphants and KN-93 treated embryos at 24hpf (a-c; Scale bar=5 μm). Otic vesicle specification is not altered in *camk2g1* morphants or KN-93 incubated embryos as assessed using *gata3* ISH (d-f; dorsal view Scale bar=100 μm). Kinocilia in morphants are the same length as control embryos (g-j; Scale bar=5 μm). Gross morphology of the otoliths was assessed at 3dpf and found to be abnormal in *camk2g1* morphants (l-n) and KN-93 treated (o,p) embryos compared to control (k; Scale bar=50 μm). Otolith fusion (l,p; arrowhead), and ectopic otolith formation (m,n,o; arrow) occur often in knockdown embryos. Over 90% of *camk2g1* morphant and over 60% of KN-93 treated embryo otoliths are abnormal (q).

Figure 4.9. Ectopic constitutively active CaMK-II reverses cyst development in *pkd2* morphants. Lateral view of control, *pkd2* morphant, and *pkd2* morphant embryos co-injected with constitutively active ($T^{287}D$) human δ_E CaMK-II at 72hpf (a-c; Scale bar=1 mm). Cloacal occlusions are rescued with ectopic CaMK-II expression (e,f,m; Scale bar=100 μm). Cilia formation is normal (g-i; Scale bar=10 μm) and anterior convolution is rescued (h-j,m; Scale bar=50 μm) assessed using acetylated tubulin and α6F Na^+K^+-ATPase immunostaining. Anterior migration is restored to near normal levels in constitutively active CaMK-II expressing pkd2 morphants (n).

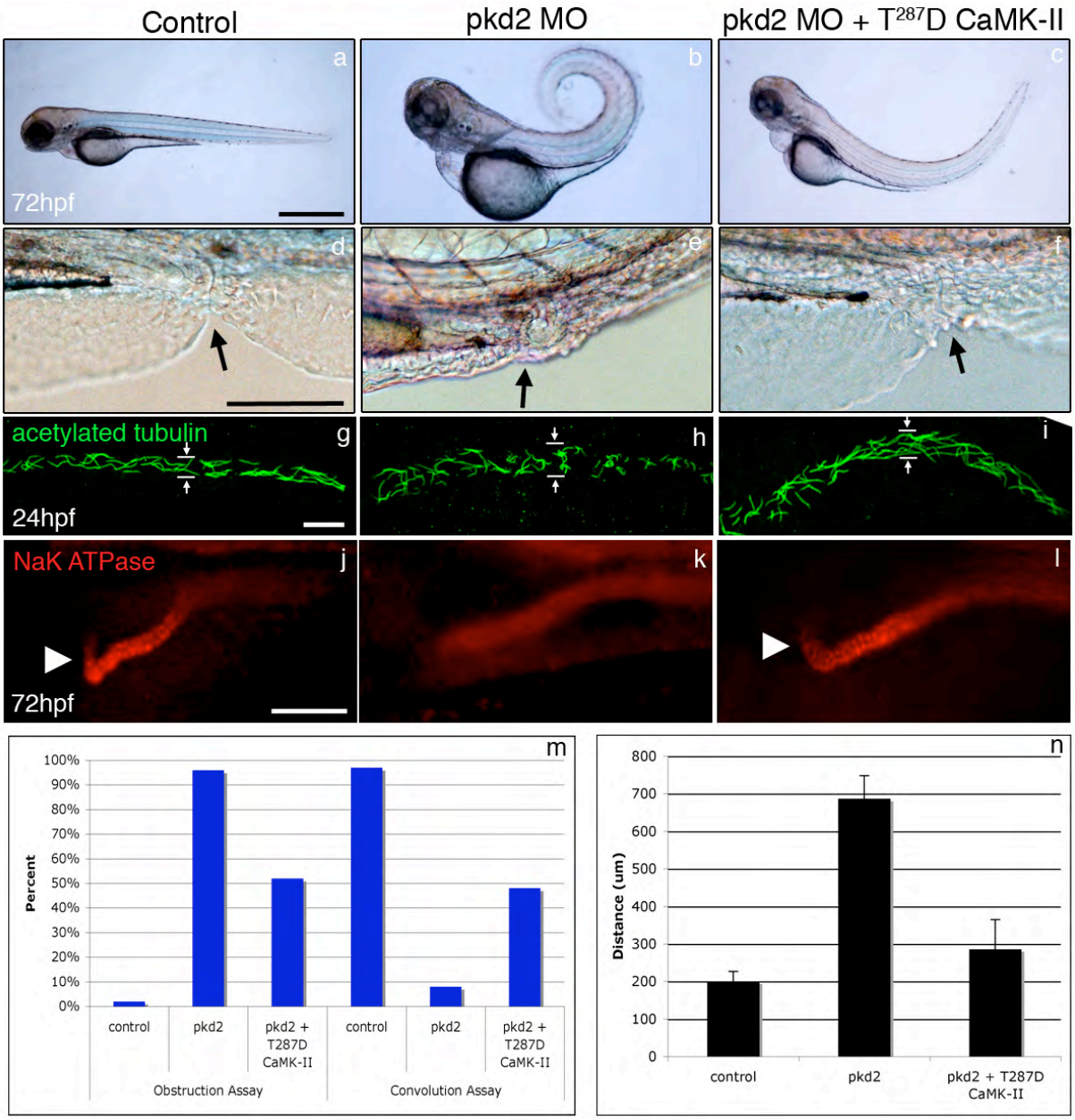
Control
pkd2 MO
pkd2 MO + T287D CaMK-II
a
b
c
72hpf
d
e
f
acetylated tubulin
g
h
i
24hpf
NaK ATPase
j
k
l
72hpf
m
Percent
100%
90%
80%
70%
60%
50%
40%
30%
20%
10%
0%
control
pkd2
pkd2 + T287D CaMK-II
control
pkd2
pkd2 + T287D CaMK-II
Obstruction Assay
Convolution Assay
n
Distance (um)
800
700
600
500
400
300
200
100
0
control
pkd2
pkd2 + T287D CaMK-II

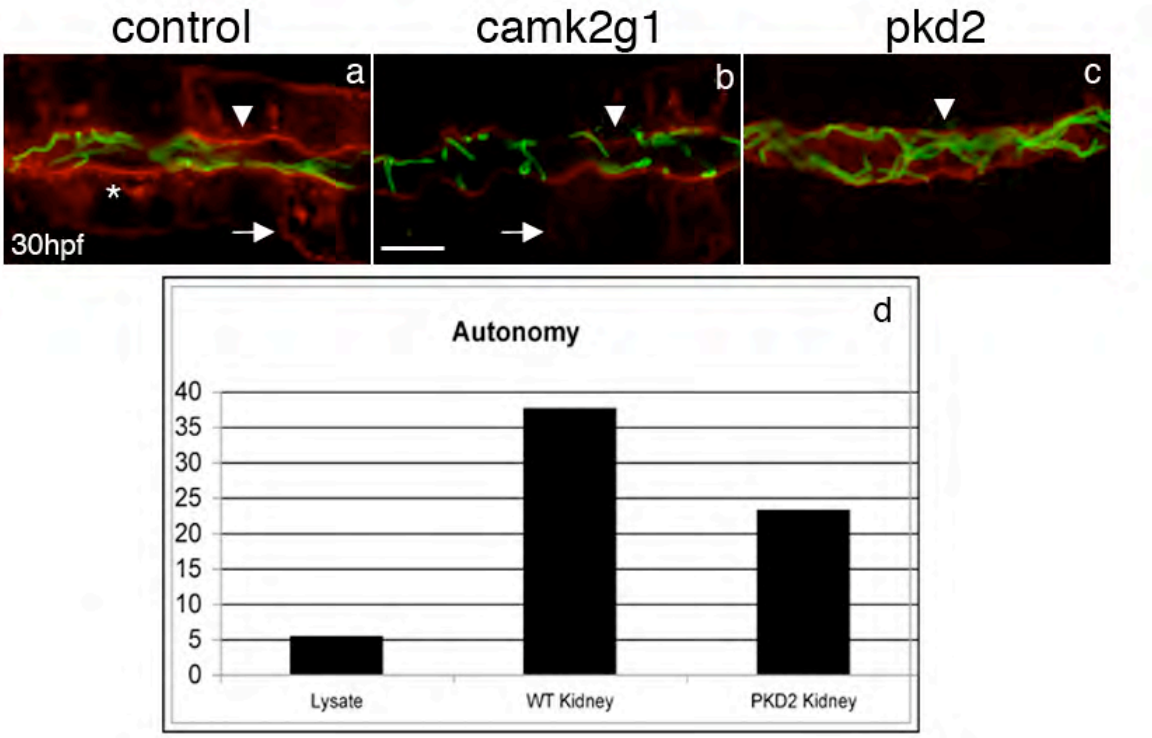

Figure 4.10. Activated CaMK-II is reduced in *camk2g1* and *pkd2* morphants. P-CaMK-II is reduced in the apical membrane (arrowhead), basolateral membrane (arrow), and cytosolic clusters (asterisk) of cam2g1 and pkd2 morphants. CaMK-II calcium independent activity is reduced in *pkd2* morphant dissected pronephros at 72hpf (d). Scale bar=10 μm

Figure 4.11. Actin polarity and organization is altered in *camk2g1* morphants. Actin localization was assessed using Phalloidin immunolabeling where control embryos have strong apical F-actin (a, arrow) and *camk2g1* morphants have strong apical and basolateral (b, arrowhead) F-actin localization in the cloaca. Actin is correctly localized in the distal pronephric duct of *camk2g1* morphants however the apical F-actin appears disorganized (c,d; Scale bar=10 μm). aPKC and γtubulin are correctly localized to the apical membrane in both the cloaca (e,f) and distal pronephric duct (g,h; Scale bar=20 μm). Cryosectioned α6F Na^+K^+-ATPase immunolabeled embryos show loss of basolateral expression as well as the formation of cysts (i,j; Scale bar=10 μm).

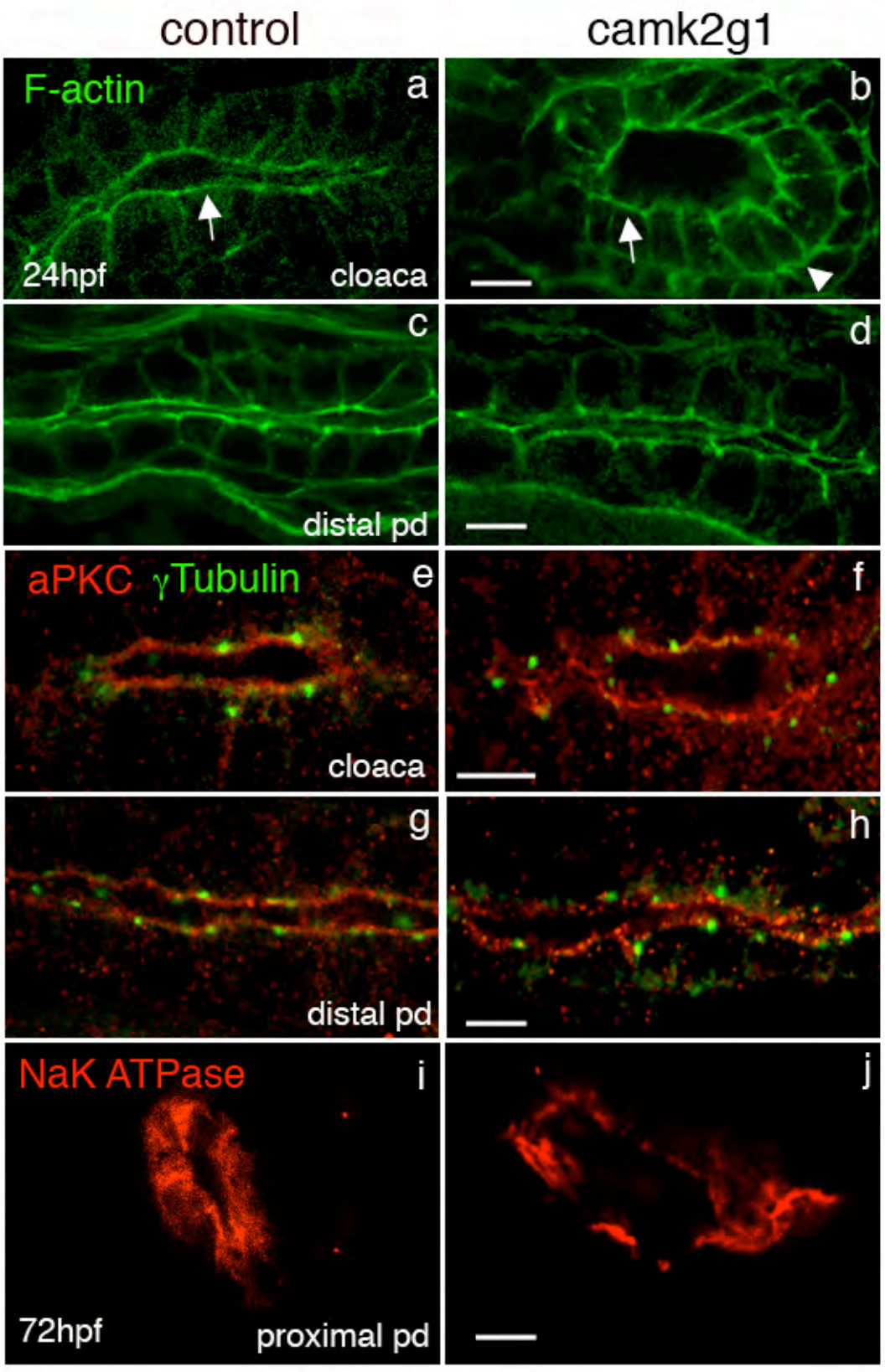
control
camk2g1
F-actin
a
b
24hpf
cloaca
c
d
distal pd
aPKC γTubulin
e
f
cloaca
g
h
distal pd
NaK ATPase
i
j
72hpf
proximal pd

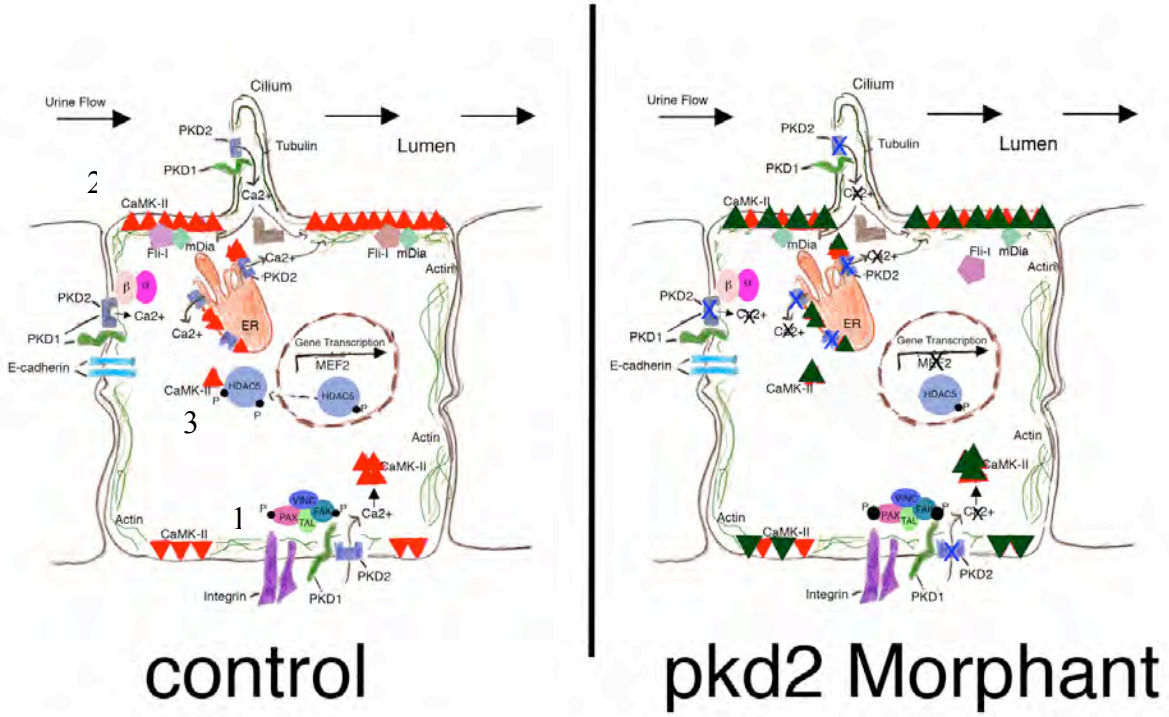

Figure 4.12. Model of CaMK-II in PKD2 Morphants. CaMK-II activation is important for many cellular processes. 1. CaMK-II is important for cell motility by promoting focal adhesion turnover. In *pkd2* and *camk2g1* morphants proximal migration is inhibited, possibly due to the inhibition of focal adhesion turnover. 2. CaMK-II binds to Fli-I to promote actin assembly and stabailization and suppression of pkd2 could alter this relationship influencing actin stability and polarity. 3. Cytosolic localization of HDAC5 promotes transcription of MEF2 target genes, in animal models of ADPKD HDAC5 is not retained in the cytosol inhibiting transcription of genes important in normal renal development.

Supplemental Movies

Supplemental Movie 3 – Video shows control kidney cilia beating at 72hpf, arrows.

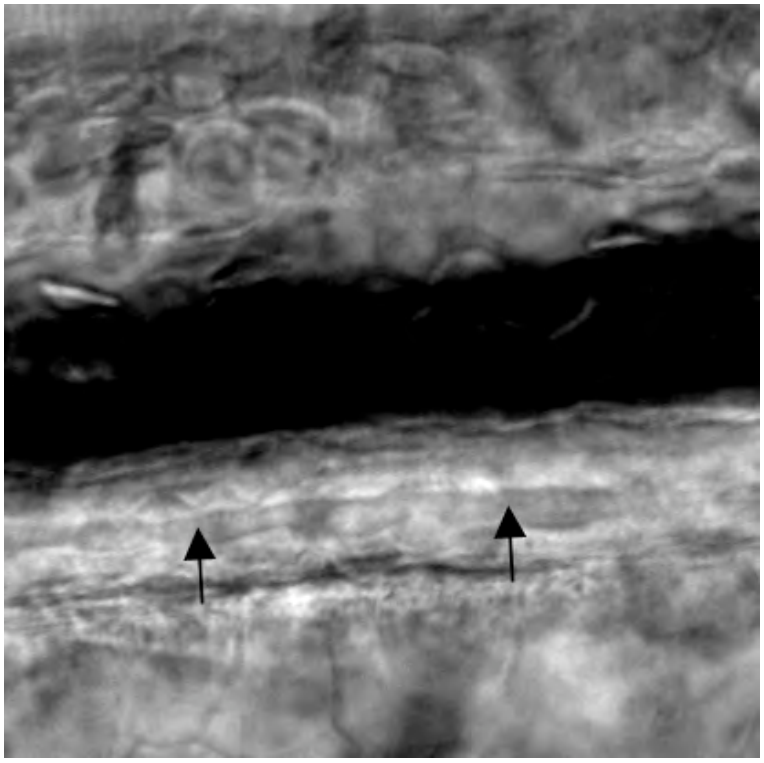

Supplemental Movie 4 – Video shows zoom of cloacal cilia beating at 72hpf, arrows.

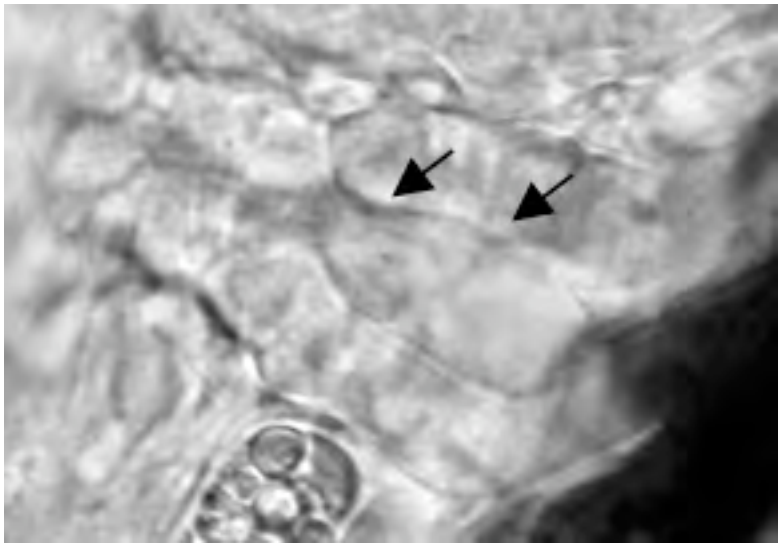

Supplemental Movie 5 – Video shows *camk2g1* kidney cilia beating at 72hpf, arrowns.

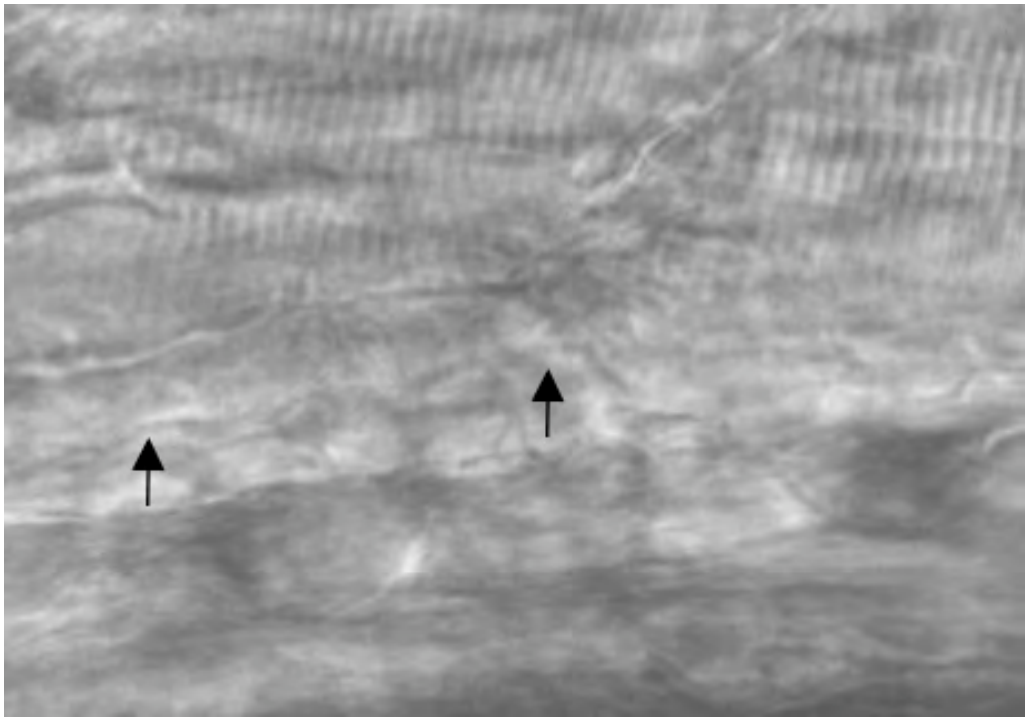

Supplemental Movie 6 – Video shows KN-93 kidney cilia beating at 72hpf, arrows.

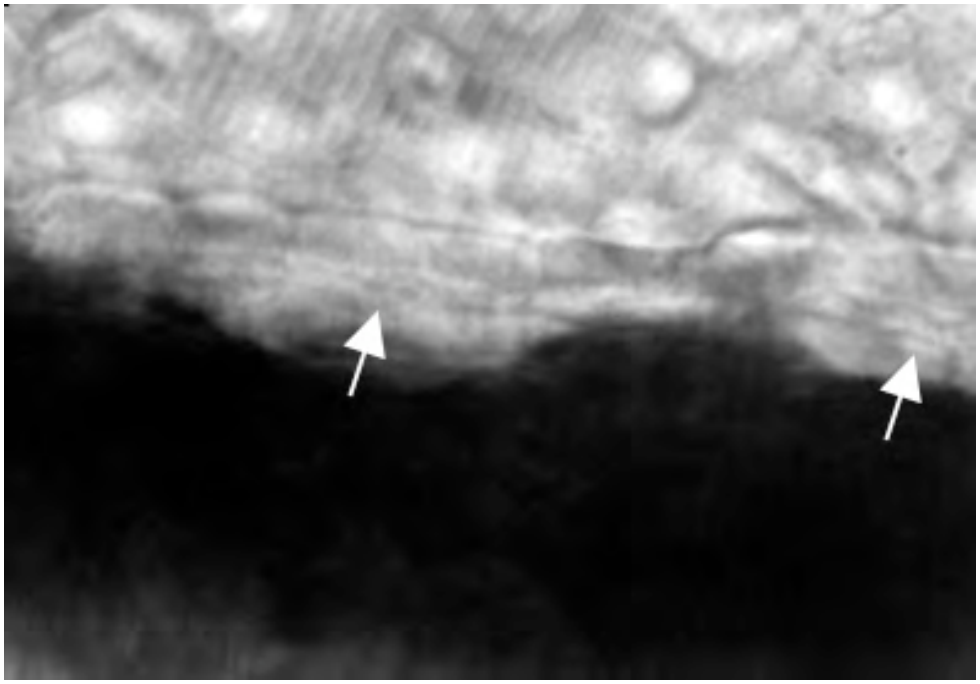

Supplemental Movie 7 – Video shows control tether cilia beating at 24hpf, arrow.

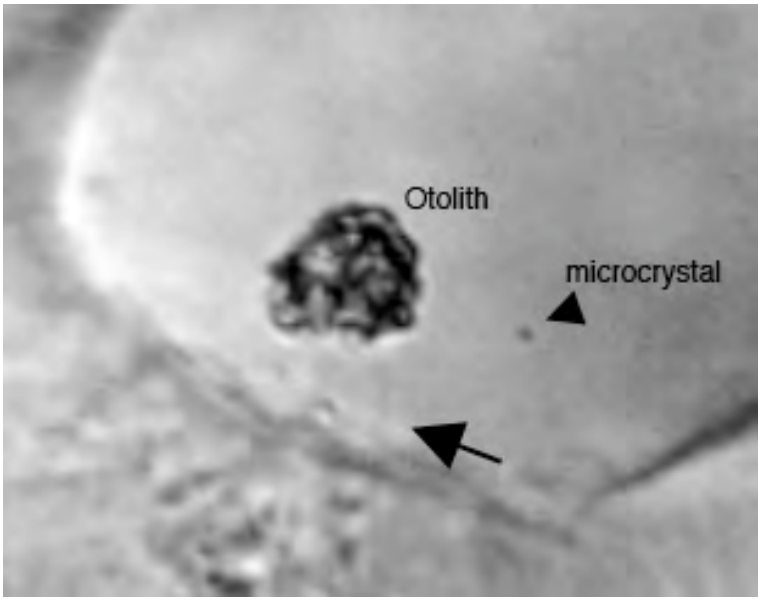

Supplemental Movie 8 – Video shows zoom of control tether cilia beating at 24hpf, arrow.

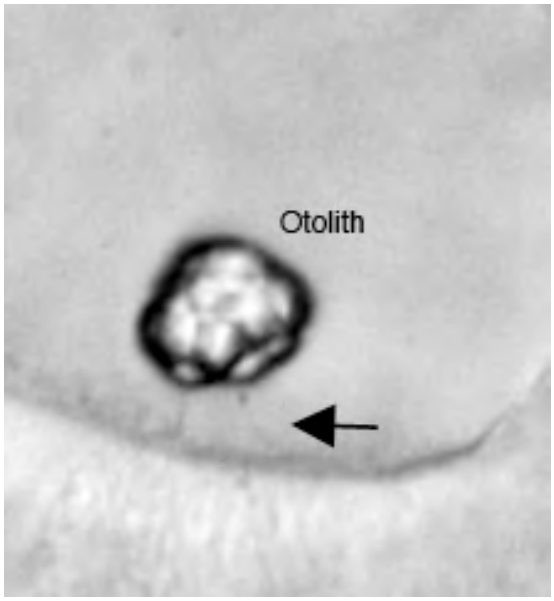

Supplemental Movie 9 – Video shows $CaCO_3$ microcrystals in control 24hpf embryo.

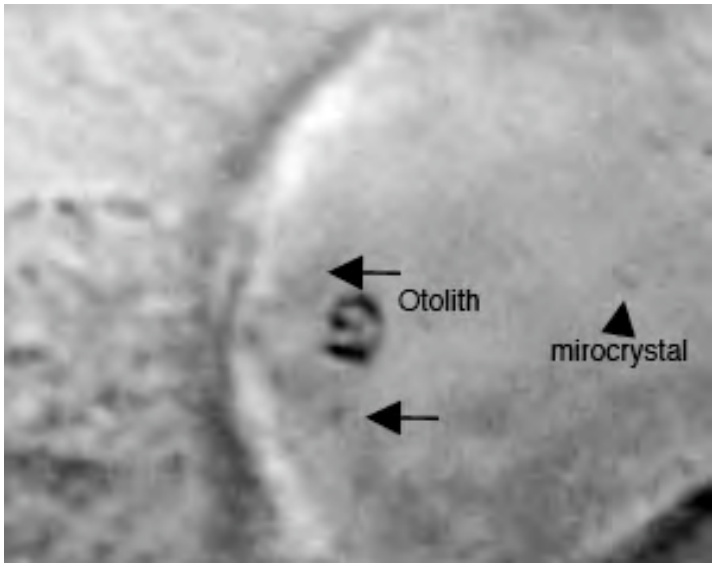

Supplemental Movie 10 –Video shows *camk2g1* morphant tether cilia beating irregularly (arrow) and altered otolith movement at 24hpf.

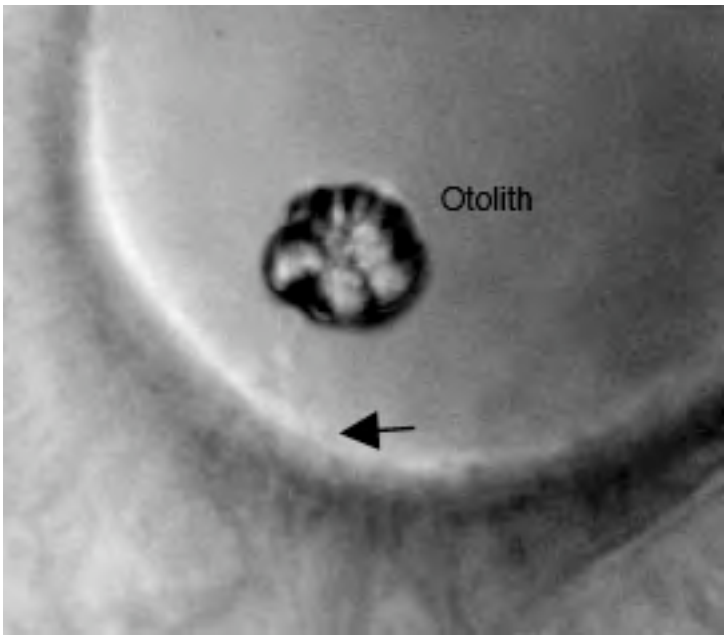

Supplemental Movie 11–Video shows *camk2g1* morphant $CaCO_3$ microcrystals and lack of tether cilia beating at 24hpf.

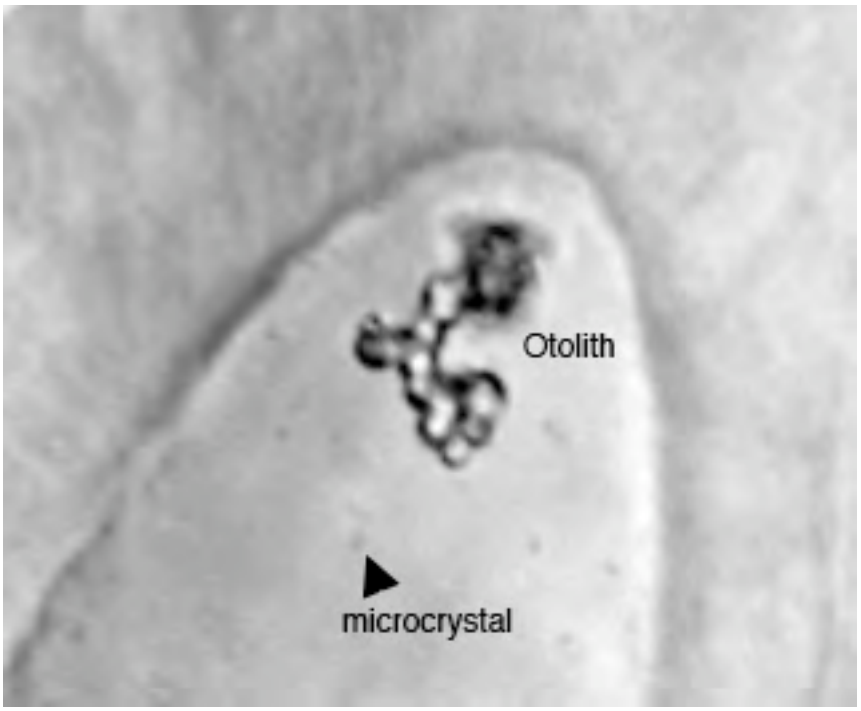

Supplemental Movie 12–Video shows *camk2g1* morphant $CaCO_3$ microcrystals and lack of tether cilia beating at 24hpf.

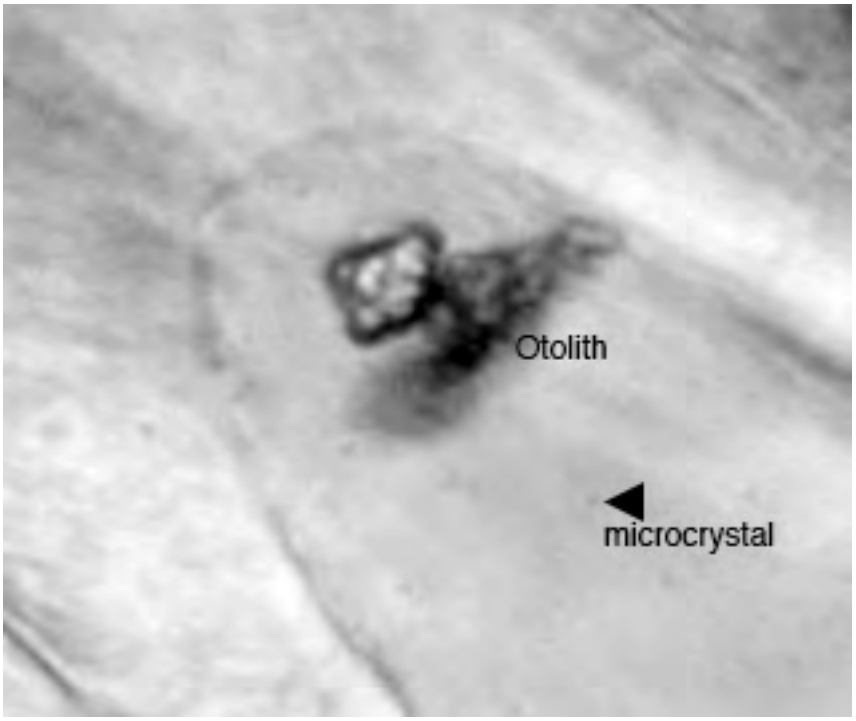

Supplemental Movie 13–Video shows entire otic placode with $CaCO_3$ microcrystals.

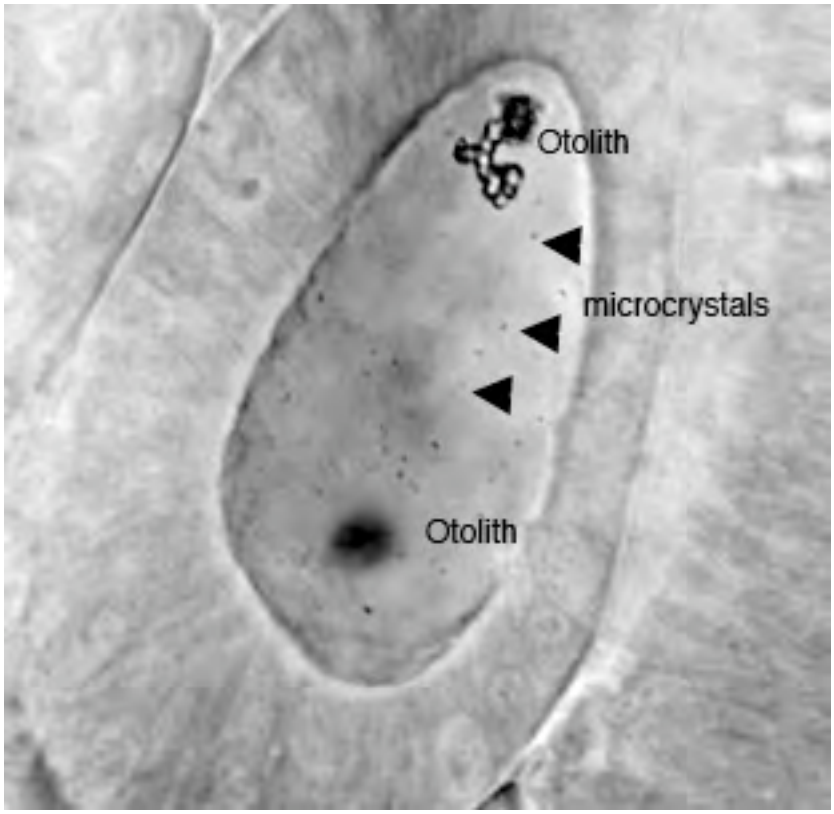

Supplemental Movie 14 – Video shows $CaCO_3$ mirocrystal and lack of tether cilia beating in KN-93 treated 24hpf embryos.

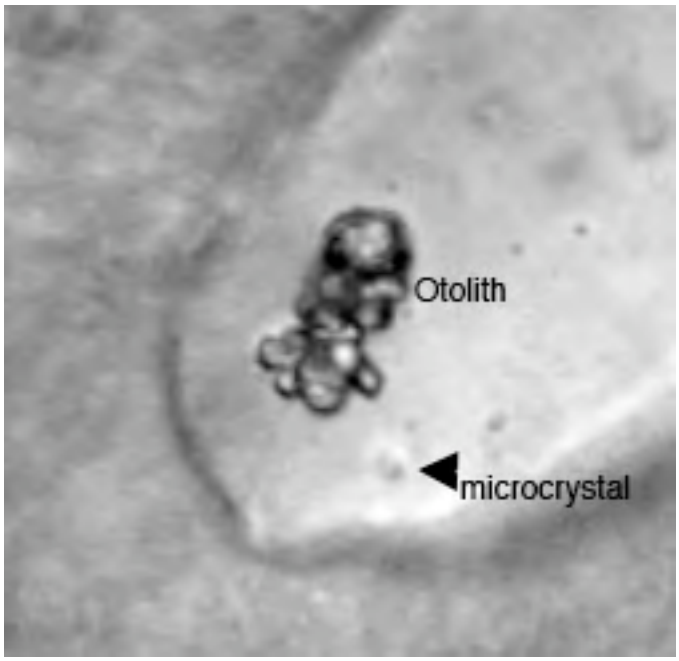

Chapter 5: Dissertation Summary

This study is the first to comprehensively analyze the expression and role of CaMK-II genes in vivo. Zebrafish are an ideal model system to analyze signaling proteins, such as CaMK-II, during development because of the transparency of the embryo, rapid development, external fertilization, and experimental techniques available. Interestingly, zebrafish retain 75% of the duplicated CaMK-II genes yielding a total of 7 catalytically active and 1 catalytically inactive, α1KAP, CaMK-II. The retention and transcription of these genes during embryogenesis demonstrates the importance of this signaling molecule in zebrafish development.

Although the studies presented here specifically address *camk2b2* and *camk2g1*, suppression of all seven genes result in unique identifiable phenotypes by 48hpf and reduced CaMK-II activity. Suppression of *camk2b2* causes bradycardia, reduced circulation, and inhibits proper pectoral fin and heart development. This phenotype is reminiscent of the *tbx5* morphant and *tbx5* mutant (hst), which is the gene mutated in patients with Holt-Oram Syndrome (also known as heart-hand syndrome). CaMK-II activity decreased significantly by 72hpf and β2 mRNA expression was reduced in *tbx5* morphant and mutant hearts and fins. Overexpression of Tbx5 in mouse NIH/3T3 fibroblasts and in zebrafish embryos caused an increase in CaMK-II activity. These results identify Tbx5 as a positive regulator of β2 CaMK-II expression in the zebrafish heart and kidney. Although Tbx5 upregulates transcription of many genes, understanding the downstream pathways in Tbx5 mutations will help in identifying possible treatments for patients with HOS.

Camk2g1 was the second gene analyzed in this study due to its unique expression pattern in the developing zebrafish kidney (pronephros). Suppression of *camk2g1* leads to hydrocephaly, otolith defects, cloacal occlusions and pronephric cysts. This phenotype mirrors that seen in *pkd2* and *pkd1* morphants, both zebrafish models of autosomal dominant polycystic kidney disease. Mutations in either PKD1 or PKD2 cause ADPKD, which is the most common kidney syndrome. Although much is known about the condition, the immediate downstream effector of PKD2 Ca^{2+} is unknown. This study identifies CaMK-II as this downstream effector, where ectopic constitutively active CaMK-II partially rescues the *pkd2* morphant cystic phenotype. In addition, activation of CaMK-II is reduced in *pkd2* morphant embryos and dissected kidneys. These results implicate CaMK-II in ADPKD pathology and identify the first Ca^{2+}-dependent effector protein that has altered activity in a vertebrate model of ADPKD.

CaMK-II is the ideal signaling molecule during development, where it is important for cell movements during gastrulation, pectoral fin and heart morphogenesis, excitation-contraction coupling, kidney development, and otolith formation. Future research in the zebrafish should provide additional insight into the role of this multifunctional signaling hub in understanding basic developmental biology in addition to human pathologies.

List of References

List of References

Abbott, A. L. and Ducibella, T. (2001). Calcium and the control of mammalian cortical granule exocytosis. *Front Biosci* **6**, D792-806.

Aguiari, G., Campanella, M., Manzati, E., Pinton, P., Banzi, M., Moretti, S., Piva, R., Rizzuto, R. and del Senno, L. (2003). Expression of polycystin-1 C-terminal fragment enhances the ATP-induced Ca2+ release in human kidney cells. *Biochem Biophys Res Commun* **301**, 657-64.

Ahn Dae-gwon, K. M. J., et al. (2002). T-box gene tbx5 is essential for formation of the pectoral limb bud. *Nature* **417**, 754-758.

Ahn, D. G., Kourakis, M. J., Rohde, L. A., Silver, L. M. and Ho, R. K. (2002). T-box gene tbx5 is essential for formation of the pectoral limb bud. *Nature* **417**, 754-8.

Allende, M. L., Amsterdam, A., Becker, T., Kawakami, K., Gaiano, N. and Hopkins, N. (1996). Insertional mutagenesis in zebrafish identifies two novel genes, pescadillo and dead eye, essential for embryonic development. *Genes Dev* **10**, 3141-55.

Anakwe, K., Robson, L., Hadley, J., Buxton, P., Church, V., Allen, S., Hartmann, C., Harfe, B., Nohno, T., Brown, A. M. et al. (2003). Wnt signalling regulates myogenic differentiation in the developing avian wing. *Development* **130**, 3503-14.

Anderson, M. E. (2007). Multiple downstream proarrhythmic targets for calmodulin kinase II: moving beyond an ion channel-centric focus. *Cardiovasc Res* **73**, 657-66.

Auman, H. J., Coleman, H., Riley, H. E., Olale, F., Tsai, H. J. and Yelon, D. (2007). Functional modulation of cardiac form through regionally confined cell shape changes. *PLoS Biol* **5**, e53.

Backs, J., Song, K., Bezprozvannaya, S., Chang, S. and Olson, E. N. (2006). CaM kinase II selectively signals to histone deacetylase 4 during cardiomyocyte hypertrophy. *J Clin Invest* **116**, 1853-64.

Bai, C. X., Kim, S., Li, W. P., Streets, A. J., Ong, A. C. and Tsiokas, L. (2008). Activation of TRPP2 through mDia1-dependent voltage gating. *Embo J* **27**, 1345-56.

Baitinger, C., Alderton, J., Poenie, M., Schulman, H. and Steinhardt, R. A. (1990). Multifunctional Ca2+/calmodulin-dependent protein kinase is necessary for nuclear envelope breakdown. *J Cell Biol* **111**, 1763-73.

Bakkers, J., Kramer, C., Pothof, J., Quaedvlieg, N. E., Spaink, H. P. and Hammerschmidt, M. (2004). Has2 is required upstream of Rac1 to govern dorsal migration of lateral cells during zebrafish gastrulation. *Development* **131**, 525-37.

Baltas, L. G., Karczewski, P. and Krause, E. G. (1995). The cardiac sarcoplasmic reticulum phospholamban kinase is a distinct delta-CaM kinase isozyme. *FEBS Lett* **373**, 71-5.

Basson, C. T., Bachinsky, D. R., Lin, R. C., Levi, T., Elkins, J. A., Soults, J., Grayzel, D., Kroumpouzou, E., Traill, T. A., Leblanc-Straceski, J. et al. (1997). Mutations in human TBX5 [corrected] cause limb and cardiac malformation in Holt-Oram syndrome. *Nat Genet* **15**, 30-35.

Basson, C. T., Cowley, G. S., Solomon, S. D., Weissman, B., Poznanski, A. K., Traill, T. A., Seidman, J. G. and Seidman, C. E. (1994). The clinical and genetic spectrum of the Holt-Oram syndrome (heart-hand syndrome). *N Engl J Medicine* **330**, 885-91.

Bayer, K. U., De Koninck, P. and Schulman, H. (2002). Alternative splicing modulates the frequency-dependent response of CaMKII to Ca(2+) oscillations. *Embo J* **21**, 3590-7.

Bayer, K. U., Harbers, K. and Schulman, H. (1998). alphaKAP is an anchoring protein for a novel CaM kinase II isoform in skeletal muscle. *Embo J* **17**, 5598-605.

Bayer, K. U., Lohler, J., Schulman, H. and Harbers, K. (1999). Developmental expression of the CaM kinase II isoforms: ubiquitous gamma- and delta-CaM kinase II are the early isoforms and most abundant in the developing nervous system. *Brain Res Mol Brain Res* **70**, 147-54.

Bayer, K. U. and Schulman, H. (2001). Regulation of signal transduction by protein targeting: the case for CaMKII. *Biochem Biophys Res Commun* **289**, 917-23.

Becker, K. A. and Hart, N. H. (1996). The cortical actin cytoskeleton of unactivated zebrafish eggs: spatial organization and distribution of filamentous actin, nonfilamentous actin, and myosin-II. *Mol Reprod Dev* **43**, 536-47.

Begemann, G. and Ingham, P. W. (2000). Developmental regulation of Tbx5 in zebrafish embryogenesis. *Mech Dev* **90**, 299-304.

Bohm, J., Heinritz, W., Craig, A., Vujic, M., Ekman-Joelsson, B. M., Kohlhase, J. and Froster, U. (2008). Functional analysis of the novel TBX5 c.1333delC mutation resulting in an extended TBX5 protein. *BMC Med Genet* **9**, 88.

Brady, R. C. and Hilfer, S. R. (1982). Optic cup formation: a calcium-regulated process. *Proc Natl Acad Sci U S A* **79**, 5587-91.

Brocke, L., Chiang, L. W., Wagner, P. D. and Schulman, H. (1999). Functional implications of the subunit composition of neuronal CaM kinase II. *J Biol Chem* **274**, 22713-22.

Brocke, L., Srinivasan, M. and Schulman, H. (1995). Developmental and regional expression of multifunctional Ca2+/calmodulin-dependent protein kinase isoforms in rat brain. *J Neurosci* **15**, 6797-808.

Bronstein, J. M., Wasterlain, C. G., Bok, D., Lasher, R. and Farber, D. B. (1988). Localization of retinal calmodulin kinase. *Exp Eye Res* **47**, 391-402.

Brown, D. D., Martz, S. N., Binder, O., Goetz, S. C., Price, B. M., Smith, J. C. and Conlon, F. L. (2005). Tbx5 and Tbx20 act synergistically to control vertebrate heart morphogenesis. *Development* **132**, 553-63.

Bruneau, B. G., Nemer, G., Schmitt, J. P., Charron, F., Robitaille, L., Caron, S., Conner, D. A., Gessler, M., Nemer, M., Seidman, C. E. et al. (2001). A murine model of Holt-Oram syndrome defines roles of the T-box transcription factor Tbx5 in cardiogenesis and disease. *Cell* **106**, 709-21.

Burgin, K. E., Waxham, M. N., Rickling, S., Westgate, S. A., Mobley, W. C. and Kelly, P. T. (1990). In situ hybridization histochemistry of Ca2+/calmodulin-dependent protein kinase in developing rat brain. *J Neurosci* **10**, 1788-98.

Burrow, C. R., Devuyst, O., Li, X., Gatti, L. and Wilson, P. D. (1999). Expression of the beta2-subunit and apical localization of Na+-K+-ATPase in metanephric kidney. *Am J Physiol* **277**, F391-403.

Cai, Y., Maeda, Y., Cedzich, A., Torres, V. E., Wu, G., Hayashi, T., Mochizuki, T., Park, J. H., Witzgall, R. and Somlo, S. (1999). Identification and characterization of polycystin-2, the PKD2 gene product. *J Biol Chem* **274**, 28557-65.

Caran, N., Johnson, L. D., Jenkins, K. J. and Tombes, R. M. (2001). Cytosolic targeting domains of gamma and delta calmodulin-dependent protein kinase II. *J Biol Chem* **276**, 42514-9.

Casuscelli, J., Schmidt, S., DeGray, B., Petri, E. T., Celic, A., Folta-Stogniew, E., Ehrlich, B. E. and Boggon, T. J. (2009). Analysis of the cytoplasmic interaction between polycystin-1 and polycystin-2. *Am J Physiol Renal Physiol* **297**, F1310-5.

Chang, D. C. and Lu, P. (2000). Multiple types of calcium signals are associated with cell division in zebrafish embryo. *Microsc Res Tech* **49**, 111-22.

Chapman, A. B., Johnson, A. M. and Gabow, P. A. (1993). Intracranial aneurysms in patients with autosomal dominant polycystic kidney disease: how to diagnose and who to screen. *Am J Kidney Dis* **22**, 526-31.

Charron, A. J., Nakamura, S., Bacallao, R. and Wandinger-Ness, A. (2000). Compromised cytoarchitecture and polarized trafficking in autosomal dominant polycystic kidney disease cells. *J Cell Biol* **149**, 111-24.

Chen, J. N. and Fishman, M. C. (1996). Zebrafish tinman homolog demarcates the heart field and initiates myocardial differentiation. *Development* **122**, 3809-16.

Chernoff, E. A. and Hilfer, S. R. (1982). Calcium dependence and contraction in somite formation. *Tissue Cell* **14**, 435-49.

Clapham, D. E. (2003). TRP channels as cellular sensors. *Nature* **426**, 517-24.

Clark, K. L., Yutzey, K. E. and Benson, D. W. (2006). Transcription factors and congenital heart defects. *Annu Rev Physiol* **68**, 97-121.

Clay, H. and Ramakrishnan, L. (2005). Multiplex fluorescent in situ hybridization in zebrafish embryos using tyramide signal amplification. *Zebrafish* **2**, 105-11.

Colantonio, J. R., Vermot, J., Wu, D., Langenbacher, A. D., Fraser, S., Chen, J. N. and Hill, K. L. (2009). The dynein regulatory complex is required for ciliary motility and otolith biogenesis in the inner ear. *Nature* **457**, 205-9.

Colbran, R. J., Smith, M. K., Schworer, C. M., Fong, Y. L. and Soderling, T. R. (1989). Regulatory domain of calcium/calmodulin-dependent protein kinase II. Mechanism of inhibition and regulation by phosphorylation. *J Biol Chem* **264**, 4800-4.

Conklin, M. W., Lin, M. S. and Spitzer, N. C. (2005). Local calcium transients contribute to disappearance of pFAK, focal complex removal and deadhesion of neuronal growth cones and fibroblasts. *Dev Biol* **287**, 201-12.

Creton, R. (2004). The calcium pump of the endoplasmic reticulum plays a role in midline signaling during early zebrafish development. *Brain Res Dev Brain Res* **151**, 33-41.

Creton, R., Speksnijder, J. E. and Jaffe, L. F. (1998). Patterns of free calcium in zebrafish embryos. *J Cell Sci* **111 (Pt 12)**, 1613-22.

Daggett, D. F., Domingo, C. R., Currie, P. D. and Amacher, S. L. (2007). Control of morphogenetic cell movements in the early zebrafish myotome. *Dev Biol* **309**, 169-79.

Digilio, M. C., Conti, E., Sarkozy, A., Mingarelli, R., Dottorini, T., Marino, B., Pizzuti, A. and Dallapiccola, B. (2002). Grouping of multiple-lentigines/LEOPARD and Noonan syndromes on the PTPN11 gene. *Am J Hum Genet* **71**, 389-94.

Dosemeci, A. and Jaffe, H. (2010). Regulation of phosphorylation at the postsynaptic density during different activity states of Ca2+/calmodulin-dependent protein kinase II. *Biochem Biophys Res Commun* **391**, 78-84.

Doyon, Y., McCammon, J. M., Miller, J. C., Faraji, F., Ngo, C., Katibah, G. E., Amora, R., Hocking, T. D., Zhang, L., Rebar, E. J. et al. (2008). Heritable targeted gene disruption in zebrafish using designed zinc-finger nucleases. *Nat Biotechnol* **26**, 702-8.

Drummond, I. (2002). The pronephros. *Results Probl Cell Differ* **40**, 322-45.

Drummond, I. (2003). Making a zebrafish kidney: a tale of two tubes. *Trends Cell Biol* **13**, 357-65.

Drummond, I. A. (2005). Kidney development and disease in the zebrafish. *J Am Soc Nephrol* **16**, 299-304.

Drummond, I. A., Majumdar, A., Hentschel, H., Elger, M., Solnica-Krezel, L., Schier, A. F., Neuhauss, S. C., Stemple, D. L., Zwartkruis, F., Rangini, Z. et al. (1998). Early development of the zebrafish pronephros and analysis of mutations affecting pronephric function. *Development* **125**, 4655-67.

Dutton, K., Dutton, J. R., Pauliny, A. and Kelsh, R. N. (2001). A morpholino phenocopy of the colourless mutant. *Genesis* **30**, 188-9.

Easley, C. A., Faison, M. O., Kirsch, T. L., Lee, J. A., Seward, M. E. and Tombes, R. M. (2006). Laminin activates CaMK-II to stabilize nascent embryonic axons. *Brain Res* **1092**, 59-68.

Easley, C. A. t., Brown, C. M., Horwitz, A. F. and Tombes, R. M. (2008). CaMK-II promotes focal adhesion turnover and cell motility by inducing tyrosine dephosphorylation of FAK and paxillin. *Cell Motil Cytoskeleton* **65**, 662-74.

Ebert, A. M., Hume, G. L., Warren, K. S., Cook, N. P., Burns, C. G., Mohideen, M. A., Siegal, G., Yelon, D., Fishman, M. C. and Garrity, D. M. (2005). Calcium extrusion is critical for cardiac morphogenesis and rhythm in embryonic zebrafish hearts. *Proc Natl Acad Sci U S A* **102**, 17705-10.

Eckfeldt, C. E., Mendenhall, E. M., Flynn, C. M., Wang, T. F., Pickart, M. A., Grindle, S. M., Ekker, S. C. and Verfaillie, C. M. (2005). Functional analysis of human hematopoietic stem cell gene expression using zebrafish. *PLoS Biol* **3**, e254.

Edman, C. F. and Schulman, H. (1994). Identification and characterization of delta B-CaM kinase and delta C-CaM kinase from rat heart, two new multifunctional Ca2+/calmodulin-dependent protein kinase isoforms. *Biochim Biophys Acta* **1221**, 89-101.

Eisenberg, C. A. and Eisenberg, L. M. (1999). WNT11 promotes cardiac tissue formation of early mesoderm. *Dev Dyn* **216**, 45-58.

Faison, M. O., Perozzi, E. F., Caran, N., Stewart, J. K. and Tombes, R. M. (2002). Axonal localization of delta Ca2+/calmodulin-dependent protein kinase II in developing P19 neurons. *Int J Dev Neurosci* **20**, 585-92.

Feinmesser, R. L., Wicks, S. J., Taverner, C. J. and Chantry, A. (1999). Ca2+/calmodulin-dependent kinase II phosphorylates the epidermal growth factor receptor on multiple sites in the cytoplasmic tail and serine 744 within the kinase domain to regulate signal generation. *J Biol Chem* **274**, 16168-73.

Feng, S., Okenka, G. M., Bai, C. X., Streets, A. J., Newby, L. J., DeChant, B. T., Tsiokas, L., Obara, T. and Ong, A. C. (2008). Identification and functional characterization of an N-terminal oligomerization domain for polycystin-2. *J Biol Chem* **283**, 28471-9.

Fleming, I. N., Elliott, C. M., Buchanan, F. G., Downes, C. P. and Exton, J. H. (1999). Ca2+/calmodulin-dependent protein kinase II regulates Tiam1 by reversible protein phosphorylation. *J Biol Chem* **274**, 12753-8.

Fleming, I. N., Elliott, C. M. and Exton, J. H. (1998). Phospholipase C-gamma, protein kinase C and Ca2+/calmodulin-dependent protein kinase II are involved in platelet-derived growth factor-induced phosphorylation of Tiam1. *FEBS Lett* **429**, 229-33.

Fliegauf, M., Benzing, T. and Omran, H. (2007). When cilia go bad: cilia defects and ciliopathies. *Nat Rev Mol Cell Biol* **8**, 880-93.

Francescatto, L., Rothschild, S. C., Myers, A. L. and Tombes, R. M. (2010). Membrane Targeted CaMK-II is the Ca^{2+} Sensor Required for Left-Right Asymmetry in Zebrafish Embryos. *In preparation*.

Gabow, P. A. (1993). Autosomal dominant polycystic kidney disease. *N Engl J Med* **329**, 332-42.

Garriock, R. J., D'Agostino, S. L., Pilcher, K. C. and Krieg, P. A. (2005). Wnt11-R, a protein closely related to mammalian Wnt11, is required for heart morphogenesis in Xenopus. *Dev Biol* **279**, 179-92.

Garrity, D. M., Childs, S. and Fishman, M. C. (2002). The heartstrings mutation in zebrafish causes heart/fin Tbx5 deficiency syndrome. *Development* **129**, 4635-45.

Gattone, V. H., 2nd, Chen, N. X., Sinders, R. M., Seifert, M. F., Duan, D., Martin, D., Henley, C. and Moe, S. M. (2009). Calcimimetic inhibits late-stage cyst growth in ADPKD. *J Am Soc Nephrol* **20**, 1527-32.

Geng, L., Burrow, C. R., Li, H. P. and Wilson, P. D. (2000). Modification of the composition of polycystin-1 multiprotein complexes by calcium and tyrosine phosphorylation. *Biochim Biophys Acta* **1535**, 21-35.

Ghosh, T. K., Packham, E. A., Bonser, A. J., Robinson, T. E., Cross, S. J. and Brook, J. D. (2001). Characterization of the TBX5 binding site and analysis of mutations that cause Holt-Oram syndrome. *Hum Mol Genet* **10**, 1983-94.

Gilland, E., Miller, A. L., Karplus, E., Baker, R. and Webb, S. E. (1999). Imaging of multicellular large-scale rhythmic calcium waves during zebrafish gastrulation. *Proc Natl Acad Sci U S A* **96**, 157-61.

Goetz, S. C., Brown, D. D. and Conlon, F. L. (2006). TBX5 is required for embryonic cardiac cell cycle progression. *Development* **133**, 2575-84.

Grandel, H. and Schulte-Merker, S. (1998). The development of the paired fins in the zebrafish (Danio rerio). *Mech Dev* **79**, 99-120.

Grantham, J. J., Geiser, J. L. and Evan, A. P. (1987). Cyst formation and growth in autosomal dominant polycystic kidney disease. *Kidney Int* **31**, 1145-52.

Grimm, D. H., Karihaloo, A., Cai, Y., Somlo, S., Cantley, L. G. and Caplan, M. J. (2006). Polycystin-2 regulates proliferation and branching morphogenesis in kidney epithelial cells. *J Biol Chem* **281**, 137-44.

Grueter, C. E., Abiria, S. A., Dzhura, I., Wu, Y., Ham, A. J., Mohler, P. J., Anderson, M. E. and Colbran, R. J. (2006). L-type Ca2+ channel facilitation mediated by phosphorylation of the beta subunit by CaMKII. *Mol Cell* **23**, 641-50.

Grueter, C. E., Colbran, R. J. and Anderson, M. E. (2007). CaMKII, an emerging molecular driver for calcium homeostasis, arrhythmias, and cardiac dysfunction. *J Mol Med* **85**, 5-14.

Grunwald, D. J. and Streisinger, G. (1992a). Induction of mutations in the zebrafish with ultraviolet light. *Genet Res* **59**, 93-101.

Grunwald, D. J. and Streisinger, G. (1992b). Induction of recessive lethal and specific locus mutations in the zebrafish with ethyl nitrosourea. *Genet Res* **59**, 103-16.

Hagemann, D., Bohlender, J., Hoch, B., Krause, E. G. and Karczewski, P. (2001). Expression of Ca2+/calmodulin-dependent protein kinase II delta-subunit isoforms in rats with hypertensive cardiac hypertrophy. *Mol Cell Biochem* **220**, 69-76.

Hanaoka, K., Qian, F., Boletta, A., Bhunia, A. K., Piontek, K., Tsiokas, L., Sukhatme, V. P., Guggino, W. B. and Germino, G. G. (2000). Co-assembly of polycystin-1 and -2 produces unique cation-permeable currents. *Nature* **408**, 990-4.

Harris, P. C., Ward, C. J., Peral, B. and Hughes, J. (1995). Autosomal dominant polycystic kidney disease: molecular analysis. *Hum Mol Genet* **4 Spec No**, 1745-9.

Harvey, S. A. and Logan, M. P. (2006). sall4 acts downstream of tbx5 and is required for pectoral fin outgrowth. *Development* **133**, 1165-73.

Hatcher, C. J., Diman, N. Y., Kim, M. S., Pennisi, D., Song, Y., Goldstein, M. M., Mikawa, T. and Basson, C. T. (2004). A role for Tbx5 in proepicardial cell migration during cardiogenesis. *Physiol Genomics* **18**, 129-40.

Hatcher, C. J., Kim, M. S., Mah, C. S., Goldstein, M. M., Wong, B., Mikawa, T. and Basson, C. T. (2001). TBX5 transcription factor regulates cell proliferation during cardiogenesis. *Dev Biol* **230**, 177-88.

Heist, E. K. and Schulman, H. (1998). The role of Ca2+/calmodulin-dependent protein kinases within the nucleus. *Cell Calcium* **23**, 103-14.

Higashi, T., Ikeda, T., Murakami, T., Shirakawa, R., Kawato, M., Okawa, K., Furuse, M., Kimura, T., Kita, T. and Horiuchi, H. (2010). Flightless-I (Fli-I) regulates the actin assembly activity of Diaphanous-related formins (DRFs), Daam1 and mDia1, in cooperation with active Rho GTPase. *J Biol Chem*.

Hoch, B., Wobus, A. M., Krause, E. G. and Karczewski, P. (2000). delta-Ca(2+)/calmodulin-dependent protein kinase II expression pattern in adult mouse heart and cardiogenic differentiation of embryonic stem cells. *J Cell Biochem* **79**, 293-300.

Hooper, K. M., Boletta, A., Germino, G. G., Hu, Q., Ziegelstein, R. C. and Sutters, M. (2005). Expression of polycystin-1 enhances endoplasmic reticulum calcium uptake and decreases capacitative calcium entry in ATP-stimulated MDCK cells. *Am J Physiol Renal Physiol* **289**, F521-30.

Horb, M. E. and Thomsen, G. H. (1999). Tbx5 is essential for heart development. *Development* **126**, 1739-51.

Hudmon, A., Lebel, E., Roy, H., Sik, A., Schulman, H., Waxham, M. N. and De Koninck, P. (2005). A mechanism for Ca2+/calmodulin-dependent protein kinase II clustering at synaptic and nonsynaptic sites based on self-association. *J Neurosci* **25**, 6971-83.

Hudmon, A. and Schulman, H. (2002a). Neuronal CA2+/calmodulin-dependent protein kinase II: the role of structure and autoregulation in cellular function. *Annu Rev Biochem* **71**, 473-510.

Hudmon, A. and Schulman, H. (2002b). Structure-function of the multifunctional Ca2+/calmodulin-dependent protein kinase II. *Biochem J* **364**, 593-611.

Hughes, J., Ward, C. J., Peral, B., Aspinwall, R., Clark, K., San Millan, J. L., Gamble, V. and Harris, P. C. (1995). The polycystic kidney disease 1 (PKD1) gene encodes a novel protein with multiple cell recognition domains. *Nat Genet* **10**, 151-60.

Igarashi, P. and Somlo, S. (2002). Genetics and pathogenesis of polycystic kidney disease. *J Am Soc Nephrol* **13**, 2384-98.

Israeli, S., Amsler, K., Zheleznova, N. and Wilson, P. D. (2010). Abnormalities in focal adhesion complex formation, regulation, and function in human autosomal recessive polycystic kidney disease epithelial cells. *Am J Physiol Cell Physiol* **298**, C831-46.

Jaffe, L. F. (1995). Calcium waves and development. *Ciba Found Symp* **188**, 4-12; discussion 12-7.

Johnson, J., Bierle, B. M., Gallicano, G. I. and Capco, D. G. (1998). Calcium/calmodulin-dependent protein kinase II and calmodulin: regulators of the meiotic spindle in mouse eggs. *Dev Biol* **204**, 464-77.

Jopling, C., van Geemen, D. and den Hertog, J. (2007). Shp2 knockdown and Noonan/LEOPARD mutant Shp2-induced gastrulation defects. *PLoS Genet* **3**, e225.

Kam, Z., Minden, J. S., Agard, D. A., Sedat, J. W. and Leptin, M. (1991). Drosophila gastrulation: analysis of cell shape changes in living embryos by three-dimensional fluorescence microscopy. *Development* **112**, 365-70.

Karls, U., Muller, U., Gilbert, D. J., Copeland, N. G., Jenkins, N. A. and Harbers, K. (1992). Structure, expression, and chromosome location of the gene for the beta subunit of brain-specific Ca2+/calmodulin-dependent protein kinase II identified by transgene integration in an embryonic lethal mouse mutant. *Mol Cell Biol* **12**, 3644-52.

Karner, C. M., Chirumamilla, R., Aoki, S., Igarashi, P., Wallingford, J. B. and Carroll, T. J. (2009). Wnt9b signaling regulates planar cell polarity and kidney tubule morphogenesis. *Nat Genet* **41**, 793-9.

Keller, R. and Danilchik, M. (1988). Regional expression, pattern and timing of convergence and extension during gastrulation of Xenopus laevis. *Development* **103**, 193-209.

Keller, R. E. (1981). An experimental analysis of the role of bottle cells and the deep marginal zone in gastrulation of Xenopus laevis. *J Exp Zool* **216**, 81-101.

Kelley, C., Blumberg, H., Zon, L. I. and Evans, T. (1993). GATA-4 is a novel transcription factor expressed in endocardium of the developing heart. *Development* **118**, 817-27.

Kilian, B., Mansukoski, H., Barbosa, F. C., Ulrich, F., Tada, M. and Heisenberg, C. P. (2003). The role of Ppt/Wnt5 in regulating cell shape and movement during zebrafish gastrulation. *Mech Dev* **120**, 467-76.

Kim, H. J., Schleiffarth, J. R., Jessurun, J., Sumanas, S., Petryk, A., Lin, S. and Ekker, S. C. (2005). Wnt5 signaling in vertebrate pancreas development. *BMC Biol* **3**, 23.

Kimmel, C. B., Ballard, W. W., Kimmel, S. R., Ullmann, B. and Schilling, T. F. (1995). Stages of embryonic development of the zebrafish. *Dev Dyn* **203**, 253-310.

Kohn, A. D. and Moon, R. T. (2005). Wnt and calcium signaling: beta-catenin-independent pathways. *Cell Calcium* **38**, 439-46.

Kottgen, M. (2007). TRPP2 and autosomal dominant polycystic kidney disease. *Biochim Biophys Acta* **1772**, 836-50.

Kramer-Zucker, A. G., Olale, F., Haycraft, C. J., Yoder, B. K., Schier, A. F. and Drummond, I. A. (2005). Cilia-driven fluid flow in the zebrafish pronephros, brain and Kupffer's vesicle is required for normal organogenesis. *Development* **132**, 1907-21.

Kuhl, M., Geis, K., Sheldahl, L. C., Pukrop, T., Moon, R. T. and Wedlich, D. (2001). Antagonistic regulation of convergent extension movements in Xenopus by Wnt/beta-catenin and Wnt/Ca2+ signaling. *Mech Dev* **106**, 61-76.

Kuhl, M., Sheldahl, L. C., Malbon, C. C. and Moon, R. T. (2000a). Ca(2+)/calmodulin-dependent protein kinase II is stimulated by Wnt and Frizzled homologs and promotes ventral cell fates in Xenopus. *J Biol Chem* **275**, 12701-11.

Kuhl, M., Sheldahl, L. C., Park, M., Miller, J. R. and Moon, R. T. (2000b). The Wnt/Ca2+ pathway: a new vertebrate Wnt signaling pathway takes shape. *Trends Genet* **16**, 279-83.

Laabich, A., Li, G. and Cooper, N. G. (2000). Calcium/calmodulin-dependent protein kinase II containing a nuclear localizing signal is altered in retinal neurons exposed to N-methyl-D-aspartate. *Brain Res Mol Brain Res* **76**, 253-65.

Lanoix, J., D'Agati, V., Szabolcs, M. and Trudel, M. (1996). Dysregulation of cellular proliferation and apoptosis mediates human autosomal dominant polycystic kidney disease (ADPKD). *Oncogene* **13**, 1153-60.

Lantinga-van Leeuwen, I. S., Dauwerse, J. G., Baelde, H. J., Leonhard, W. N., van de Wal, A., Ward, C. J., Verbeek, S., Deruiter, M. C., Breuning, M. H., de Heer, E. et al. (2004). Lowering of Pkd1 expression is sufficient to cause polycystic kidney disease. *Hum Mol Genet* **13**, 3069-77.

Lantinga-van Leeuwen, I. S., Leonhard, W. N., van der Wal, A., Breuning, M. H., de Heer, E. and Peters, D. J. (2007). Kidney-specific inactivation of the Pkd1 gene induces rapid cyst formation in developing kidneys and a slow onset of disease in adult mice. *Hum Mol Genet* **16**, 3188-96.

Lantsman, K. and Tombes, R. M. (2005). CaMK-II oligomerization potential determined using CFP/YFP FRET. *Biochim Biophys Acta* **1746**, 45-54.

Lee, T. S., Karl, R., Moosmang, S., Lenhardt, P., Klugbauer, N., Hofmann, F., Kleppisch, T. and Welling, A. (2006). Calmodulin kinase II is involved in voltage-dependent facilitation of the L-type Cav1.2 calcium channel: Identification of the phosphorylation sites. *J Biol Chem* **281**, 25560-7.

Li, Y., Wright, J. M., Qian, F., Germino, G. G. and Guggino, W. B. (2005). Polycystin 2 interacts with type I inositol 1,4,5-trisphosphate receptor to modulate intracellular Ca2+ signaling. *J Biol Chem* **280**, 41298-306.

Lin, F., Hiesberger, T., Cordes, K., Sinclair, A. M., Goldstein, L. S., Somlo, S. and Igarashi, P. (2003). Kidney-specific inactivation of the KIF3A subunit of kinesin-II inhibits renal ciliogenesis and produces polycystic kidney disease. *Proc Natl Acad Sci U S A* **100**, 5286-91.

Lin, Y. H., Park, Z. Y., Lin, D., Brahmbhatt, A. A., Rio, M. C., Yates, J. R., 3rd and Klemke, R. L. (2004). Regulation of cell migration and survival by focal adhesion targeting of Lasp-1. *J Cell Biol* **165**, 421-32.

Lister, J. A., Close, J. and Raible, D. W. (2001). Duplicate mitf genes in zebrafish: complementary expression and conservation of melanogenic potential. *Dev Biol* **237**, 333-44.

Little, G. H., Bai, Y., Williams, T. and Poizat, C. (2007). Nuclear calcium/calmodulin-dependent protein kinase IIdelta preferentially transmits signals to histone deacetylase 4 in cardiac cells. *J Biol Chem* **282**, 7219-31.

Liu, N. and Cooper, N. G. (1996). The Ca2+/calmodulin-dependent protein kinase II-associated protein complex isolated from chicken retina. *J Mol Neurosci* **7**, 1-12.

Liu, Y., Pathak, N., Kramer-Zucker, A. and Drummond, I. A. (2007). Notch signaling controls the differentiation of transporting epithelia and multiciliated cells in the zebrafish pronephros. *Development* **134**, 1111-22.

Lo, S. H., Yu, Q. C., Degenstein, L., Chen, L. B. and Fuchs, E. (1997). Progressive kidney degeneration in mice lacking tensin. *J Cell Biol* **136**, 1349-61.

Lorca, T., Cruzalegui, F. H., Fesquet, D., Cavadore, J. C., Mery, J., Means, A. and Doree, M. (1993). Calmodulin-dependent protein kinase II mediates inactivation of MPF and CSF upon fertilization of Xenopus eggs. *Nature* **366**, 270-3.

Low, S. H., Vasanth, S., Larson, C. H., Mukherjee, S., Sharma, N., Kinter, M. T., Kane, M. E., Obara, T. and Weimbs, T. (2006). Polycystin-1, STAT6, and P100 function in a pathway that transduces ciliary mechanosensation and is activated in polycystic kidney disease. *Dev Cell* **10**, 57-69.

Lu, J. H., Lu, J. K., Choo, S. L., Li, Y. C., Yeh, H. W., Shiue, J. F. and Yeh, V. C. (2008). Cascade effect of cardiac myogenesis gene expression during cardiac looping in tbx5 knockdown zebrafish embryos. *J Biomed Sci* **15**, 779-87.

Lu, W., Fan, X., Basora, N., Babakhanlou, H., Law, T., Rifai, N., Harris, P. C., Perez-Atayde, A. R., Rennke, H. G. and Zhou, J. (1999). Late onset of renal and hepatic cysts in Pkd1-targeted heterozygotes. *Nat Genet* **21**, 160-1.

Lu, W., Peissel, B., Babakhanlou, H., Pavlova, A., Geng, L., Fan, X., Larson, C., Brent, G. and Zhou, J. (1997). Perinatal lethality with kidney and pancreas defects in mice with a targetted Pkd1 mutation. *Nat Genet* **17**, 179-81.

Lu, W., Shen, X., Pavlova, A., Lakkis, M., Ward, C. J., Pritchard, L., Harris, P. C., Genest, D. R., Perez-Atayde, A. R. and Zhou, J. (2001). Comparison of Pkd1-targeted mutants reveals that loss of polycystin-1 causes cystogenesis and bone defects. *Hum Mol Genet* **10**, 2385-96.

Lundberg, M. S., Curto, K. A., Bilato, C., Monticone, R. E. and Crow, M. T. (1998). Regulation of vascular smooth muscle migration by mitogen-activated protein kinase and calcium/calmodulin-dependent protein kinase II signaling pathways. *J Mol Cell Cardiol* **30**, 2377-89.

Madgwick, S., Levasseur, M. and Jones, K. T. (2005). Calmodulin-dependent protein kinase II, and not protein kinase C, is sufficient for triggering cell-cycle resumption in mammalian eggs. *J Cell Sci* **118**, 3849-59.

Maier, L. S. (2009). Role of CaMKII for signaling and regulation in the heart. *Front Biosci* **14**, 486-96.

Maier, L. S. and Bers, D. M. (2002). Calcium, calmodulin, and calcium-calmodulin kinase II: heartbeat to heartbeat and beyond. *J Mol Cell Cardiol* **34**, 919-39.

Malliri, A., van Es, S., Huveneers, S. and Collard, J. G. (2004). The Rac exchange factor Tiam1 is required for the establishment and maintenance of cadherin-based adhesions. *J Biol Chem* **279**, 30092-8.

Mangos, S., Lam, P. Y., Zhao, A., Liu, Y., Mudumana, S., Vasilyev, A., Liu, A. and Drummond, I. A. (2010). The ADPKD genes pkd1a/b and pkd2 regulate extracellular matrix formation. *Dis Model Mech*.

Markoulaki, S., Matson, S., Abbott, A. L. and Ducibella, T. (2003). Oscillatory CaMKII activity in mouse egg activation. *Dev Biol* **258**, 464-74.

Markoulaki, S., Matson, S. and Ducibella, T. (2004). Fertilization stimulates long-lasting oscillations of CaMKII activity in mouse eggs. *Dev Biol* **272**, 15-25.

Marks, P. W. and Maxfield, F. R. (1990). Transient increases in cytosolic free calcium appear to be required for the migration of adherent human neutrophils. *J Cell Biol* **110**, 43-52.

Martinez-Barbera, J. P., Toresson, H., Da Rocha, S. and Krauss, S. (1997). Cloning and expression of three members of the zebrafish Bmp family: Bmp2a, Bmp2b and Bmp4. *Gene* **198**, 53-9.

Matthews, R. P., Guthrie, C. R., Wailes, L. M., Zhao, X., Means, A. R. and McKnight, G. S. (1994). Calcium/calmodulin-dependent protein kinase types II and IV differentially regulate CREB-dependent gene expression. *Mol Cell Biol* **14**, 6107-16.

Mayford, M., Bach, M. E., Huang, Y. Y., Wang, L., Hawkins, R. D. and Kandel, E. R. (1996). Control of memory formation through regulated expression of a CaMKII transgene. *Science* **274**, 1678-83.

Milutinovic, J., Fialkow, P. J., Agodoa, L. Y., Phillips, L. A., Rudd, T. G. and Bryant, J. I. (1984). Autosomal dominant polycystic kidney disease: symptoms and clinical findings. *Q J Med* **53**, 511-22.

Mitra, S. K., Hanson, D. A. and Schlaepfer, D. D. (2005). Focal adhesion kinase: in command and control of cell motility. *Nat Rev Mol Cell Biol* **6**, 56-68.

Mochizuki, T., Wu, G., Hayashi, T., Xenophontos, S. L., Veldhuisen, B., Saris, J. J., Reynolds, D. M., Cai, Y., Gabow, P. A., Pierides, A. et al. (1996). PKD2, a gene for polycystic kidney disease that encodes an integral membrane protein. *Science* **272**, 1339-42.

Montgomery, R. L., Davis, C. A., Potthoff, M. J., Haberland, M., Fielitz, J., Qi, X., Hill, J. A., Richardson, J. A. and Olson, E. N. (2007). Histone deacetylases 1 and 2 redundantly regulate cardiac morphogenesis, growth, and contractility. *Genes Dev* **21**, 1790-802.

Moon, R. T., Bowerman, B., Boutros, M. and Perrimon, N. (2002). The promise and perils of Wnt signaling through beta-catenin. *Science* **296**, 1644-6.

Morita, M., Iguchi, A. and Takemura, A. (2009). Roles of calmodulin and calcium/calmodulin-dependent protein kinase in flagellar motility regulation in the coral Acropora digitifera. *Mar Biotechnol (NY)* **11**, 118-23.

Morris, T. A., DeLorenzo, R. J. and Tombes, R. M. (1998). CaMK-II inhibition reduces cyclin D1 levels and enhances the association of p27kip1 with Cdk2 to cause G1 arrest in NIH 3T3 cells. *Exp Cell Res* **240**, 218-27.

Moy, G. W., Mendoza, L. M., Schulz, J. R., Swanson, W. J., Glabe, C. G. and Vacquier, V. D. (1996). The sea urchin sperm receptor for egg jelly is a modular protein with extensive homology to the human polycystic kidney disease protein, PKD1. *J Cell Biol* **133**, 809-17.

Myers, D. C., Sepich, D. S. and Solnica-Krezel, L. (2002). Convergence and extension in vertebrate gastrulae: cell movements according to or in search of identity? *Trends Genet* **18**, 447-55.

Nagao, S., Nishii, K., Yoshihara, D., Kurahashi, H., Nagaoka, K., Yamashita, T., Takahashi, H., Yamaguchi, T., Calvet, J. P. and Wallace, D. P. (2008). Calcium channel inhibition accelerates polycystic kidney disease progression in the Cy/+ rat. *Kidney Int* **73**, 269-77.

Naiche, L. A., Harrelson, Z., Kelly, R. G. and Papaioannou, V. E. (2005). T-box genes in vertebrate development. *Annu Rev Genet* **39**, 219-39.

Nasevicius, A. and Ekker, S. C. (2000). Effective targeted gene 'knockdown' in zebrafish. *Nat Genet* **26**, 216-20.

Nauli, S. M., Alenghat, F. J., Luo, Y., Williams, E., Vassilev, P., Li, X., Elia, A. E., Lu, W., Brown, E. M., Quinn, S. J. et al. (2003). Polycystins 1 and 2 mediate mechanosensation in the primary cilium of kidney cells. *Nat Genet* **33**, 129-37.

Ng, J. K., Kawakami, Y., Buscher, D., Raya, A., Itoh, T., Koth, C. M., Rodriguez Esteban, C., Rodriguez-Leon, J., Garrity, D. M., Fishman, M. C. et al. (2002). The limb identity gene Tbx5 promotes limb initiation by interacting with Wnt2b and Fgf10. *Development* **129**, 5161-70.

Nigg, E. A. and Raff, J. W. (2009). Centrioles, centrosomes, and cilia in health and disease. *Cell* **139**, 663-78.

Nixon, V. L., Levasseur, M., McDougall, A. and Jones, K. T. (2002). Ca(2+) oscillations promote APC/C-dependent cyclin B1 degradation during metaphase arrest and completion of meiosis in fertilizing mouse eggs. *Curr Biol* **12**, 746-50.

Nomura, M., Yoshida, M. and Morisawa, M. (2004). Calmodulin/calmodulin-dependent protein kinase II mediates SAAF-induced motility activation of ascidian sperm. *Cell Motil Cytoskeleton* **59**, 28-37.

Obara, T., Mangos, S., Liu, Y., Zhao, J., Wiessner, S., Kramer-Zucker, A. G., Olale, F., Schier, A. F. and Drummond, I. A. (2006). Polycystin-2 immunolocalization and function in zebrafish. *J Am Soc Nephrol* **17**, 2706-18.

Oh, J. S., Manzerra, P. and Kennedy, M. B. (2004). Regulation of the neuron-specific Ras GTPase-activating protein, synGAP, by Ca2+/calmodulin-dependent protein kinase II. *J Biol Chem* **279**, 17980-8.

Palmer, A. E. and Tsien, R. Y. (2006). Measuring calcium signaling using genetically targetable fluorescent indicators. *Nat Protoc* **1**, 1057-65.

Pandur, P., Lasche, M., Eisenberg, L. M. and Kuhl, M. (2002). Wnt-11 activation of a non-canonical Wnt signalling pathway is required for cardiogenesis. *Nature* **418**, 636-41.

Panizzi, J. R., Jessen, J. R., Drummond, I. A. and Solnica-Krezel, L. (2007). New functions for a vertebrate Rho guanine nucleotide exchange factor in ciliated epithelia. *Development* **134**, 921-31.

Pei, Y., Watnick, T., He, N., Wang, K., Liang, Y., Parfrey, P., Germino, G. and St George-Hyslop, P. (1999). Somatic PKD2 mutations in individual kidney and liver cysts support a "two-hit" model of cystogenesis in type 2 autosomal dominant polycystic kidney disease. *J Am Soc Nephrol* **10**, 1524-9.

Pennekamp, P., Karcher, C., Fischer, A., Schweickert, A., Skryabin, B., Horst, J., Blum, M. and Dworniczak, B. (2002). The ion channel polycystin-2 is required for left-right axis determination in mice. *Curr Biol* **12**, 938-43.

Peterkin, T., Gibson, A. and Patient, R. (2007). Redundancy and evolution of GATA factor requirements in development of the myocardium. *Dev Biol* **311**, 623-35.

Pfleiderer, P. J., Lu, K. K., Crow, M. T., Keller, R. S. and Singer, H. A. (2004). Modulation of vascular smooth muscle cell migration by calcium/ calmodulin-dependent protein kinase II-delta 2. *Am J Physiol Cell Physiol* **286**, C1238-45.

Pillai, R., Coverdale, L. E., Dubey, G. and Martin, C. C. (2004). Histone deacetylase 1 (HDAC-1) required for the normal formation of craniofacial cartilage and pectoral fins of the zebrafish. *Dev Dyn* **231**, 647-54.

Piontek, K. B., Huso, D. L., Grinberg, A., Liu, L., Bedja, D., Zhao, H., Gabrielson, K., Qian, F., Mei, C., Westphal, H. et al. (2004). A functional floxed allele of Pkd1 that can be conditionally inactivated in vivo. *J Am Soc Nephrol* **15**, 3035-43.

Plageman, T. F., Jr. and Yutzey, K. E. (2006). Microarray analysis of Tbx5-induced genes expressed in the developing heart. *Dev Dyn* **235**, 2868-80.

Poole, A. W. and Jones, M. L. (2005). A SHPing tale: perspectives on the regulation of SHP-1 and SHP-2 tyrosine phosphatases by the C-terminal tail. *Cell Signal* **17**, 1323-32.

Postlethwait, J., Amores, A., Cresko, W., Singer, A. and Yan, Y. L. (2004). Subfunction partitioning, the teleost radiation and the annotation of the human genome. *Trends Genet* **20**, 481-90.

Praetorius, H. A. and Spring, K. R. (2001). Bending the MDCK cell primary cilium increases intracellular calcium. *J Membr Biol* **184**, 71-9.

Praetorius, H. A. and Spring, K. R. (2003). Removal of the MDCK cell primary cilium abolishes flow sensing. *J Membr Biol* **191**, 69-76.

Pyati, U. J., Cooper, M. S., Davidson, A. J., Nechiporuk, A. and Kimelman, D. (2006). Sustained Bmp signaling is essential for cloaca development in zebrafish. *Development* **133**, 2275-84.

Qian, F., Boletta, A., Bhunia, A. K., Xu, H., Liu, L., Ahrabi, A. K., Watnick, T. J., Zhou, F. and Germino, G. G. (2002). Cleavage of polycystin-1 requires the receptor for egg jelly domain and is disrupted by human autosomal-dominant polycystic kidney disease 1-associated mutations. *Proc Natl Acad Sci U S A* **99**, 16981-6.

Qian, F., Germino, F. J., Cai, Y., Zhang, X., Somlo, S. and Germino, G. G. (1997). PKD1 interacts with PKD2 through a probable coiled-coil domain. *Nat Genet* **16**, 179-83.

Rallis, C., Bruneau, B. G., Del Buono, J., Seidman, C. E., Seidman, J. G., Nissim, S., Tabin, C. J. and Logan, M. P. (2003). Tbx5 is required for forelimb bud formation and continued outgrowth. *Development* **130**, 2741-51.

Ramirez, M. T., Zhao, X. L., Schulman, H. and Brown, J. H. (1997). The nuclear deltaB isoform of Ca2+/calmodulin-dependent protein kinase II regulates atrial natriuretic factor gene expression in ventricular myocytes. *J Biol Chem* **272**, 31203-8.

Ren, Y., Meng, S., Mei, L., Zhao, Z. J., Jove, R. and Wu, J. (2004). Roles of Gab1 and SHP2 in paxillin tyrosine dephosphorylation and Src activation in response to epidermal growth factor. *J Biol Chem* **279**, 8497-505.

Rich, R. C. and Schulman, H. (1998). Substrate-directed function of calmodulin in autophosphorylation of Ca2+/calmodulin-dependent protein kinase II. *J Biol Chem* **273**, 28424-9.

Roelfsema, J. H. and Breuning, M. H. (1996). The long walk toward the PKD1 gene. The European PKD1 Consortium. *Adv Nephrol Necker Hosp* **25**, 131-45.

Rosenberg, O. S., Deindl, S., Sung, R. J., Nairn, A. C. and Kuriyan, J. (2005). Structure of the autoinhibited kinase domain of CaMKII and SAXS analysis of the holoenzyme. *Cell* **123**, 849-60.

Roszko, I., Sawada, A. and Solnica-Krezel, L. (2009). Regulation of convergence and extension movements during vertebrate gastrulation by the Wnt/PCP pathway. *Semin Cell Dev Biol* **20**, 986-97.

Rothschild, S. C., Easley, C. A. t., Francescatto, L., Lister, J. A., Garrity, D. M. and Tombes, R. M. (2009). Tbx5-mediated expression of Ca(2+)/calmodulin-dependent protein kinase II is necessary for zebrafish cardiac and pectoral fin morphogenesis. *Dev Biol* **330**, 175-84.

Rothschild, S. C., Lister, J. A. and Tombes, R. M. (2007). Differential expression of CaMK-II genes during early zebrafish embryogenesis. *Dev Dyn* **236**, 295-305.

Schneider, M. F. and Rodney, G. G. (2004). Peptide and protein modulation of local Ca2+ release events in permeabilized skeletal muscle fibers. *Biol Res* **37**, 613-6.

Schoenebeck, J. J. and Yelon, D. (2007). Illuminating cardiac development: Advances in imaging add new dimensions to the utility of zebrafish genetics. *Semin Cell Dev Biol* **18**, 27-35.

Schottenfeld, J., Sullivan-Brown, J. and Burdine, R. D. (2007). Zebrafish curly up encodes a Pkd2 ortholog that restricts left-side-specific expression of southpaw. *Development* **134**, 1605-15.

Schulman, H., Hanson, P. I. and Meyer, T. (1992). Decoding calcium signals by multifunctional CaM kinase. *Cell Calcium* **13**, 401-11.

Seville, R. A., Nijjar, S., Barnett, M. W., Masse, K. and Jones, E. A. (2002). Annexin IV (Xanx-4) has a functional role in the formation of pronephric tubules. *Development* **129**, 1693-704.

Seward, M. E., Easley, C. A. t., McLeod, J. J., Myers, A. L. and Tombes, R. M. (2008). Flightless-I, a gelsolin family member and transcriptional regulator, preferentially binds directly to activated cytosolic CaMK-II. *FEBS Lett* **582**, 2489-95.

Sheldahl, L. C., Slusarski, D. C., Pandur, P., Miller, J. R., Kuhl, M. and Moon, R. T. (2003). Dishevelled activates Ca2+ flux, PKC, and CamKII in vertebrate embryos. *J Cell Biol* **161**, 769-77.

Shen, K. and Meyer, T. (1999). Dynamic control of CaMKII translocation and localization in hippocampal neurons by NMDA receptor stimulation. *Science* **284**, 162-6.

Shimeld, S. M. (2004). Calcium turns sinister in left-right asymmetry. *Trends Genet* **20**, 277-80.

Shimomura, A., Ogawa, Y., Kitani, T., Fujisawa, H. and Hagiwara, M. (1996). Calmodulin-dependent protein kinase II potentiates transcriptional activation through activating transcription factor 1 but not cAMP response element-binding protein. *J Biol Chem* **271**, 17957-60.

Shimomura, O., Inouye, S., Musicki, B. and Kishi, Y. (1990). Recombinant aequorin and recombinant semi-synthetic aequorins. Cellular Ca2+ ion indicators. *Biochem J* **270**, 309-12.

Silva, A. J., Paylor, R., Wehner, J. M. and Tonegawa, S. (1992). Impaired spatial learning in alpha-calcium-calmodulin kinase II mutant mice. *Science* **257**, 206-11.

Singer, H. A., Benscoter, H. A. and Schworer, C. M. (1997). Novel Ca2+/calmodulin-dependent protein kinase II gamma-subunit variants expressed in vascular smooth muscle, brain, and cardiomyocytes. *J Biol Chem* **272**, 9393-400.

Singh, P., Leddy, J. J., Chatzis, G. J., Salih, M. and Tuana, B. S. (2005). Alternative splicing generates a CaM kinase IIbeta isoform in myocardium that targets the sarcoplasmic reticulum through a putative alphaKAP and regulates GAPDH. *Mol Cell Biochem* **270**, 215-21.

Skouloudaki, K., Puetz, M., Simons, M., Courbard, J. R., Boehlke, C., Hartleben, B., Engel, C., Moeller, M. J., Englert, C., Bollig, F. et al. (2009). Scribble participates in Hippo signaling and is required for normal zebrafish pronephros development. *Proc Natl Acad Sci U S A* **106**, 8579-84.

Slusarski, D. C., Yang-Snyder, J., Busa, W. B. and Moon, R. T. (1997). Modulation of embryonic intracellular Ca2+ signaling by Wnt-5A. *Dev Biol* **182**, 114-20.

Soderling, T. R. (2000). CaM-kinases: modulators of synaptic plasticity. *Curr Opin Neurobiol* **10**, 375-80.

Solnica-Krezel, L., Schier, A. F. and Driever, W. (1994). Efficient recovery of ENU-induced mutations from the zebrafish germline. *Genetics* **136**, 1401-20.

Srinivasan, M., Edman, C. F. and Schulman, H. (1994). Alternative splicing introduces a nuclear localization signal that targets multifunctional CaM kinase to the nucleus. *J Cell Biol* **126**, 839-52.

St Amand, A. L. and Klymkowsky, M. W. (2001). Cadherins and catenins, Wnts and SOXs: embryonic patterning in Xenopus. *Int Rev Cytol* **203**, 291-355.

Stefanovic, S., Windsor, M., Nagata, K. I., Inagaki, M. and Wileman, T. (2005). Vimentin rearrangement during African swine fever virus infection involves retrograde transport along microtubules and phosphorylation of vimentin by calcium calmodulin kinase II. *J Virol* **79**, 11766-75.

Stemmann, O., Zou, H., Gerber, S. A., Gygi, S. P. and Kirschner, M. W. (2001). Dual inhibition of sister chromatid separation at metaphase. *Cell* **107**, 715-26.

Stevens, I., Derua, R., Rondelez, E., Waelkens, E., Merlevede, W. and Goris, J. (1999). Identification of cyk, a cyclin B2 kinase, as a novel calcium/calmodulin-dependent protein kinase II and its role during Xenopus laevis oocyte maturation. *Exp Cell Res* **252**, 303-18.

Strausberg, R. L., Feingold, E. A., Grouse, L. H., Derge, J. G., Klausner, R. D., Collins, F. S., Wagner, L., Shenmen, C. M., Schuler, G. D., Altschul, S. F. et al. (2002). Generation and initial analysis of more than 15,000 full-length human and mouse cDNA sequences. *Proc Natl Acad Sci U S A* **99**, 16899-903.

Streisinger, G., Coale, F., Taggart, C., Walker, C. and Grunwald, D. J. (1989). Clonal origins of cells in the pigmented retina of the zebrafish eye. *Dev Biol* **131**, 60-9.

Streisinger, G., Singer, F., Walker, C., Knauber, D. and Dower, N. (1986). Segregation analyses and gene-centromere distances in zebrafish. *Genetics* **112**, 311-9.

Streisinger, G., Walker, C., Dower, N., Knauber, D. and Singer, F. (1981). Production of clones of homozygous diploid zebra fish (Brachydanio rerio). *Nature* **291**, 293-6.

Sugai, R., Takeuchi, M., Okuno, S. and Fujisawa, H. (1996). Molecular cloning of a novel protein containing the association domain of calmodulin-dependent protein kinase II. *J Biochem* **120**, 773-9.

Sumanas, S., Kim, H. J., Hermanson, S. and Ekker, S. C. (2001). Zebrafish frizzled-2 morphant displays defects in body axis elongation. *Genesis* **30**, 114-8.

Sun, G., Lewis, L. E., Huang, X., Nguyen, Q., Price, C. and Huang, T. (2004a). TBX5, a gene mutated in Holt-Oram syndrome, is regulated through a GC box and T-box binding elements (TBEs). *J Cell Biochem* **92**, 189-99.

Sun, P., Lou, L. and Maurer, R. A. (1996). Regulation of activating transcription factor-1 and the cAMP response element-binding protein by Ca2+/calmodulin-dependent protein kinases type I, II, and IV. *J Biol Chem* **271**, 3066-73.

Sun, Z., Amsterdam, A., Pazour, G. J., Cole, D. G., Miller, M. S. and Hopkins, N. (2004b). A genetic screen in zebrafish identifies cilia genes as a principal cause of cystic kidney. *Development* **131**, 4085-93.

Sweeton, D., Parks, S., Costa, M. and Wieschaus, E. (1991). Gastrulation in Drosophila: the formation of the ventral furrow and posterior midgut invaginations. *Development* **112**, 775-89.

Tada, M., Concha, M. L. and Heisenberg, C. P. (2002). Non-canonical Wnt signalling and regulation of gastrulation movements. *Semin Cell Dev Biol* **13**, 251-60.

Tahara, M., Tasaka, K., Masumoto, N., Mammoto, A., Ikebuchi, Y. and Miyake, A. (1996). Dynamics of cortical granule exocytosis at fertilization in living mouse eggs. *Am J Physiol* **270**, C1354-61.

Takeuchi, J. K., Koshiba-Takeuchi, K., Suzuki, T., Kamimura, M., Ogura, K. and Ogura, T. (2003). Tbx5 and Tbx4 trigger limb initiation through activation of the Wnt/Fgf signaling cascade. *Development* **130**, 2729-39.

Takeuchi, M. and Fujisawa, H. (1997). Perinuclear membrane localization of alphaKAP, a protein produced from a gene within the gene of calmodulin-dependent protein kinase IIalpha. *J Biochem* **122**, 494-7.

Takeuchi, Y., Yamamoto, H., Fukunaga, K., Miyakawa, T. and Miyamoto, E. (2000). Identification of the isoforms of Ca(2+)/Calmodulin-dependent protein kinase II in rat astrocytes and their subcellular localization. *J Neurochem* **74**, 2557-67.

Tao, Y., Kim, J., Faubel, S., Wu, J. C., Falk, S. A., Schrier, R. W. and Edelstein, C. L. (2005a). Caspase inhibition reduces tubular apoptosis and proliferation and slows disease progression in polycystic kidney disease. *Proc Natl Acad Sci U S A* **102**, 6954-9.

Tao, Y., Kim, J., Stanley, M., He, Z., Faubel, S., Schrier, R. W. and Edelstein, C. L. (2005b). Pathways of caspase-mediated apoptosis in autosomal-dominant polycystic kidney disease (ADPKD). *Kidney Int* **67**, 909-19.

Tao, Y., Zafar, I., Kim, J., Schrier, R. W. and Edelstein, C. L. (2008). Caspase-3 gene deletion prolongs survival in polycystic kidney disease. *J Am Soc Nephrol* **19**, 749-55.

Tartaglia, M. and Gelb, B. D. (2005). Noonan syndrome and related disorders: genetics and pathogenesis. *Annu Rev Genomics Hum Genet* **6**, 45-68.

Tartaglia, M., Mehler, E. L., Goldberg, R., Zampino, G., Brunner, H. G., Kremer, H., van der Burgt, I., Crosby, A. H., Ion, A., Jeffery, S. et al. (2001). Mutations in PTPN11, encoding the protein tyrosine phosphatase SHP-2, cause Noonan syndrome. *Nat Genet* **29**, 465-8.

Tatone, C., Delle Monache, S., Iorio, R., Caserta, D., Di Cola, M. and Colonna, R. (2002). Possible role for Ca(2+) calmodulin-dependent protein kinase II as an effector of the fertilization Ca(2+) signal in mouse oocyte activation. *Mol Hum Reprod* **8**, 750-7.

Tatone, C., Iorio, R., Francione, A., Gioia, L. and Colonna, R. (1999). Biochemical and biological effects of KN-93, an inhibitor of calmodulin-dependent protein kinase II, on the initial events of mouse egg activation induced by ethanol. *J Reprod Fertil* **115**, 151-7.

Tobimatsu, T. and Fujisawa, H. (1989). Tissue-specific expression of four types of rat calmodulin-dependent protein kinase II mRNAs. *J Biol Chem* **264**, 17907-12.

Tombes, R. M., Faison, M. O. and Turbeville, J. M. (2003). Organization and evolution of multifunctional Ca(2+)/CaM-dependent protein kinase genes. *Gene* **322**, 17-31.

Tombes, R. M., Grant, S., Westin, E. H. and Krystal, G. (1995). G1 cell cycle arrest and apoptosis are induced in NIH 3T3 cells by KN-93, an inhibitor of CaMK-II (the multifunctional Ca2+/CaM kinase). *Cell Growth Differ* **6**, 1063-70.

Tombes, R. M. and Krystal, G. W. (1997). Identification of novel human tumor cell-specific CaMK-II variants. *Biochim Biophys Acta* **1355**, 281-92.

Tombes, R. M., Mikkelsen, R. B., Jarvis, W. D. and Grant, S. (1999). Downregulation of delta CaM kinase II in human tumor cells. *Biochim Biophys Acta* **1452**, 1-11.

Tombes, R. M., Peloquin, J. G. and Borisy, G. G. (1991). Specific association of an M-phase kinase with isolated mitotic spindles and identification of two of its substrates as MAP4 and MAP1B. *Cell Regul* **2**, 861-74.

Tombes, R. M. and Peppers, L. S. (1995). Sea urchin fertilization stimulates CaM kinase-II (multifunctinoal (Type II) Ca^{2+}/CaM kinase) activity and association with $p34^{cdc2}$. *Dev Growth Differ* **37**, 589-596.

Tsiokas, L. (2009). Function and regulation of TRPP2 at the plasma membrane. *Am J Physiol Renal Physiol* **297**, F1-9.

Tsiokas, L., Kim, S. and Ong, E. C. (2007). Cell biology of polycystin-2. *Cell Signal* **19**, 444-53.

Urquidi, V. and Ashcroft, S. J. (1995). A novel pancreatic beta-cell isoform of calcium/calmodulin-dependent protein kinase II (beta 3 isoform) contains a proline-rich tandem repeat in the association domain. *FEBS Lett* **358**, 23-6.

Vadlamudi, R. K., Adam, L., Nguyen, D., Santos, M. and Kumar, R. (2002). Differential regulation of components of the focal adhesion complex by heregulin: role of phosphatase SHP-2. *J Cell Physiol* **190**, 189-99.

Vandorpe, D. H., Chernova, M. N., Jiang, L., Sellin, L. K., Wilhelm, S., Stuart-Tilley, A. K., Walz, G. and Alper, S. L. (2001). The cytoplasmic C-terminal fragment of polycystin-1 regulates a Ca2+-permeable cation channel. *J Biol Chem* **276**, 4093-101.

Vasilyev, A., Liu, Y., Mudumana, S., Mangos, S., Lam, P. Y., Majumdar, A., Zhao, J., Poon, K. L., Kondrychyn, I., Korzh, V. et al. (2009). Collective cell migration drives morphogenesis of the kidney nephron. *PLoS Biol* **7**, e9.

Walker, C. and Streisinger, G. (1983). Induction of Mutations by gamma-Rays in Pregonial Germ Cells of Zebrafish Embryos. *Genetics* **103**, 125-136.

Wallingford, J. B., Ewald, A. J., Harland, R. M. and Fraser, S. E. (2001). Calcium signaling during convergent extension in Xenopus. *Curr Biol* **11**, 652-61.

Wallingford, J. B., Fraser, S. E. and Harland, R. M. (2002). Convergent extension: the molecular control of polarized cell movement during embryonic development. *Dev Cell* **2**, 695-706.

Wang, Z. and Yang, Z. Q. (2000). Casein kinase II phosphorylation of caldesmon downregulates myosin-caldesmon interactions. *Biochemistry* **39**, 11114-20.

Waxman, J. S., Keegan, B. R., Roberts, R. W., Poss, K. D. and Yelon, D. (2008). Hoxb5b acts downstream of retinoic acid signaling in the forelimb field to restrict heart field potential in zebrafish. *Dev Cell* **15**, 923-34.

Webb, S. E. and Miller, A. L. (2000). Calcium signalling during zebrafish embryonic development. *Bioessays* **22**, 113-23.

Webb, S. E. and Miller, A. L. (2006). Ca2+ signaling during vertebrate somitogenesis. *Acta Pharmacol Sin* **27**, 781-90.

Westerfield, M. (1993). The Zebrafish Book: A guide for the laboratory use of zebrafish (Brachydanio rerio). *University of Oregon Press, Eugene OR*.

Westfall, T. A., Brimeyer, R., Twedt, J., Gladon, J., Olberding, A., Furutani-Seiki, M. and Slusarski, D. C. (2003a). Wnt-5/pipetail functions in vertebrate axis formation as a negative regulator of Wnt/beta-catenin activity. *J Cell Biol* **162**, 889-98.

Westfall, T. A., Hjertos, B. and Slusarski, D. C. (2003b). Requirement for intracellular calcium modulation in zebrafish dorsal-ventral patterning. *Dev Biol* **259**, 380-91.

Whitaker, M. (2006). Calcium at fertilization and in early development. *Physiol Rev* **86**, 25-88.

Whitaker, M. J. and Steinhardt, R. A. (1982). Ionic regulation of egg activation. *Q Rev Biophys* **15**, 593-666.

Wienholds, E., van Eeden, F., Kosters, M., Mudde, J., Plasterk, R. H. and Cuppen, E. (2003). Efficient target-selected mutagenesis in zebrafish. *Genome Res* **13**, 2700-7.

Wilson, P. D. (2001). Polycystin: new aspects of structure, function, and regulation. *J Am Soc Nephrol* **12**, 834-45.

Wilson, P. D. (2004a). Polycystic kidney disease. *N Engl J Med* **350**, 151-64.

Wilson, P. D. (2004b). Polycystic kidney disease: new understanding in the pathogenesis. *Int J Biochem Cell Biol* **36**, 1868-73.

Wilson, P. D. (2008). Mouse models of polycystic kidney disease. *Curr Top Dev Biol* **84**, 311-50.

Wilson, P. D., Devuyst, O., Li, X., Gatti, L., Falkenstein, D., Robinson, S., Fambrough, D. and Burrow, C. R. (2000). Apical plasma membrane mispolarization of NaK-ATPase in polycystic kidney disease epithelia is associated with aberrant expression of the beta2 isoform. *Am J Pathol* **156**, 253-68.

Wilson, P. D. and Falkenstein, D. (1995). The pathology of human renal cystic disease. *Curr Top Pathol* **88**, 1-50.

Wilson, P. D., Geng, L., Li, X. and Burrow, C. R. (1999). The PKD1 gene product, "polycystin-1," is a tyrosine-phosphorylated protein that colocalizes with alpha2beta1-integrin in focal clusters in adherent renal epithelia. *Lab Invest* **79**, 1311-23.

Wilson, V. and Conlon, F. L. (2002). The T-box family. *Genome Biol* **3**, REVIEWS3008.

Wingert, R. A. and Davidson, A. J. (2008). The zebrafish pronephros: a model to study nephron segmentation. *Kidney Int* **73**, 1120-7.

Wingert, R. A., Selleck, R., Yu, J., Song, H. D., Chen, Z., Song, A., Zhou, Y., Thisse, B., Thisse, C., McMahon, A. P. et al. (2007). The cdx genes and retinoic acid control the positioning and segmentation of the zebrafish pronephros. *PLoS Genet* **3**, 1922-38.

Winston, N. J. and Maro, B. (1995). Calmodulin-dependent protein kinase II is activated transiently in ethanol-stimulated mouse oocytes. *Dev Biol* **170**, 350-2.

Woo, D. (1995). Apoptosis and loss of renal tissue in polycystic kidney diseases. *N Engl J Med* **333**, 18-25.

Wu, G., D'Agati, V., Cai, Y., Markowitz, G., Park, J. H., Reynolds, D. M., Maeda, Y., Le, T. C., Hou, H., Jr., Kucherlapati, R. et al. (1998). Somatic inactivation of Pkd2 results in polycystic kidney disease. *Cell* **93**, 177-88.

Wu, X. and McMurray, C. T. (2001). Calmodulin kinase II attenuation of gene transcription by preventing cAMP response element-binding protein (CREB) dimerization and binding of the CREB-binding protein. *J Biol Chem* **276**, 1735-41.

Xia, S., Li, X., Johnson, T., Seidel, C., Wallace, D. P. and Li, R. (2010). Polycystin-dependent fluid flow sensing targets histone deacetylase 5 to prevent the development of renal cysts. *Development* **137**, 1075-84.

Yamaguchi, T., Hempson, S. J., Reif, G. A., Hedge, A. M. and Wallace, D. P. (2006). Calcium restores a normal proliferation phenotype in human polycystic kidney disease epithelial cells. *J Am Soc Nephrol* **17**, 178-87.

Yamaguchi, T., Wallace, D. P., Magenheimer, B. S., Hempson, S. J., Grantham, J. J. and Calvet, J. P. (2004). Calcium restriction allows cAMP activation of the B-Raf/ERK pathway, switching cells to a cAMP-dependent growth-stimulated phenotype. *J Biol Chem* **279**, 40419-30.

Yang, Y., Zhu, W. Z., Joiner, M. L., Zhang, R., Oddis, C. V., Hou, Y., Yang, J., Price, E. E., Gleaves, L., Eren, M. et al. (2006). Calmodulin kinase II inhibition protects against myocardial cell apoptosis in vivo. *Am J Physiol Heart Circ Physiol* **291**, H3065-75.

Yelon, D. (2001). Cardiac patterning and morphogenesis in zebrafish. *Developmental Dynamics* **222**, 552-63.

Yoder, B. K., Hou, X. and Guay-Woodford, L. M. (2002). The polycystic kidney disease proteins, polycystin-1, polycystin-2, polaris, and cystin, are co-localized in renal cilia. *J Am Soc Nephrol* **13**, 2508-16.

Yu, J., He, S., Friedman, J. S., Akimoto, M., Ghosh, D., Mears, A. J., Hicks, D. and Swaroop, A. (2004). Altered expression of genes of the Bmp/Smad and Wnt/calcium signaling pathways in the cone-only Nrl-/- mouse retina, revealed by gene profiling using custom cDNA microarrays. *J Biol Chem* **279**, 42211-20.

Zalk, R., Lehnart, S. E. and Marks, A. R. (2007). Modulation of the ryanodine receptor and intracellular calcium. *Annu Rev Biochem* **76**, 367-85.

Zhang, R., Khoo, M. S., Wu, Y., Yang, Y., Grueter, C. E., Ni, G., Price, E. E., Jr., Thiel, W., Guatimosim, S., Song, L. S. et al. (2005). Calmodulin kinase II inhibition protects against structural heart disease. *Nat Med* **11**, 409-17.

Zhang, T., Kohlhaas, M., Backs, J., Mishra, S., Phillips, W., Dybkova, N., Chang, S., Ling, H., Bers, D. M., Maier, L. S. et al. (2007). CaMKIIdelta isoforms differentially affect calcium handling but similarly regulate HDAC/MEF2 transcriptional responses. *J Biol Chem* **282**, 35078-87.

Zhang, T., Maier, L. S., Dalton, N. D., Miyamoto, S., Ross, J., Jr., Bers, D. M. and Brown, J. H. (2003). The deltaC isoform of CaMKII is activated in cardiac hypertrophy and induces dilated cardiomyopathy and heart failure. *Circ Res* **92**, 912-9.

Vita

Sarah Chase Rothschild was born on October 30, 1978 in New Bedford, Massachusetts. She graduated from Old Rochester Regional High School in Mattapoisett, MA in 1996. She subsequently earned a Bachelor of Arts in Economics and Political Science from the University of Mary Washington in Fredericksburg, VA, in 2000. In 2006, she began her graduate studies in Integrative Life Sciences at Virginia Commonwealth University, under the tutelage of Robert M. Tombes, Ph.D. She received the Phi Kappa Phi Honor Society Award and was selected to attend the Marine Biological Laboratory summer course in zebrafish development and genetics. In May of 2010, she will begin a post-doctoral fellowship with Robert M. Tombes, Ph.D. to continue working on the link between CaMK-II and autosomal dominant polycystic kidney disease.

Manuscripts resulting from the present dissertation research:

Rothschild, S. C., Lister, J. A. and Tombes, R. M. (2007). Differential expression of CaMK-II genes during early zebrafish embryogenesis. *Dev Dyn* 236, 295-305.

Rothschild, S. C., Easley, C. A. t., Francescatto, L., Lister, J. A., Garrity, D. M. and Tombes, R. M. (2009). Tbx5-mediated expression of Ca(2+)/calmodulin-dependent protein kinase II is necessary for zebrafish cardiac and pectoral fin morphogenesis. *Dev Biol* 330, 175-84.